Calculation of the Fire Resistance of Wood Based Boards and Wall Constructions

Fredlund, Bertil

1990

LUND UNIVERSITY • SWEDEN
INSTITUTE OF SCIENCE AND TECHNOLOGY
DEPARTMENT OF FIRE SAFEFTY ENGINEERING

CODEN: SE - LUTVDG/TVBB - 3053
ISSN 0284 - 933X

BERTIL FREDLUND

CALCULATION OF THE FIRE RESISTANCE OF WOOD BASED BOARDS AND WALL CONSTRUCTIONS

LUND 1990

PREFACE

The project is a part of the research programme "Timber constructions and fire" and has been financed by funds from the Swedish Fire Research Board. The aim of the project is to illustrate the possibility of calculating the fire resistance of building panels and wall constructions. The work has been planned in consultation with the steering group "Timber construction and fire" of the Swedish Fire Research Board.

The members of the steering group have been as follows:

Vidar Sjödin, chairman	Rockwool Inc.
Birgit Östman, secretary	Swedish Institute for Wood Technology Research
Bengt Bengtsson	Swedish Wood Panel Inc.
Hans Ohlsson	National Board of Physical Planning and Building
Ulf Wickström	The Swedish National Testing Institute
Kai Ödéen	Royal Institute of Technology, Stockholm
Jan Hagstedt	Swedish Timber Council

The calculations in this work are based on the model developed by the author and presented in [1]. The simulations comprise a total of 23 different calculation cases. The calculations have been compared with experimentally determined fire resistances in most of the cases. In two cases the influence of a varied opening factor for a fire compartment type A is studied.

This document refers to research grants 814-89-1 and 814-89-2 from the Swedish Fire Research Board within the limits of the special programme "Timber constructions and Fire" to the author's company Bedec Engineering. The special programme is a collaboration between the Swedish Fire Research Board, the Swedish Council for Building Research, the Swedish National Board for Technical Development and the Swedish Institute for Wood Technology Research.

The author wishes to thank Marianne Abrahamsson who typed the final version of the manuscript and Lewis J Gruber for correction of the English language.

Lund, January 1990
Bertil Fredlund

TABLE OF CONTENTS

1 INTRODUCTION

Traditionally, the fire resistance of building components and building structures is determined by experiments according to the internationally accepted test method ISO 834 or its Swedish counterpart SIS 02 48 20. For example, testing of a wall in a full scale furnace implies that samples of the dimension 3x3 m are used. The wall samples are installed in a vertical position on one side of the furnace. The temperature in the furnace is then increased according to the requirements in the test method. If a loadbearing structure is tested, external load is applied to the structure.

The fire resistance of a building component is defined as the time when some of the following performance requirements are no longer complied with.

- The insulation requirement, i.e. the rise in temperature on the unexposed face is not allowed to exceed 140 °C on average or 180 °C for a single point

- The integrity requirement, i.e. the building component is not allowed to be penetrated by flames or hot gases

- The loadbearing requirement. This requirement is to be excluded for non-loadbearing structures

In the following theoretical analysis it is the first requirement, i.e. when the rise in temperature on the unexposed face exceeds 140 °C, that determines the fire resistance of the walls and the wood based boards studied.

Since full scale testing is very expensive, small scale tests have been developed [2]. These methods are however only possible to use when non-loadbearing structures are tested.

It is of course desirable to be able to estimate the fire resistance by analytical methods. In this connection the addition principle might be mentioned. The method is based on adding the fire resistances of separate building components to a total fire resistance of a building structure. The fire resistance of the separate building components is determined from experiments.

The objective of this study is to demonstrate that he fire resistance can be calculated on the basis of analytical treatment instead of the results of furnace tests. The calculations in this work are based on the model developed by the author and presented in [1].

The calculated fire resistances are compared with those measured in tests in accordance with ISO 834 and presented in [2] and [3].

2 DESCRIPTION OF THE ANALYTICAL MODEL

In this chapter the theoretical model according to [1] is summarised. The formulation is based on energy and mass transfer in two dimensions.

2.1 Heat transfer analysis

Energy transfer is assumed to occur as thermal conduction and convective flow as volatile pyrolysis products and water vapour move along the pore system of the wood material.

One fundamental assumption is that for each arbitrary point and time there is total thermodynamic equilibrium, i.e. the solid phase and the gaseous phase in the material have the same temperature over a small space about the considered point. We also neglect the contributions due to the work done by pressure.

The original moist wood material is assumed to be divided into four phases: active wood material which forms volatile pyrolysis products, a charcoal phase which can be oxidised at the surface of the material, water in the liquid phase, and water vapour.

The energy content per unit volume is assumed to be equal to the sum of the energy contents of each constituent material. In calculating the temperature rise in the material, the effect of thermal inertia in the gaseous phase can be ignored.

The energy released internally is obtained as the sum of the rate of pyroysis times the reaction energy and the rate of vaporisation times the latent heat of vaporisation respectively, attention being paid to the sign of the phase transformation energies (vaporisation or condensation). In this context, consideration must also be given to the differences in energy content (enthalpy) of the reacting substance and the reaction products.

Pyrolysis is assumed to conform to a mean reaction which is described by an Arrhenius function. Vaporisation is assumed to conform to a relationship which is obtained if the pore system is fully saturated so long as there is water left in the pore system. The oxidation of charcoal at the surface of the material is also assumed to conform to a type of Arrhenius function. The thermal properties of the wood mate-

rial are calculated as weighted mean values of the concentrations of the constituent materials obtained at the time under consideration.

The boundary conditions consist of an exchange of energy with the surroundings. The energy flow at the boundary comprises radiation and convection. The convective energy flow is influenced by outward flow of gases at the boundary.

The fundamental equation for conservation of energy in two dimensions can be summarised as

$$\frac{\delta}{\delta x}\left(\lambda_x \frac{\delta T}{\delta x}\right) + \frac{\delta}{\delta y}\left(\lambda_y \frac{\delta T}{\delta y}\right) - \kappa_x \frac{\delta T}{\delta x} - \kappa_y \frac{\delta T}{\delta y} - \rho c \frac{\delta T}{\delta t} + Q_1^* + Q_w^* = 0 \qquad (2.1)$$

where

T	=	temperature, K
x,y	=	positional coordinates in the x and y directions, respectively, m
λ_x,λ_y	=	thermal conductivity in the x and y directions, respectively, $Wm^{-1}K^{-1}$
κ_x,κ_y	=	convective terms in the x and y directions, respectively, Wm^{-2}
ρ	=	mass per unit volume, kgm^{-3}
c	=	specific heat capacity, $Jkg^{-1}K^{-1}$
t	=	time, s
Q_1^*	=	net exothermic effect in conjunction with pyrolysis, $Jm^{-3}s^{-1}$
Q_w^*	=	net exothermic effect in conjunction with vaporisation of water, $Jm^{-3}s^{-1}$

The convective terms κ_x and κ_y are defined as

$$\kappa_x = m_{xg}c_g + m_{xv}c_v \qquad (2.2)$$

$$\kappa_y = m_{yg}c_g + m_{yv}c_v \qquad (2.3)$$

where

m_{xg},m_{yg}	=	flow of volatile pyrolysis products in x and y directions, respectively, $kgm^{-2}s^{-1}$
m_{xv},m_{yv}	=	vapour flow in x and y directions, respectively, $kgm^{-2}s^{-1}$
c_g	=	specific heat capacity of volatile pyrolysis products, $Jkg^{-1}K^{-1}$
c_v	=	specific heat capacity of vapour, $Jkg^{-1}K^{-1}$

The net exothermic effect in conjunction with pyrolysis Q_1^* and vaporisation Q_w^* is defined as

$$Q_1^* = -\Delta H_1 \frac{\delta \rho_1}{\delta t} + H_g \frac{\delta \rho_g}{\delta t} \tag{2.4}$$

$$Q_w^* = -\Delta H_w \frac{\delta \rho_w}{\delta t} + H_v \frac{\delta \rho_v}{\delta t} \tag{2.5}$$

where

$\Delta H_1, \Delta H_w$ = enthalpy change due to pyrolysis and vaporisation, respectively, Jkg^{-1}

H_g, H_v = enthalpy of volatile pyrolysis products and vapour, respectively, Jkg^{-1}

$\delta_1, \delta_g, \delta_w, \delta_v$ = mass per unit volume of active material, volatile pyrolysis products, water and vapour, respectively, kgm^{-3}

The enthalpy change due to pyrolysis ΔH_1 and vaporisation ΔH_w is given by

$$\Delta H_1 = H_1 - H_g - L_g \tag{2.6}$$

$$\Delta H_w = H_w - H_v - L_v \tag{2.7}$$

where

H_1, H_w = enthalpy of active material and water, respectively, Jkg^{-1}

L_g, L_v = heat of reaction and latent heat of vaporisation, respectively, Jkg^{-1}

Equations (2.4) and (2.5) contain the derivatives with respect to time of ρ, ρ_g, ρ_w and ρ_v for which we need expressions. These derivatives can be written as

$$\frac{\delta \rho_1}{\delta t} = -\rho_1 \, b \, e^{-(E_A/RT)} \tag{2.8}$$

$$\frac{\delta \rho_g}{\delta t} = -\frac{\delta \rho_1}{\delta t} - \frac{\delta m_{xg}}{\delta x} - \frac{\delta m_{yg}}{\delta y} \tag{2.9}$$

$$\frac{\delta \rho_w}{\delta t} = -G_v \tag{2.10}$$

$$\frac{\delta \rho_v}{\delta t} = -\frac{\delta \rho_w}{\delta t} - \frac{\delta m_{xv}}{\delta x} - \frac{\delta m_{yv}}{\delta y} \qquad (2.11)$$

where

b = preexperimental rate constant for pyrolysis, s^{-1}

E_A = activation energy, $Jmol^{-1}$

R = universal gas constant, $Jmol^{-1}K^{-1}$

G_v = rate of generation of water vapour, $kgm^{-3}s^{-1}$

Explicit expressions for the vaporisation term G_v in equation (2.10) and for the flow terms m_{xg}, m_{yg}, m_{xv} and m_{yv} are given in Section 2.2.

2.2 Mass transfer analysis

Generally speaking, transfer of water may take place in both the gaseous and liquid phases. In a number of models, this problem is studied in connection with the drying of wood. In the drying processes in question, however, mass transfer is normally very slow, and vapour transfer due to pressure differences can therefore usually be ignored.

It is stated in [4] that in certain cases a reasonable assumption is to divide the moisture flow into a vapour flow and a water flow. An important example given is drying in conjunction with relatively rapid heating, when account must be taken of the fact that the heat flow is different from the total energy flow. At moderate moisture contents, there are no continuous water phases, and moisture flow takes place essentially in the vapour phase.

Generally speaking, the forces driving the moisture flow are dependent on differences in concentration, temperature gradients and pressure gradients. The flow due to differences in concentration is assumed to conform to Fick's law. The pressure gradients in the material initiate a flow which is assumed to conform to Darcy's law.

According to the universal gas law, temperature changes in the gaseous phase in a volume which is largely constant give rise to a change in pressure. In fire exposure applications, however, this pressure change is small compared to the pressure changes due to vaporisation of water, giving a steep pressure rise [5].

The model for mass transfer of volatile pyrolysis products and water vapour which is presented here is based on gas flows driven by pressure gradients. Flow is given according to Darcy's law. Mass transfer in the liquid phase is considerably slower than that in the gaseous phase and can therefore be neglected.

We assume that the two gaseous phases, water vapour and volatile pyrolysis products, follow the universal gas law. This applies for dilute gases, i.e. low pressure and not very low temperatures. The saturation pressure for water vapour is a function of temperature and can, as a good approximation, be assumed to follow an exponential function. The fundamental assumption made here is that vaporisation is sufficiently rapid for complete saturation of water vapour in the pores to be possible. This holds so long as there is water in the liquid phase at the point in the material which is under consideration.

The total pressure is obtained according to Dalton's law as the sum of the partial pressures of water vapour and volatile pyrolysis products.

The comprehensive differential equation for the mass flow in the two directions x and y is

$$\frac{\delta}{\delta x}\left(\varphi_x \frac{\delta P}{\delta x}\right) + \frac{\delta}{\delta y}\left(\varphi_y \frac{\delta P}{\delta y}\right) + \psi P + G^* - \omega \frac{\delta P}{\delta t} = 0 \qquad (2.12)$$

where

P	=	total pressure, Pa
φ_x, φ_y	=	mass transfer coefficient in x and y directions, respectively, mole s kg^{-1}
ψ	=	thermal expansion coefficient, mole $J^{-1}s^{-1}$
G^*	=	total rate of molar production of water vapour and volatile pyrolysis products, mole $m^{-3}s^{-1}$
ω	=	mass capacity coefficient, mole J^{-1}

The rate of molar production of volatile pyrolysis products and water vapour is defined as

$$G^* = \frac{G_v}{M_w} + \frac{G_g}{M_g} \qquad (2.13)$$

where

M_w, M_g = molar mass of water and volatile pyrolysis products, respectively, kg mole^{-1}

G_v, G_g = rate of generation of water vapour and volatile pyrolysis products, respectively, kgm^{-3}s^{-1}

The production of volatile pyrolysis products G_g is given by an Arrhenius relationship according to equation (2.8); we have

$$G_g = \rho_1 \, b \, e^{-(E_A/RT)} \tag{2.14}$$

A relationship for the production of water vapour G_v is needed in equation (2.13). For a known temperature and pressure distribution, G_v can be calculated from the relationship

$$G_v = \frac{M_w \pi_g k_1}{RT^2} e^{\frac{k_2}{T}} \left[\frac{k_2}{T} - 1\right] \frac{\delta T}{\delta t} - \frac{\delta}{\delta x}\left[\frac{\rho_v}{\rho_v + \rho_g} \alpha_x \frac{\delta P}{\delta x}\right] - \frac{\delta}{\delta y}\left[\frac{\rho_v}{\rho_v + \rho_g} \alpha_y \frac{\delta P}{\delta y}\right] \tag{2.15}$$

where

α_x, α_y = mass transfer coefficient in x and y directions, respectively, s

k_1, k_2 = constants in expression for saturation pressure of water vapour k_1=414 kPa, k_2=4820 K

The relationship between the mass transfer coefficients α_x, α_y and φ_x, φ_y is given by

$$\varphi_i = \frac{\frac{\rho_v}{M_w} + \frac{\rho_g}{M_g}}{\rho_v + \rho_g} \alpha_i \tag{2.16}$$

where

i = direction concerned, x or y

Equation (2.15) contains temperatures and pressures which, during the iterative calculation, are obtained from the immediately preceding calculation step.

When a new pressure distribution has been calculated, the corresponding gas and vapour flows can be calculated according to

$$m_{ij} = \frac{\rho_j}{\rho_v + \rho_g} m_i \qquad (2.17)$$

where

i = direction concerned, x or y

j = volatile pyrolysis products or water vapour

m = mass flow, $kgm^{-2}s^{-1}$

Finally, for known mass flows the change in concentration of volatile pyrolysis products and water vapour can be calculated from the relationship

$$\frac{\delta m_{xg}}{\delta x} + \frac{\delta m_{yg}}{\delta y} = G_g - \frac{\delta \rho_g}{\delta t} \qquad (2.18)$$

$$\frac{\delta m_{xv}}{\delta x} + \frac{\delta m_{yv}}{\delta y} = G_v - \frac{\delta \rho_v}{\delta t} \qquad (2.19)$$

2.3 Initial and boundary conditions for the energy and mass conservation equations

In order that equations (2.1) and (2.12) may be solved, the boundary and initial conditions must be specified. The initial conditions are given by the initial temperature and pressure distribution in the solid phase at the reference time zero. The boundary conditions for the energy conservation equation are specified as prescribed energy flow rates or temperatures at the boundaries. The mass flow at all boundaries is determined by the fact that the pressure along the boundaries is outward pressure.

2.4 Solution techniques

The heat balance and mass balance equations set out contain non-linear boundary conditions and material properties which vary with temperature, pressure and mass fraction of the substance in different states. Analytical solutions are available only for linear applications of simple geometries and simple boundary conditions. The only way in which a solution can be obtained in a more general case is therefore a numerical method.

The method chosen in this case is the finite element method. A description of the finite element approximation and the evaluation of all the element matrices using 4-node isoparametric elements are given in [1].

The integration with respect to time is an implicit single step method. The implicit method is unconditionally stable but this obviously does not imply that the size of the computational increments is subject to limitations. The limiting factors are due to the physical nature of the problem. Examples that may be mentioned are that the changes in boundary conditions and non-linearities in the transfer and capacity matrices must be reproduced in a reasonable manner.

3 MATERIAL PROPERTIES

In this chapter, the material data for the model developed are put together. Experimental determination of physical data did not form part of this project. The data given have thus been collected by studies of the literature. In certain cases, the physical data have been estimated on the basis of information found in the literature.

Generally speaking, it is difficult to obtain reliable material data for material properties at elevated temperatures. For wood, the reasons are that the properties of the original material are subject to a large scatter, and that there are practical difficulties in determining material parameters at high temperatures.

In order that calculations may be carried out according to the model developed, we need information concerning material properties for the following components

- solid wood
- chipboard
- fibre board
- plasterboard
- mineral wool
- glass wool
- charcoal
- calcinated gypsum
- water
- water vapour
- volatile pyrolysis products

The material properties we need are thermal conductivity, specific heat capacity, reaction rate and heat of reaction, surface reaction rate, permeability and dynamic viscosity.

3.1 Material properties of wood based boards and building panels of wood

In the calculations which have been carried out, all the material data have been taken from [1]. We do not distinguish between the thermal properties of solid wood, chipboard or fibre board. The only input data which have been varied are thickness, density and moisture content.

3.1.1 Thermal conductivity of wood and charcoal

The thermal conductivity of the original wood varies as a function of the mass per unit volume of dry wood material, water content and temperature. During pyrolysis the wood material decomposes to charcoal and volatile pyrolysis products. For the partially charred material, the thermal conductivity is assumed to vary linearly between the original wood material and the final charcoal. The effect of the temperature on the thermal conductivity of charcoal, and the moisture content in the wood are taken into consideration. The thermal conductivity of wood as a function of moisture content and density for radial heat transfer is given by MacLean [6].

The thermal conductivities of dry wood material and charcoal as a function of temperature are illustrated in Figure 3.1.

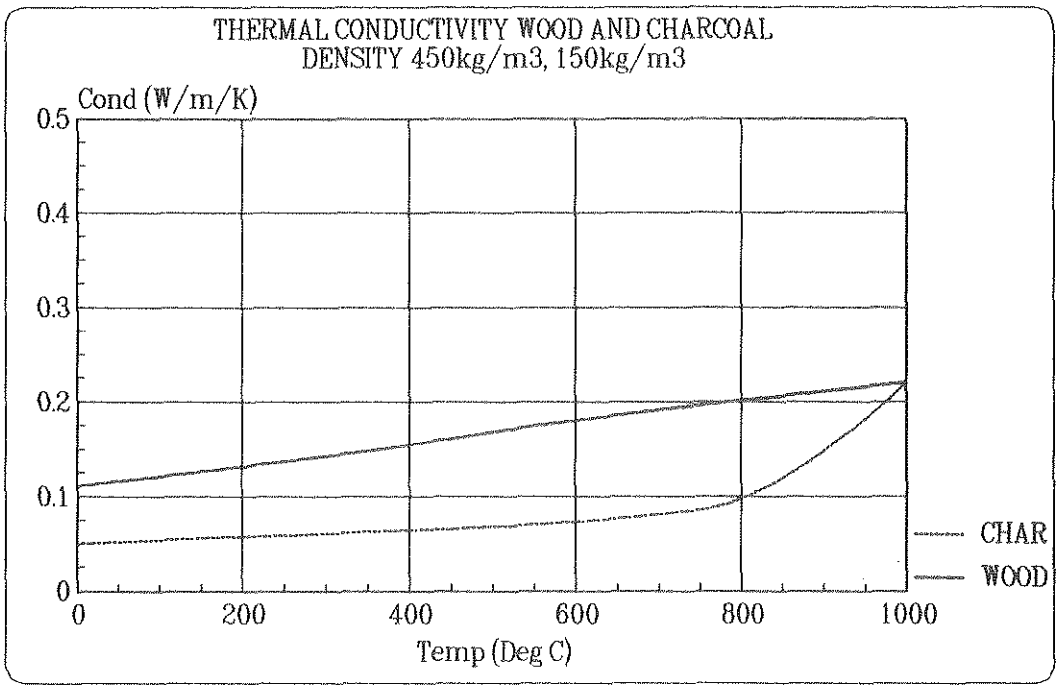

Figure 3.1 Thermal conductivity of dry wood material and charcoal as a function of temperature

3.1.2 Specific heat capacity of wood and pyrolysis products

In the calculations of energy transfer and the heat generated internally in conjunction with phase changes we need information concerning specific heat capacity as a function of temperature for the constituent materials.

Figure 3.2 shows the specific heat capacity as a function of temperature for original wood, charcoal, volatile pyrolysis products and water vapour.

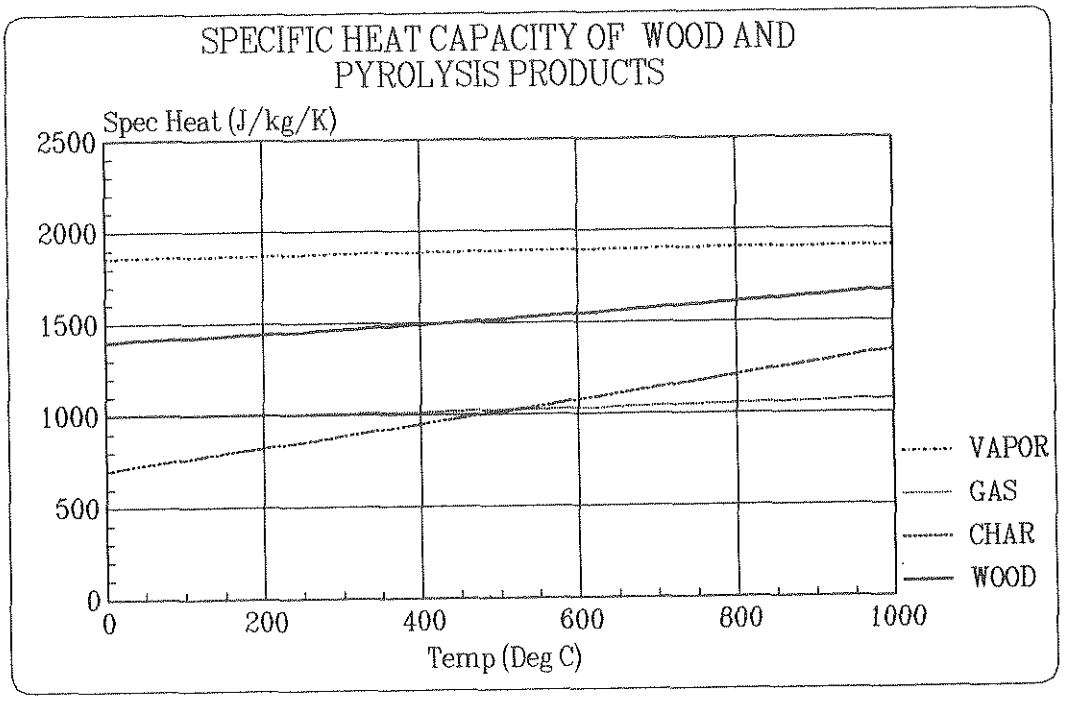

Figure 3.2 Specific heat capacity of original wood, charcoal, volatile pyrolysis products and water vapour as a function of temperature

3.1.3 The kinetics of wood pyrolysis

The process of pyrolysis is assumed to conform to a mean reaction described by an Arrhenius function according to equation (2.8), and repeated here

$$\frac{\delta \rho_1}{\delta t} = -\rho_1 \, b \, e^{-(E_A/RT)} \qquad (3.1)$$

where

E_A = activation energy, $Jmol^{-1}$
R = universal gas constant, 8.314 $Jmol^{-1}K^{-1}$
b = preexperimental rate constant for pyrolysis, s^{-1}
ρ_1 = mass per unit volume of active material, kgm^{-3}
T = temperature, K
t = time, s

In the calculations the following numerical data have been used

E_A = 26300 $Jmol^{-1}$
b = 0.55 s^{-1}

Since there is great uncertainty regarding the heat of reaction, it has been decided that in the simulations described in this report, this parameter would not be used in order to fit the calculation results to experiments. Quite simply, as a temporary solution, we assume that the heat of reaction h_g=0.

3.1.4 Surface reactions

It is assumed that the chemical reaction at the surface is described by the following empirical equation [7]

$$|\dot{s}| = T_s \, \beta \, e^{-(E_A/RT_s)} \qquad (3.2)$$

where

s = rate of recession of material surface due to the reaction, ms^{-1}
T_s = surface temperature, K
β = empirical constant, $s^{-1}K^{-1}$
E_A = activation energy, $Jmol^{-1}$
R = universal gas constant, $Jmol^{-1}K^{-1}$

In the calculations the following numerical data have been used

$$\beta = 10^{-7}\ s^{-1}K^{-1}$$
$$E_A = 25770\ Jmol^{-1}$$

The heat of reaction at the surface of the material is obtained if we assume that the reaction occurs between carbon and oxygen, with carbon monoxide as the reaction product. The carbon monoxide then reacts with oxygen in the transition layer outside the solid phase and forms carbon dioxide. The heat of reaction at the surface of the material, given by the first reaction, is

$$\Delta H_s = -\ 395.5\ kJmol^{-1}$$

3.1.5 Permeability of wood and charcoal

The permeability of wood and building panels of wood varies considerably. In addition, if the description of the material also includes the carbon layer, it is further complicated as a result of shrinkage and cracking. In [1], these problems are further discussed and the permeability estimated.

In the computer program the variation in permeability D is given by

$$D = k_{D1}\, e^{k_{D2}\left(1 - \frac{\rho-\rho_2}{\rho_0-\rho_2}\right)} \qquad (3.3)$$

where

k_{D1} = preexponential constant depending on material, m^2
k_{D2} = exponential constant
ρ = current density, kgm^{-3}
ρ_2 = density of charcoal, kgm^{-3}
ρ_0 = original density, kgm^{-3}

In the simulations the following numerical data have been used

$$k_{D1} = 0.15 \cdot 10^{-15}\ m^2$$
$$k_{D2} = 11$$

3.1.6 Dynamic viscosity

Mass transfer of volatile pyrolysis products and water vapour occurs under the influence of gradients in total pressure. The dynamic viscosity of the gases varies as a function of temperature. In [1] the dynamic viscosity of volatile pyrolysis products is given, based on experiments according to [8].

The weighted mean value of the dynamic viscosity of the volatile pyrolysis products together with water vapour is given in Figure 3.3.

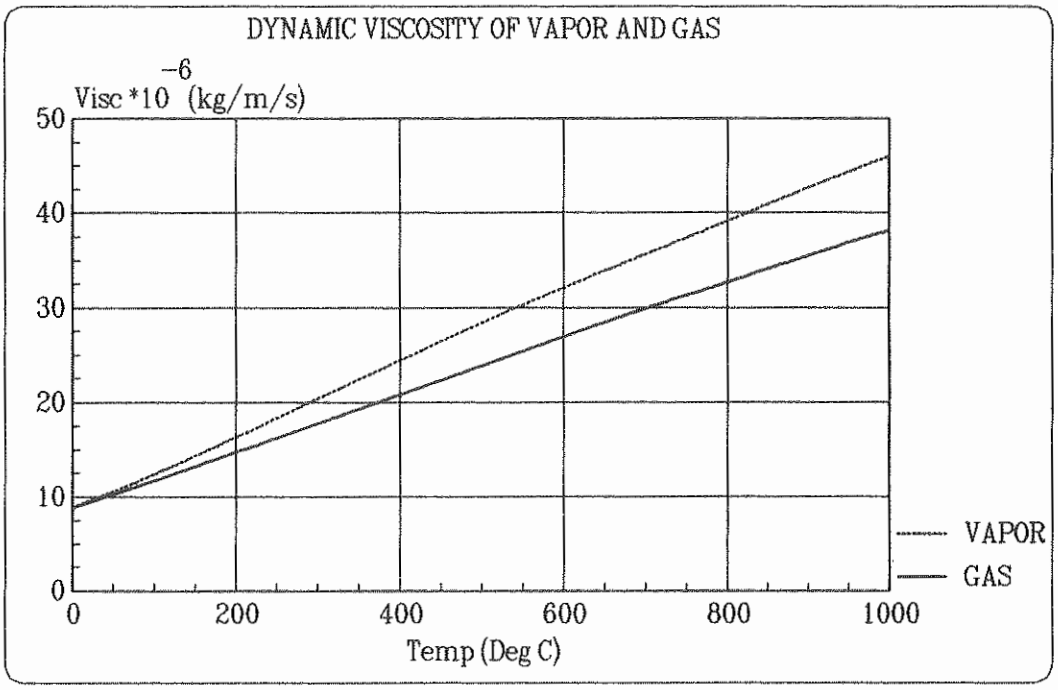

Figure 3.3 Dynamic viscosity of volatile pyrolysis products and water vapour

3.2 Material properties of plasterboard

The thermal properties of plaster vary as a function of density, chemical composition and temperature. Gypsum is calcium sulphate consisting of two moles of hydration water per one mole calcium sulphate, $CaSO_4 \cdot 2H_2O$. By weight gypsum consists of 21% hydration water and 79% calcium sulphate.

If the gypsum is heated it is calcined, i.e. the hydration water vanishes. Calcination occurs mainly in two steps. At 100 °C 3/4 of the hydration water vanishes according to the reaction

$$CaSO_4 \cdot 2H_2O + \text{Energy} \;\Longrightarrow\; CaSO_4 \cdot 0.5H_2O + 1.5H_2O \qquad (3.4)$$

The energy needed for this reaction is 515 $kJkg^{-1}$ gypsum or 3270 $kJkg^{-1}$ released water. In addition, energy of 2260 $kJkg^{-1}$ is required for vaporisation of the water.

The remaining part of the hydration water is released at 210 °C according to

$$CaSO_4 \cdot 0.5H_2O + \text{Energy} \;\Longrightarrow\; CaSO_4 \cdot 0.5H_2O \qquad (3.4)$$

The energy required for this reaction is 185 $kJkg^{-1}$ gypsum or 2967 $kJkg^{-1}$ released water. Even in this reaction the vaporisation energy must be added.

At 360 °C a further reaction takes place. The calcium sulphate is changed to a more stable form. The reaction is slightly exotermic and is therefore neglected in the calculations.

In order that the calculations may be carried out, we need the thermal properties of gypsum for the following phases

- original gypsum $CaSO_4 \cdot 2H_2O$
- partly calcined gypsum $CaSO_4 \cdot 05H_2O$
- calcium sulphate $CaSO_4$

3.2.1 Thermal conductivity of plasterboard

On the basis of the measurements according to [9] the thermal conductivity has been calculated for the three phases of gypsum. The measured thermal conductivity is adapted to the theoretical model [1] in the following way

- The measured thermal conductivity is extrapolated linearly from 780 °C to 1000 °C

- The relationship above 210 °C, that is $CaSO_4$, is extrapolated linearly down to 0 °C. At 0 °C we get the thermal conductivity 0.10 $Wm^{-1}K^{-1}$

- The measured thermal conductivity at 0 °C is 0.28 $Wm^{-1}K^{-1}$. The difference between 0.28 and 0.10 $Wm^{-1}K^{-1}$ is assumed to depend on the water content, 21% by weight, in the original plasterboard. In this context we make no difference between hydration water and free water. This means that the thermal conductivity remains constant at a constant temperature until the water is transferred from the point under consideration due to pressure gradients.

- The thermal conductivity of plasterboard is assumed to vary linearly with the mass per unit volume of the constituent components calcium sulphate and water. If the fraction of water is denoted u, we have the following relationship

$$\lambda_{gyps}\,\rho_{gyps} = \lambda_{CaSO4}\,(1-u)\rho_{gyps} + \lambda_{H2O}\,u\,\rho_{gyps} \qquad (3.6)$$

where

λ_{gyps} = thermal conductivity of gypsum
ρ_{gyps} = density of plasterboard
λ_{CaSO_4} = thermal conductivity of $CaSO_4$ according to extrapolated relationship in [9]
λ_{H_2O} = resulting conductivity of water evaluated according to equation (3.6) at 0 °C

The thermal conductivity of plasterboard as a function of temperature and degree of calcination according to equation (3.6) is plotted in Figure 3.4.

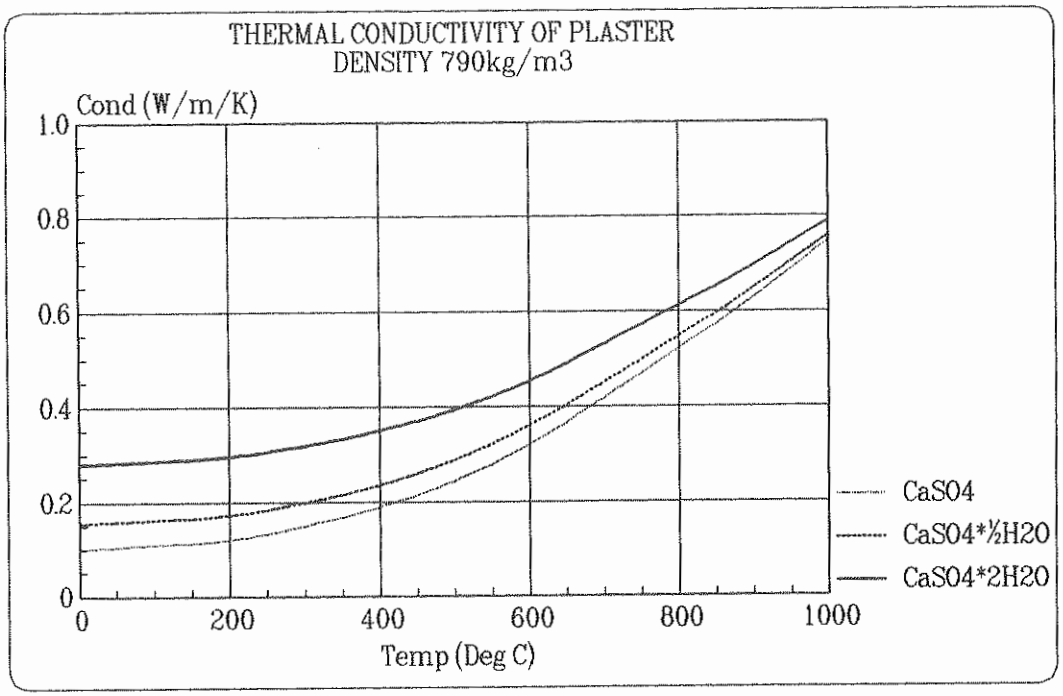

Figure 3.4 Thermal conductivity of plasterboard as a function of temperature and the degree of calcination

3.2.2 Specific heat capacity of plasterboard

The specific heat capacity of gypsum as a function of temperature and degree of calcination is given in [10]. The specific heat capacity is specified at 25, 400, 600, 800 and 1000 °C and given in cal $K^{-1}mol^{-1}$. The data are recalculated in $Jkg^{-1}K^{-1}$ and extrapolated linearly to 0 °C. The curves are plotted in Figure 3.5.

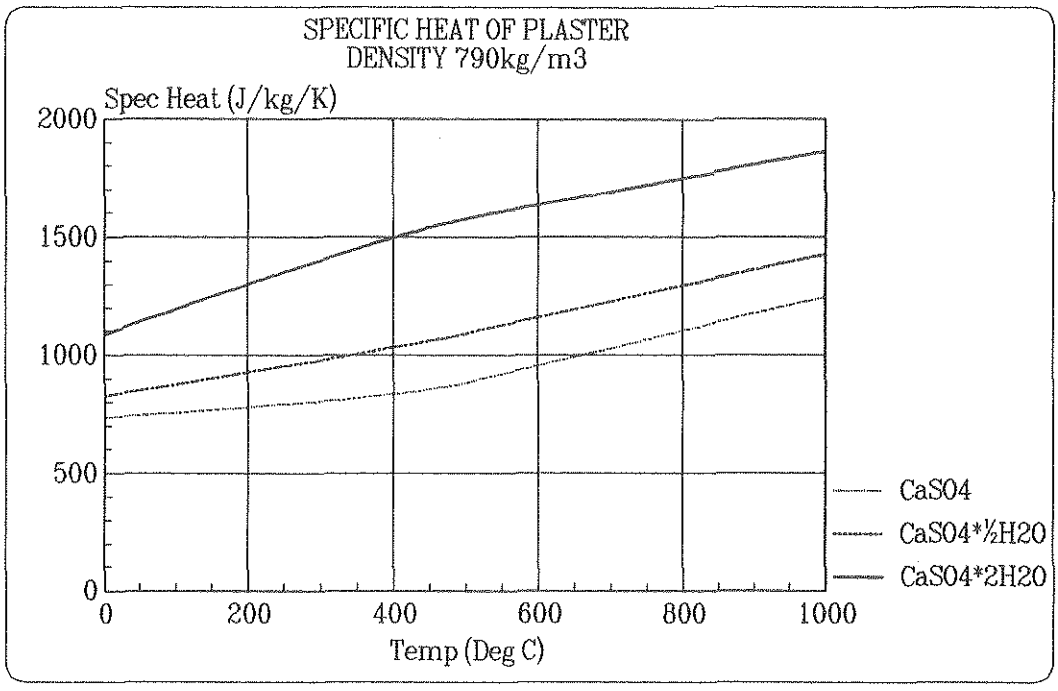

Figure 3.5 Specific heat capacity of plasterboard as a function of temperature and degree of calcination

3.2.3 Permeability of plasterboard

In order to carry out the calculations of the movement of free water in the plasterboard, we need the permeability of the material. In [11] the permeability is reported equal to $0.38 \cdot 10^{-12}$ m^2. The value is taken from an unpublished report from the Swedish Plywood Association (1978). We also need a relationship of the variation of permeability as a function of calcination. To my knowledge, there are no such data reported. As a temporary solution we assume a variation of the permeability according to equation (3.3).

In the simulations the following numerical data have been used

$k_{D1} = 0.38 \cdot 10^{-12}$ m^2
$k_{D2} = 5$
$\rho_2 = 624.1$ kgm^{-3}
$\rho_0 = 790$ kgm^{-3}

The constant k_{D2} is assumed and gives 148 times increased permeability of $CaSO_4$ compared with the original plasterboard.

3.2.4 Temperature criterion for the loss of plasterboard

From tests a reasonable temperature criterion for the loss of plasterboard turned out to be 550 °C at the rear face of the board. This criterion is used in the calculation for want of better criteria.

3.3 Material data of glass wool and mineral wool

In some of the calculations there is an insulating material present. The required thermal properties are presented in this section.

3.3.1 Thermal conductivity of glass wool and mineral wool

Based on data from the manufacturer of glass wool and mineral wool, and tests of softening temperatures of the insulating materials, an approximate relationship of the thermal conductivity as a function of temperature has been derived according to Figure 3.6.

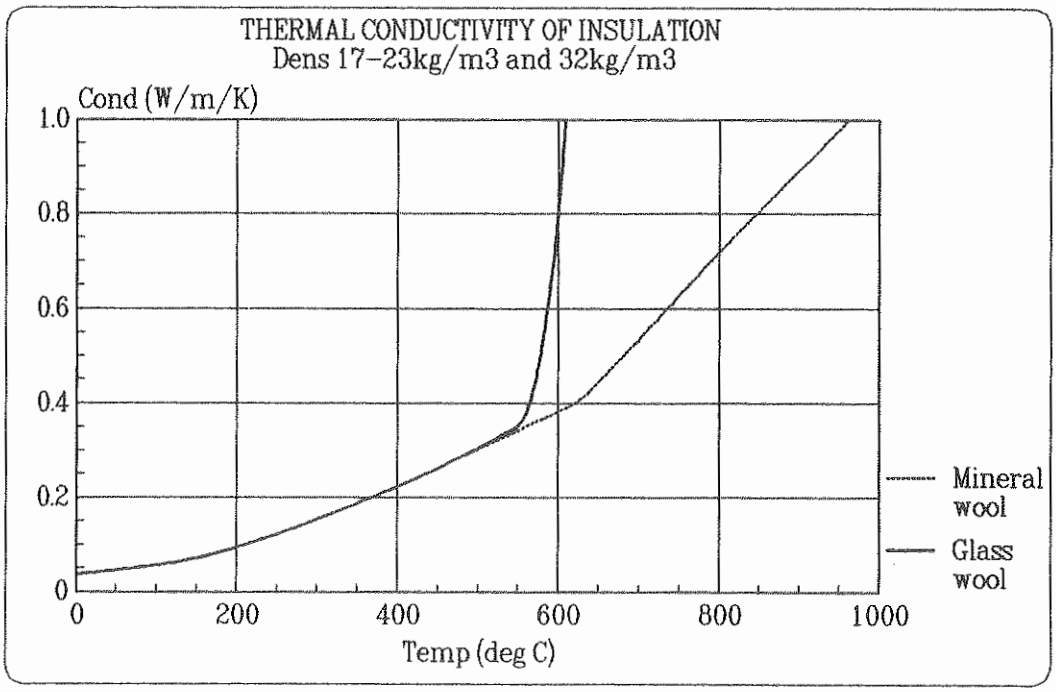

Figure 3.6 Thermal conductivity of glass wool ρ=17-23 kgm^{-3} and mineral wool ρ=32 kgm^{-3} as a function of temperature. The effect of the softening of glass wool above 600 °C and the softening of mineral wool above 750 °C is taken into consideration.

To reproduce the effect of softening of glass wool above 600 °C, the thermal conductivity has been increased. At 670 °C the thermal conductivity is assumed to be 3 $Wm^{-1}K^{-1}$ and above 800 °C to be 10 $Wm^{-1}K^{-1}$. A linear interpolation is performed for intermediate temperatures.

A similar procedure is used for mineral wool. But the softening of mineral wool arises in two steps. At 700-800 °C the deformation is about 30% of the original thickness. Between 750 and 1150 °C the resultant thermal conductivity is calculated as 1/0.7 times the linearly extrapolated values of thermal conductivity data from the manufacturer. At 1150 °C the deformation of the mineral wool is about 50% of the original thickness and the resultant thermal conductivity is assumed to be twice the linearly extrapolated values.

3.3.2 Specific heat capacity of glass wool and mineral wool

The relationship for the specific heat capacity of glass wool and mineral wool as a function of temperature is set out in Figure 3.7.

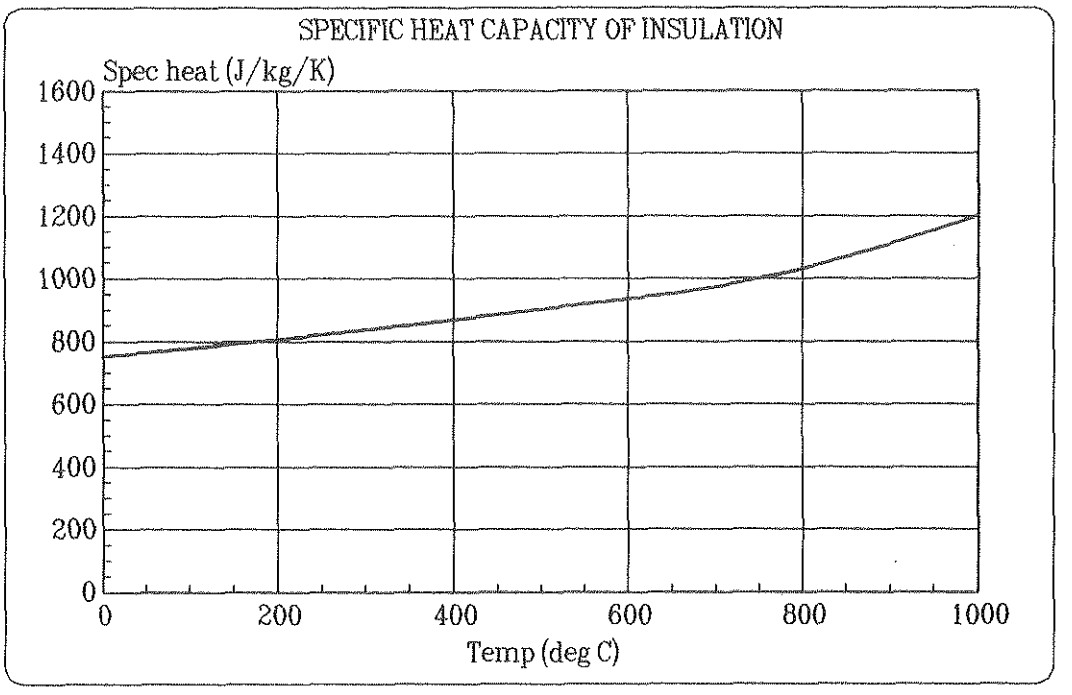

Figure 3.7 Specific heat capacity of glass wool and mineral wool as a function of temperature

3.3.3 Permeability of glass wool and mineral wool

The permeability of glass wool and mineral wool is assumed to be constant at $0.2 \cdot 10^{-8}$ m^2. This gives us the following constants in equation (3.3)

$$k_{D1} = 0.2 \cdot 10^{-8} \text{ m}^2$$
$$k_{D2} = 0$$

4 NUMERICAL RESULTS

In this study 23 different calculation cases are presented. Some of the results of the calculations which have been carried out are presented in this chapter. The presentation is given in diagrams in which the three different calculated quantities temperature, density and moisture ratio, have been set out as a function of the distance from the surface exposed to fire at different times. For practical reasons all calculated data cannot be given in this chapter. A complete presentation is however available in Appendix A.

The different calculation cases are presented in Tables 4.1 and 4.2. The numerical results presented in this chapter are based on calculations carried out with the one dimensional version of the computer program WOOD1. The input data for the simulations are based on the material data put together in Chapter 3.

Table 4.1 Summary of calculation cases for wood based boards

Calculation case	Material	Thickness	Density	Moisture ratio		Boundary condition*	
		mm	kgm^{-3}	%		Front side	Rear face
1	Chipboard	12	700	0.5		ISO834	no insulation
2	Chipboard	12	700	8.0		ISO834	no insulation
3	Chipboard	12	700	11.0		ISO834	no insulation
4	Chipboard	12	700	8.0		200 MJm^{-2} 0.04 $m^{1/2}$	no insulation
5	Chipboard	12	700	8.0		200 MJm^{-2} 0.08 $m^{1/2}$	no insulation
6	Chipboard	19	700	8.0		ISO834	no insulation
7	Fibre board	9	800	0.5		ISO834	no insulation
8	Fibre board	9	800	8.0		ISO834	no insulation
9	Fibre board	9	800	11.0		ISO834	no insulation
10	Fibre board	9	800	8.0		ISO834	insulation
11	Wood boarding	13	500	4.0		ISO834	no insulation
12	Wood boarding	13	500	13.0		ISO834	no insulation
13	Plasterboard	12	790	21.0	**	ISO834	no insulation
14	Plasterboard	13	790	21.0	**	ISO834	no insulation

* ISO834 means that the gas temperature follows ISO834. The fire load 200 MJm^{-2} and the opening factors 0.04 $m^{1/2}$ and 0.08 $m^{1/2}$ respectively in a fire compartment type A define the fire exposure.
The air temperature in the room at the rear face is 20 °C. Insulation means the provision of 100 mm mineral wool behind the wood material.

** Hydration water

Table 4.2 Summary of calculation cases for wall constructions

Calculation case	Material *	Thickness mm	Density kgm^{-3}	Moisture ratio %	
15	Fibre board	9	800	8.0	
	Glass wool	95	23	0.0	
	Asphalt board	13	350	8.0	
16	Chipboard	10	700	8.0	
	Glass wool	70	17	0.0	
	Chipboard	10	700	8.0	
17	Chipboard	10	700	8.0	
	Mineral wool	70	32	0.0	
	Chipboard	10	700	8.0	
18	Chipboard	12	700	8.0	
	Mineral wool	100	32	0.0	
	Chip board	12	700	8.0	
19	Chipboard	19	700	8.0	
	Mineral wool	25	32	0.0	
	Chipboard	19	700	8.0	
20	Chipboard	19	700	8.0	
	Chipboard	19	700	8.0	
	Mineral wool	25	32	0.0	
	Chipboard	19	700	8.0	
21	Chipboard	19	700	8.0	
	Mineral wool	100	32	0.0	
	Chipboard	19	700	8.0	
22	Plasterboard	13	790	21.0	hydration water
	Mineral wool	25	32	0.0	
	Plasterboard	13	790	21.0	hydration water
23	Plasterboard	13	790	21.0	hydration water
	Mineral wool	45	32	0.0	
	Plasterboard	13	790	21.0	hydration water

* The front side (towards the fire) is given first

In all calculation cases given in Table 4.2, the boundary conditions on the front side follow the gas temperature time curve according to ISO834. The air temperature in the room at the rear face is constant, 20 °C.

4.1 Chipboard

In Figures 4.1a to 4.1c the calculated temperature, density and moisture distributions are given at different times for a 12 mm chipboard with moisture ratio of 8.0% (calculation case number 2).

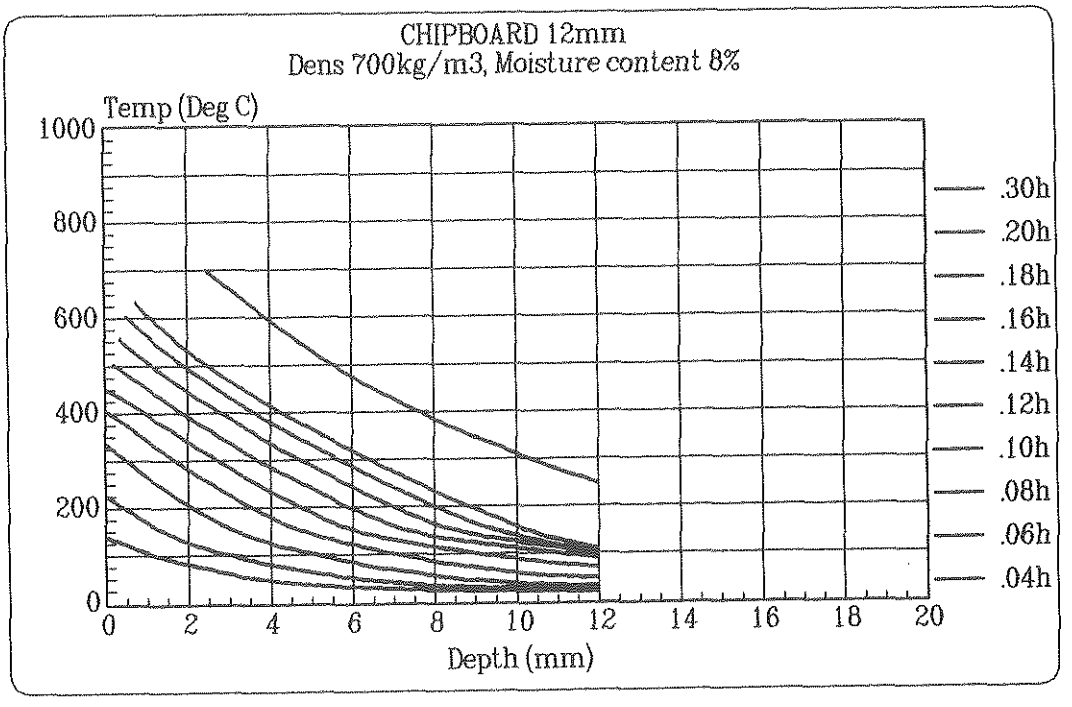

Figure 4.1a Calculation case number 2. Temperature distribution in a 12 mm chipboard at different times. The density is 700 kgm^{-3} and the moisture ratio is 8.0 %. Fire exposure according to ISO834.

Figure 4.1a gives the fire resistance, i.e. when the rise in temperature on the unexposed face exceeds 140 °C. The fire resistance is 14 min and 18 sec. In figure 4.1a we can also read out the regression of the exposed surface. At 12 minutes the regression is about 1 mm and at 18 minutes 2.5 mm.

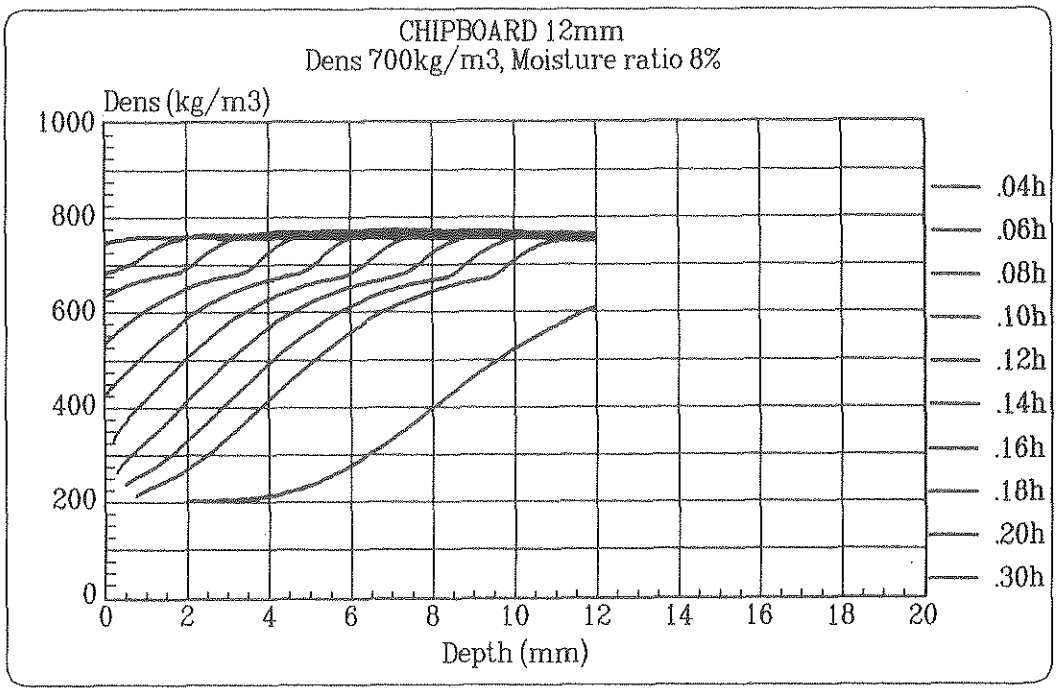

Figure 4.1b Calculation case number 2. Density distribution in a 12 mm chipboard at different times. The original dry density is 700 kgm^{-3} and the moisture ratio is 8.0%. Fire exposure according to ISO834.

In Figure 4.1b the effect of pyrolysis on the density is summarised. From the relationship we can also see when the material has dried out. This is indicated by the density level 700 kgm^{-3}.

If the beginning of the charring zone is defined as the point when 20% of the original dry material is lost, we have for chipboard (ρ_0=700 kgm^{-3}) the level 560 kgm^{-3}. The charring depth at 12 minutes according to Figure 4.1b is then 6 mm giving a mean charring rate of 0.5 mm min^{-1}. This is a reasonable charring rate according to experiments.

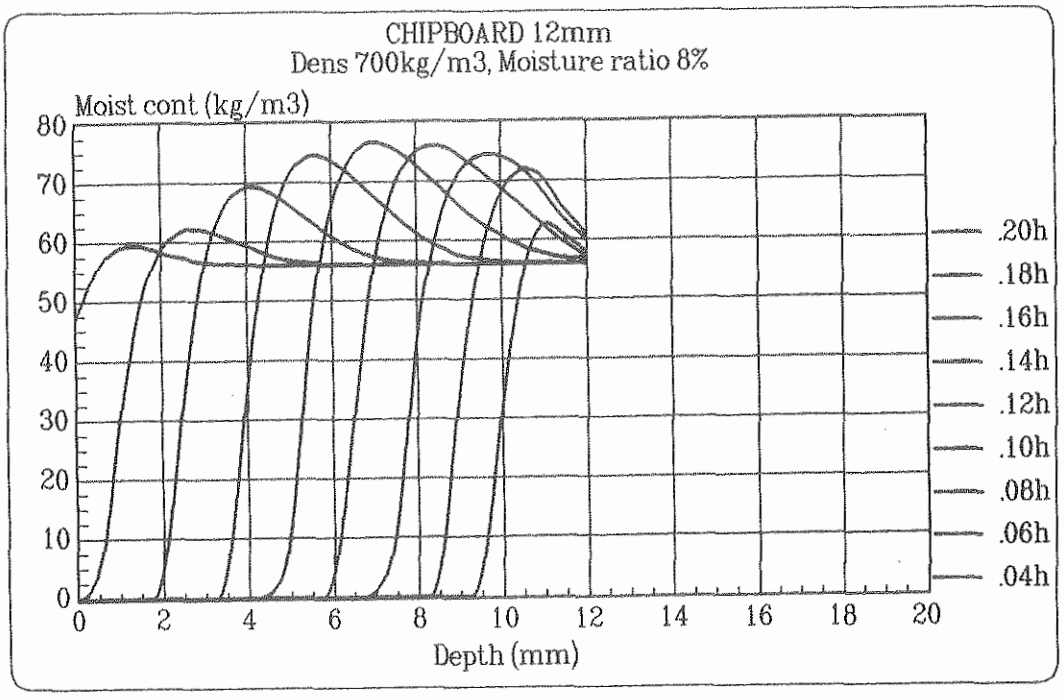

Figure 4.1c Calculation case number 2. Moisture distribution in a 12 mm chipboard at different times. The density is 700 kgm^{-3} and the moisture content is 8.0%. Fire exposure according to ISO834.

In Figure 4.1c the drying process of the chipboard is more clearly seen. Owing to pressure gradients which arise, there is a gradual and steep rise in moisture ratio. In those parts of the material where the temperature is above 100 °C, vaporisation occurs. The pressure gradients give rise to a mass flow directed towards the cooler parts of the material where the vapour condenses.

Figures on pages 72 to 77 in the Appendix set out the complete set of the calculation cases 1 to 6 for the chipboard. The results from these calculations are summarised in Table 4.3

Table 4.3 Calculated fire resistance of chipboard, density 700 kgm^{-3}

Calculation case No	Thickness mm	Moisture ratio %	Fire resistance min:sec
1	12	0.5	10:21
2	12	8.0	14:18
3	12	11.0	15:55
4 *	12	8.0	11:24
5 **	12	8.0	9:00
6	19	8.0	26:06

* Fire compartment type A, 200 MJm^{-2}, 0.04 $m^{1/2}$

** Fire compartment type A, 200 MJm^{-2}, 0.08 $m^{1/2}$

From Table 4.3 the importance of taking the initial moisture ratio into account is evident. We can also conclude that in a natural fire characterized by a fire compartment type A, a fire load of 200 MJm^{-2} and opening factor of 0.04 $m^{1/2}$ and 0.08 $m^{1/2}$ respectively, the fire resistance is reduced by 3 to 5.5 minutes.

4.2 Fibre board

In Figures 4.2a to 4.2c the calculated temperature, density and moisture distributions are given at different times for a 9 mm fibre board with moisture ratio of 8.0% (calculation case number 8).

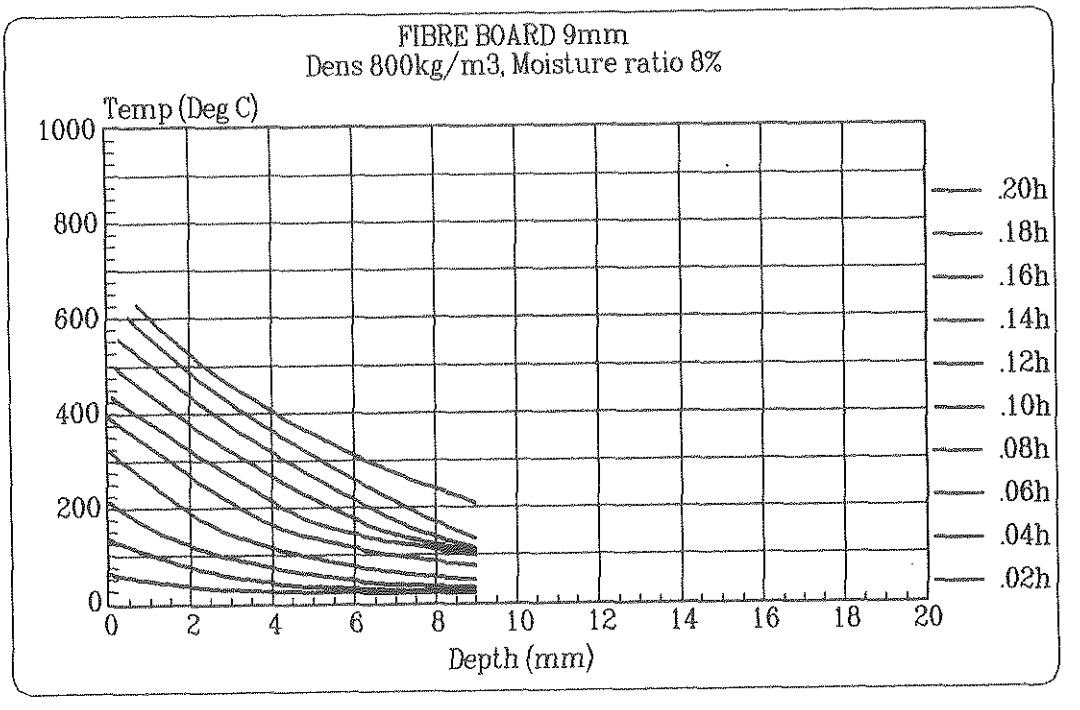

Figure 4.2a Calculation case number 8. Temperature distribution in a 9 mm fibre board at different times. The density is 800 kgm^{-3} and the moisture ratio is 8.0%. Fire exposure according to ISO834.

Figure 4.2a gives the fire resistance. The temperature rise on the unexposed face exceeds 140 °C after 11 min and 12 sec. The regression of the exposed surface at 12 minutes is only about 1 mm according to Figure 4.2a.

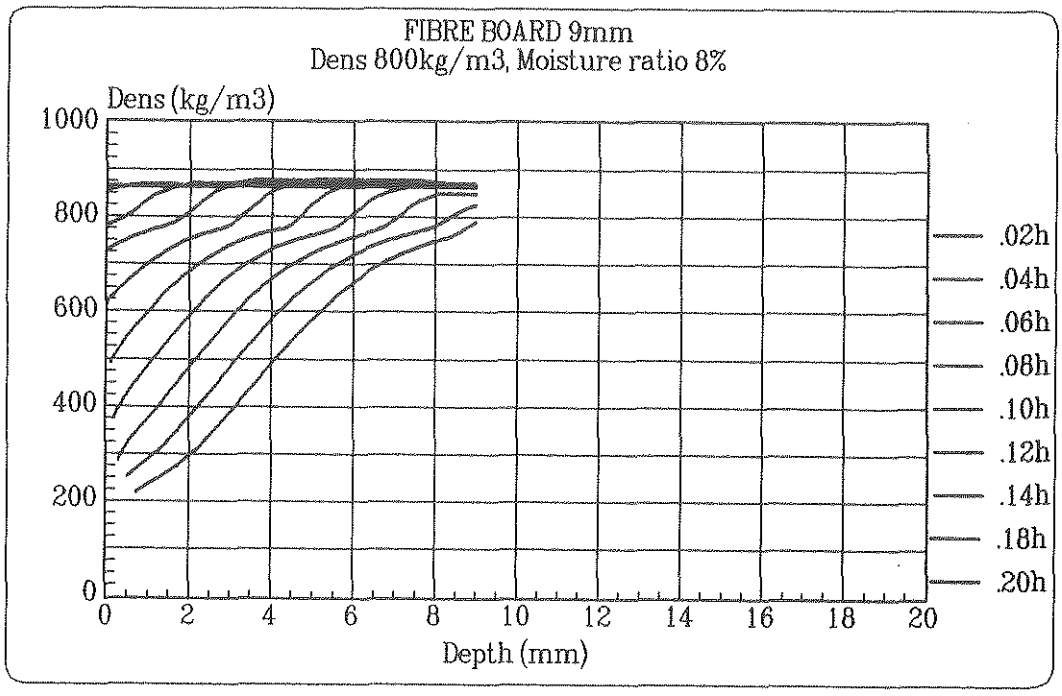

Figure 4.2b Calculation case number 8. Density distribution in a 9 mm fibre board at different times. The original dry density is 800 kgm^{-3} and the moisture ratio is 8.0%. Fire exposure according to ISO834.

In Figure 4.2b the effect of pyrolysis on the density is summarised. From the relationship we can also see when the material has dried out. This is indicated by the density level 800 kgm^{-3}.

In the same way as in Subsection 4.1, the beginning of the charring zone is determined from Figure 4.2b at the density level 640 kgm^{-3}. The charring depth at 12 minutes according to Figure 4.2b is then 5.5 mm giving a mean charring rate of 0.46 mm min^{-1}.

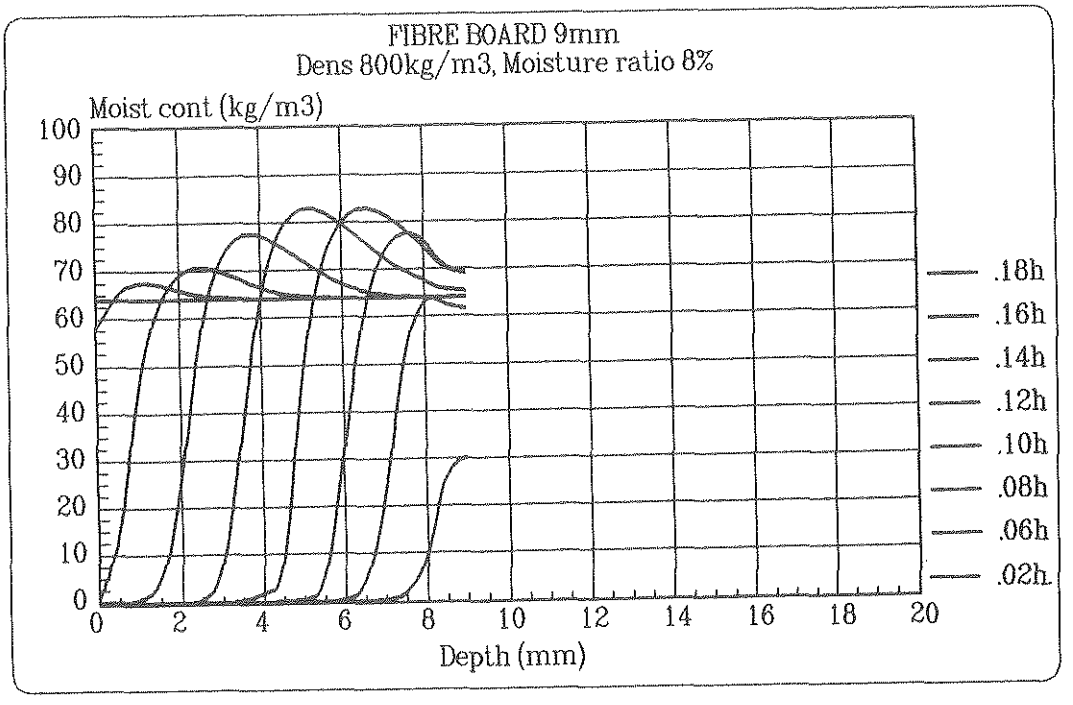

Figure 4.2c Calculation case number 8. Moisture distribution in a 9 mm fibre board at different times. The density is 800 kgm^{-3} and the moisture content is 8.0%. Fire exposure according to ISO834.

In Figure 4.2c the drying process owing to pressure gradients is illustrated.

Figures on pages 78 to 81 in the Appendix set out the complete set of calculation cases 7 to 10 for the fibre board. The results from these calculations are summarised in Table 4.4.

Table 4.4 Calculated fire resistance of fibre board, density 800 kgm^{-3}

Calculation case No	Thickness mm	Moisture ratio %	Fire resistance min:sec
7	9	0.5	8:12
8	9	8.0	11:12
9	9	11.0	12:16
10 *	9	8.0	9:48

* With 100 mm mineral wool behind the fibre board

From Table 4.4 the importance of taking the initial moisture ratio into account is evident. We can also conclude that the mineral wool behind the fibre board has a marked influence on the fire resistance

4.3 Wood board

In Figures 4.3a to 4.3c the calculated temperature, density and moisture distributions are given at different times for a 13 mm wood boarding with a moisture ratio of 4.0% (calculation case number 11).

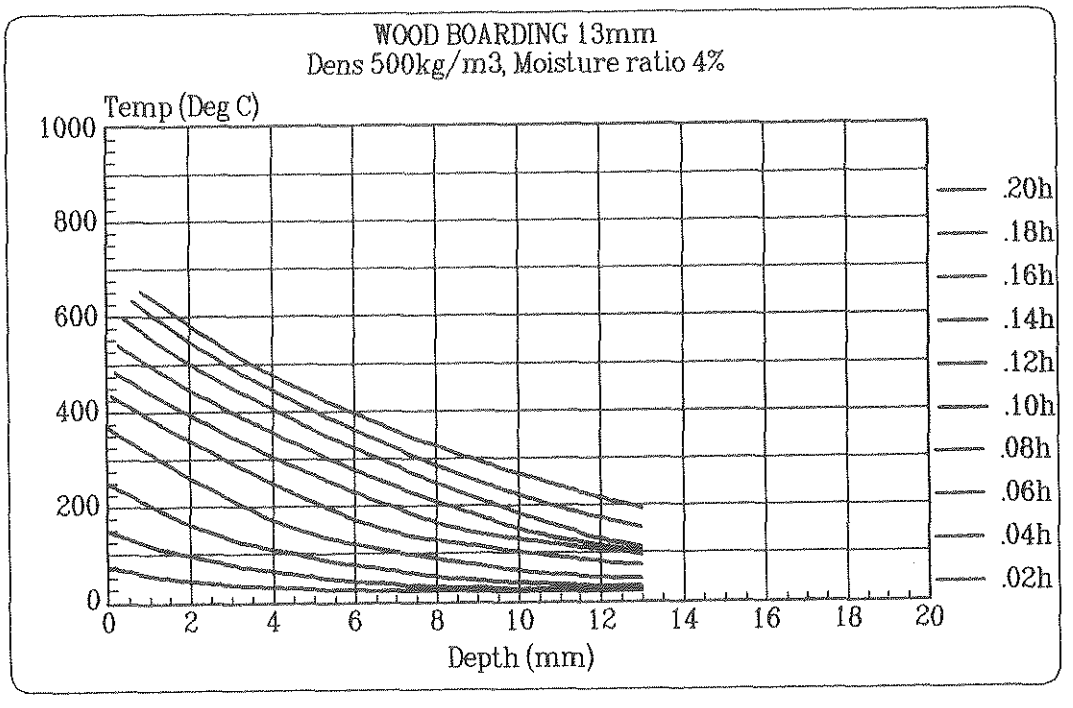

Figure 4.3a Calculation case number 11. Temperature distribution in a 13 mm wood boarding at different times. The density is 500 kgm^{-3} and the moisture ratio is 4.0%. Fire exposure according to ISO834.

Figure 4.3a gives the fire resistance. The temperature rise on the unexposed face exceeds 140 °C after 11 min and 2 sec. The regression of the exposed surface at 12 minutes is about 1 mm according to Figure 4.3a.

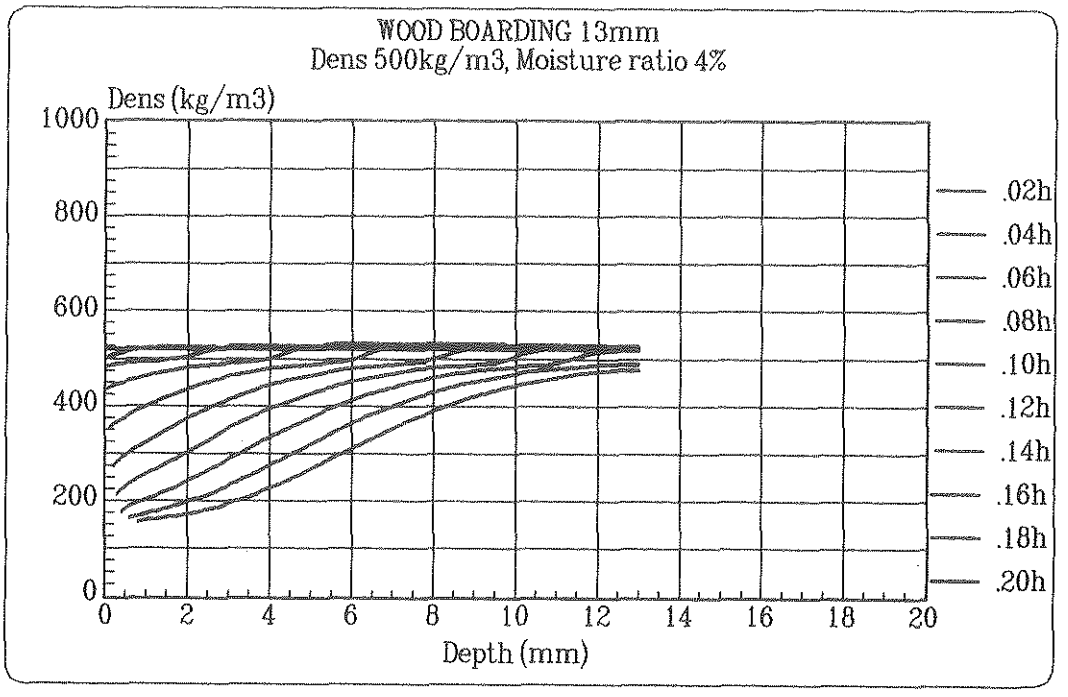

Figure 4.3b Calculation case number 11. Density distribution in a 13 mm wood boarding at different times. The original dry density is 500 kgm^{-3} and the moisture ratio is 4.0%. Fire exposure according to ISO834.

In Figure 4.3b the effect of pyrolysis on the density is summarised. From the relationship we also can see when the material has dried out. This is indicated by the density level 500 kgm^{-3}.

In the same way as in Subsections 4.1 and 4.2, the beginning of the charring zone is determined from Figure 4.3b at the density level 400 kgm^{-3}. The charring depth at 12 min according to Figure 4.3b is then 8.5 mm giving a mean charring rate of 0.71 mm min^{-1}. This is a reasonable charring rate according to experiments.

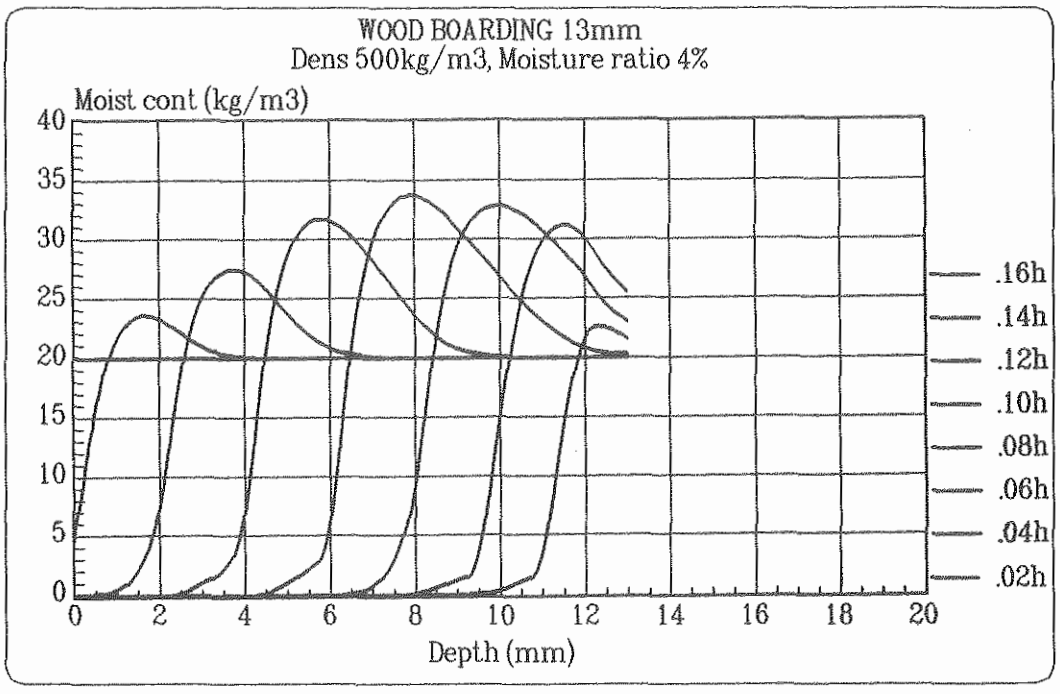

Figure 4.3c Calculation case number 11. Moisture distribution in a 13 mm wood boarding at different times. The density is 500 kgm^{-3} and the moisture ratio is 4.0%. Fire exposure according to ISO834.

In Figure 4.3c the drying process owing to pressure gradients is illustrated.

Figures on pages 82 to 83 in the Appendix set out the complete set of calculation cases 11 and 12 for the wood boarding. The results from these calculations are summarised in Table 4.5.

Table 4.5 Calculated fire resistance of wood boarding, density 800 kgm^{-3}

Calculation case No	Thickness mm	Moisture ratio %	Fire resistance min:sec
11	13	4.0	11:02
12	13	12.0	14:18

From Table 4.5 the importance of taking the initial moisture ratio into account is evident.

4.4 Plasterboard

In Figures 4.4a and 4.4b, the calculated temperature and density distributions are given at different times for a 13 mm plasterboard (calculation case number 14).

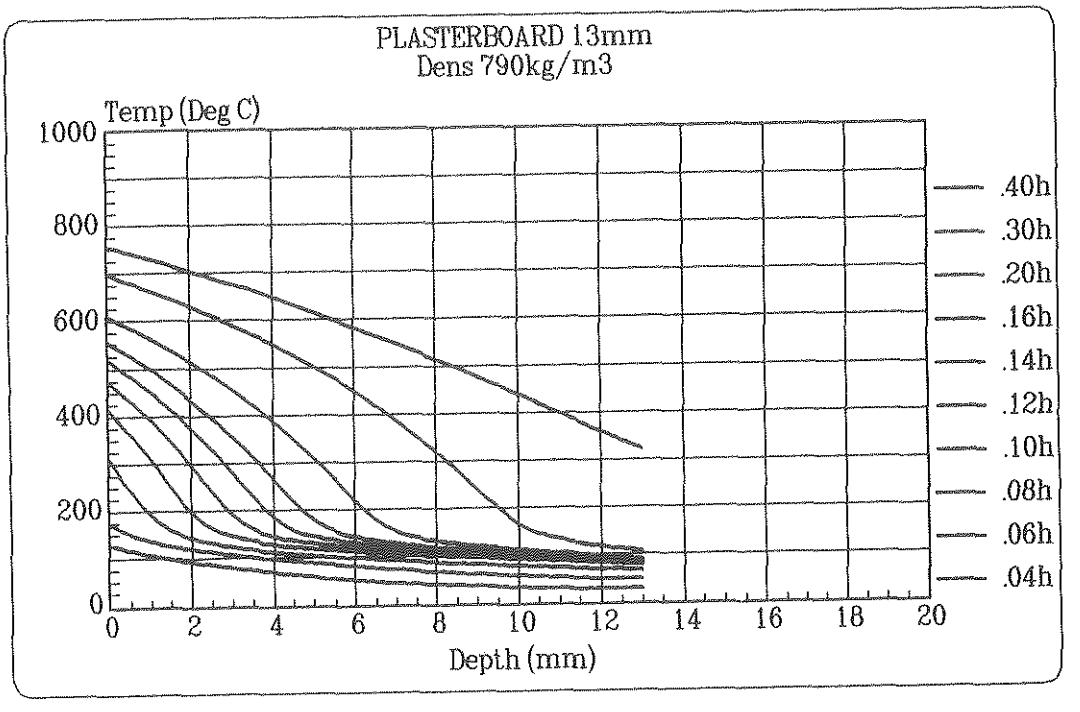

Figure 4.4a Calculation case number 14. Temperature distribution in a 13 mm plasterboard at different times. The density is 790 kgm^{-3}. Fire exposure according to ISO834.

Figure 4.4a gives the fire resistance. The temperature rise on the unexposed face exceeds 140°C after 19 min and 32 sec. Compared with the 13 mm wood boarding the fire resistance is approximately increased by 5 minutes. This is due to all the hydration water in the plasterboard that has to evaporate before the temperature rises above 100 °C.

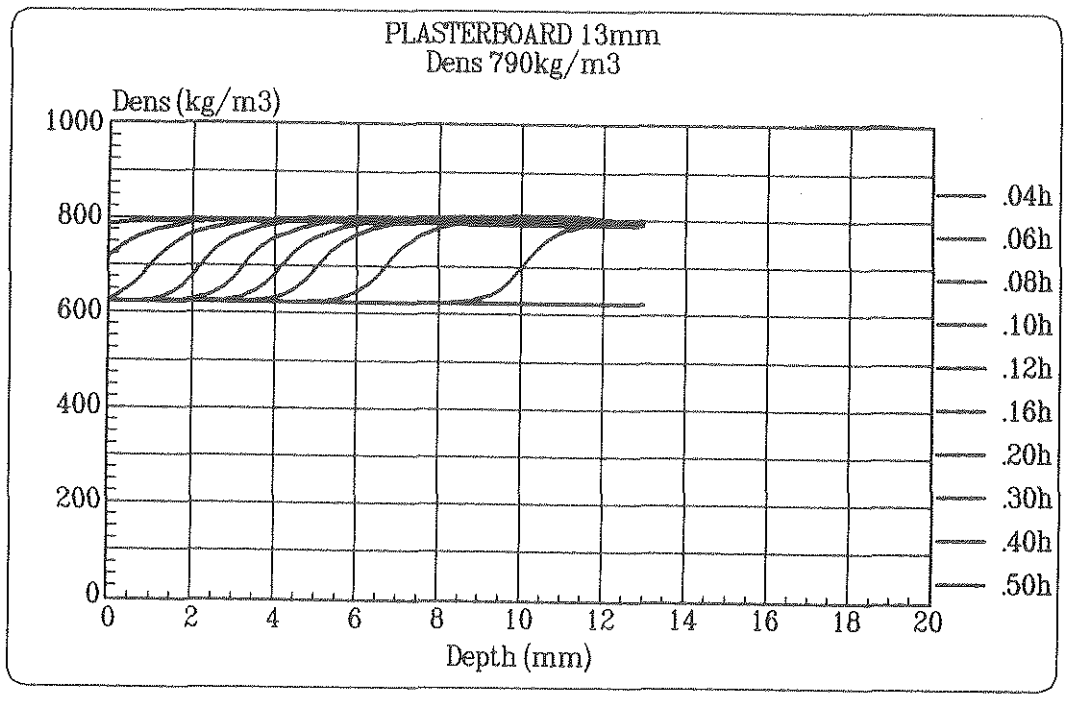

Figure 4.4b Calculation case number 14. Density distribution in a 13 mm plasterboard at different times. The original density is 790 kgm^{-3}. Including 21% hydration water. Fire exposure according to ISO834.

In Figure 4.4b the effect of calcination is summarised. From the relationship we can see when the material has been fully calcined. This is indicated by the density level 624.1 kgm^{-3}.

Figures on page 84 in the Appendix set out the complete set of calculation cases 13 and 14 for the plasterboard. The results from these calculations are summarised in Table 4.6.

Table 4.6 Calculated fire resistance of plasterboard, density 790 kgm^{-3}

Calculation case No	Thickness mm	Fire resistance min:sec
13	12	18:56
14	13	19:32

From Table 4.6 we can see the effect of the thickness of the plasterboard. Increasing the thickness by 1 mm from 12 mm gives an increased fire resistance of 36 seconds.

4.5 Wall constructions

In this subsection the description of the process in two wall constructions is given. The two calculation cases reported are number 19 with 19 mm chipboard and 25 mm mineral wool, and number 22 with 13 mm plasterboard and 25 mm mineral wool. The complete set of calculation cases 15 to 23 on wall constructions is given in the Appendix in Figures on pages 85 to 93.

In Figures 4.5a to 4.5c, the calculated temperature, density and moisture distributions are given at different times for a wall construction with 19 mm chipboard + 25 mm mineral wool + 19 mm chipboard (calculation case number 19).

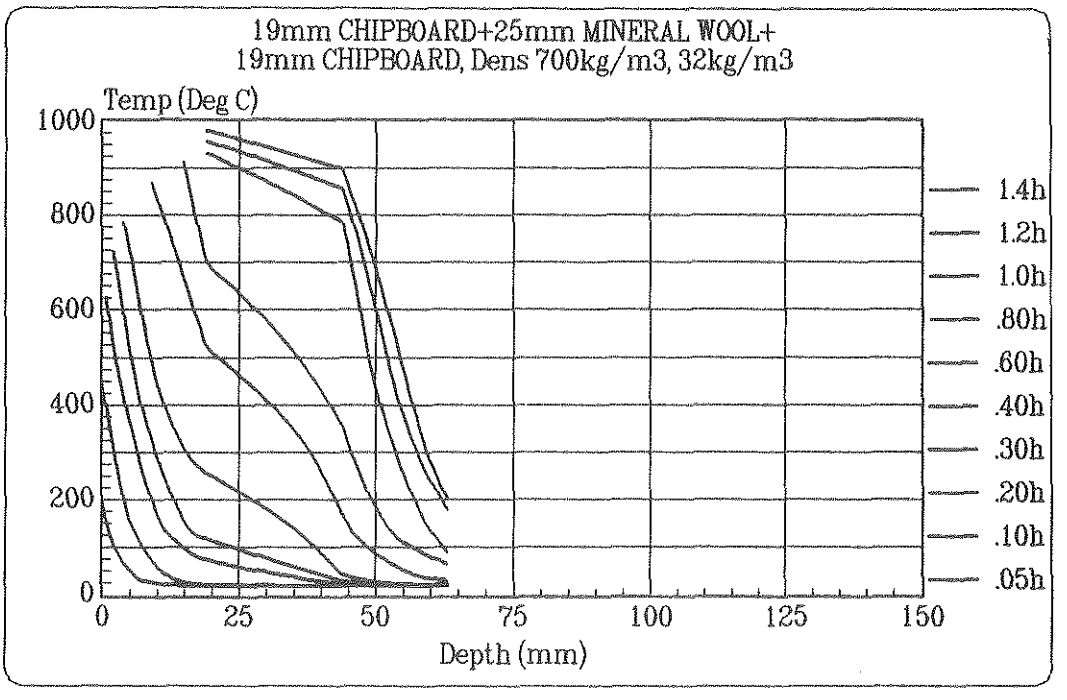

Figure 4.5a Calculation case number 19. Temperature distribution in a wall construction with 19 mm chipboard + 25 mm mineral wool + 19 mm chipboard at different times. The density of the chipboard is 700kgm^{-3} and the density of the mineral wool is 32 kgm^{-3}. The moisture ratio in the chipboard is 8.0%. Fire exposure according to ISO834.

Figure 4.5a gives the fire resistance for each material layer. The temperature rise behind each material exceeds 140 °C after 21 min and 5 sec (first chipboard), 35 min and 41 sec (second chipboard).

In Figure 4.5b the effect of pyrolysis on the density and the chipboard is summarised. From the relationship we can also see when the two chipboards have dried out. This is indicated by the density level 700 kgm^{-3}.

In the same way as in the previous subsections the charring zone can be determined from Figure 4.5b at the density level 560 kgm^{-3}.

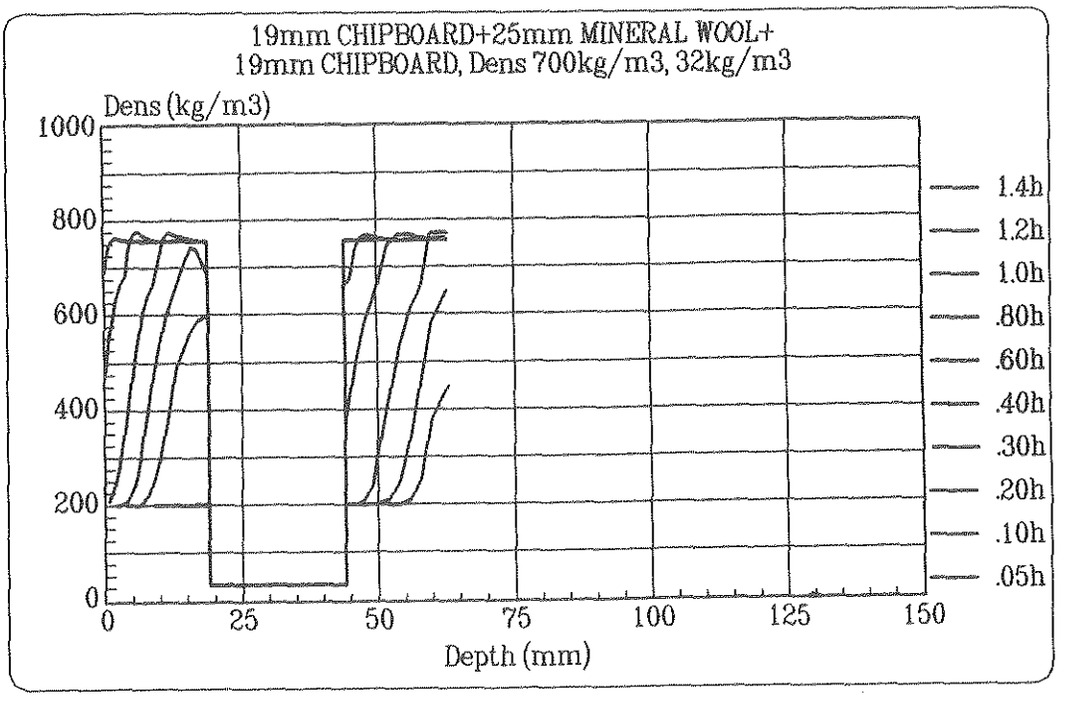

Figure 4.5b Calculation case number 19. Density distribution in a wall construction with 19 mm chipboard + 25 mm mineral wool + 19 mm chipboard at different times. The density of the chipboard is 700kgm^{-3} and the density of the mineral wool is 32 kgm^{-3}. The moisture ratio in the chipboard is 8.0%. Fire exposure according to ISO834.

In Figure 4.5c the drying process owing to pressure gradients is illustrated. In the calculations it is assumed that the total pressure in the insulation layer remains at atmospheric due to leaking through the boards.

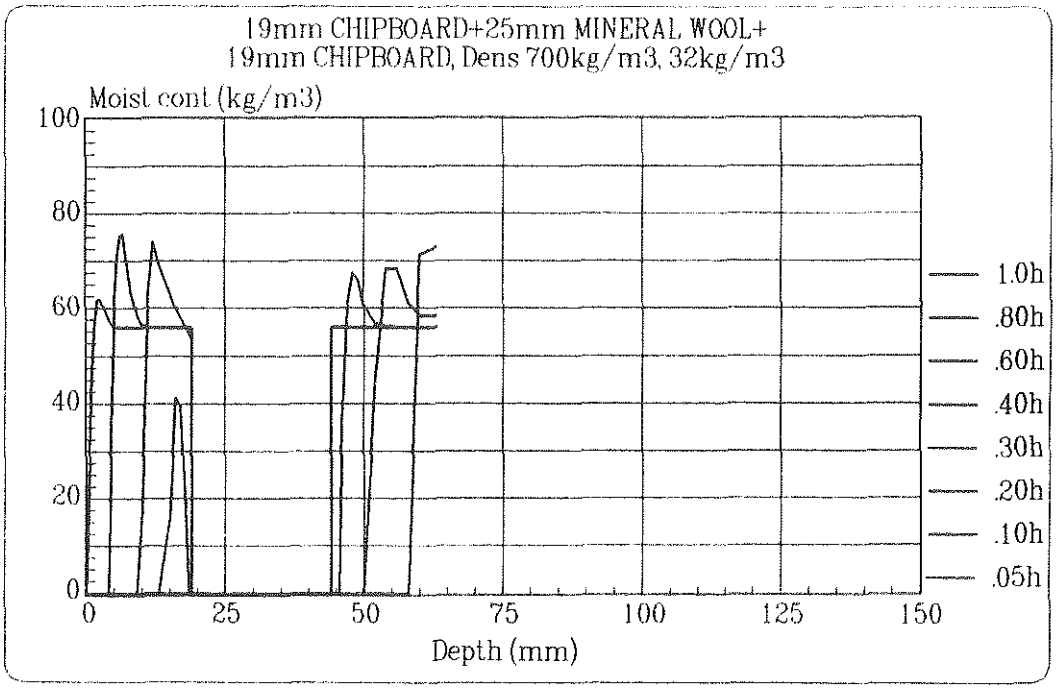

Figure 4.5c Calculation case number 19. Moisture distribution in a wall construction with 19 mm chipboard + 25 mm mineral wool + 19 mm chipboard at different times. The original dry density of the chipboard is 700kgm^{-3} and the density of the mineral wool is 32 kgm^{-3}. The initial moisture ratio in the chipboard is 8.0% and in the mineral wool 0.0%. Fire exposure according to ISO834.

In Figures 4.6a and 4.6b the calculated temperature and density distributions are given at different times for a wall construction with 13 mm plasterboard + 25 mm mineral wool + 13 mm plasterboard (calculation case number 22).

Figure 4.6a gives the fire resistance for each material layer. The temperature rise behind each material exceeds 140 °C after 18 min and 20 sec (first plasterboard), 24 min and 57 sec (mineral wool) and finally, 55 min and 55 sec (second plasterboard). In Figure 4.6a we can also determine the time for the loss of the first plasterboard, i.e. when the temperature criterion 550 °C at the rear face is satisfied. The loss time is 24 min.

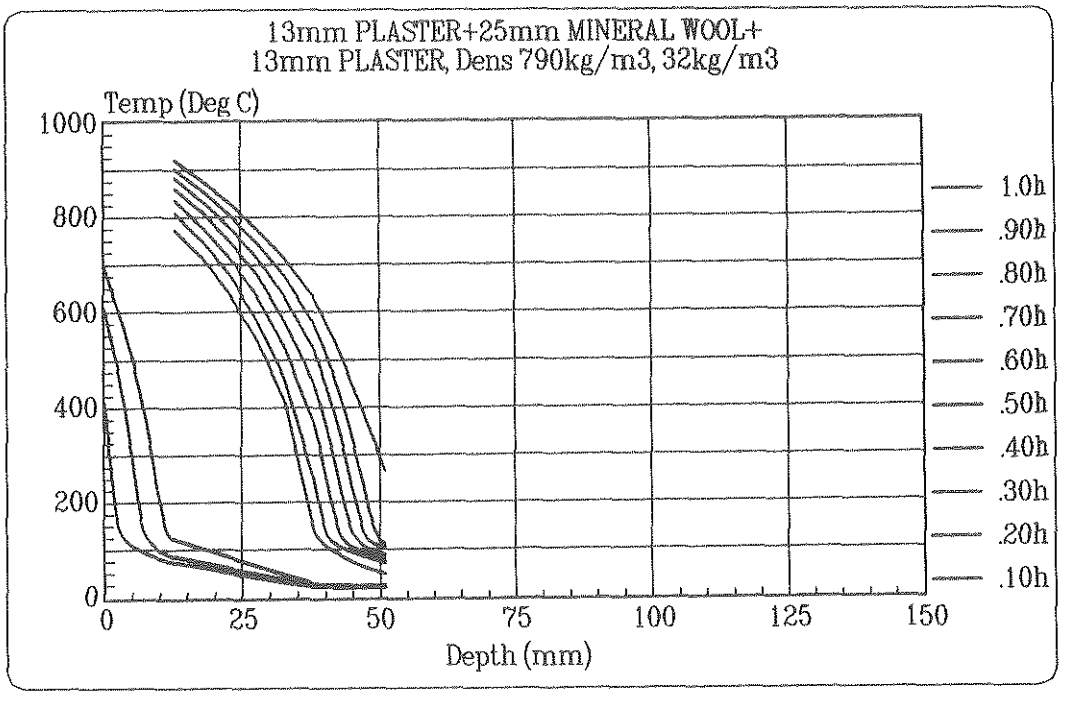

Figure 4.6a Calculation case number 22. Temperature distribution in a wall construction with 13 mm plasterboard + 25 mm mineral wool + 13 mm plasterboard at different times. The density of the plasterboard is 790 kgm^{-3} and the density of the mineral wool is 32 kgm^{-3}. Fire exposure according to ISO834.

In Figure 4.6b, the effect of calcination on the density of the plasterboard is summarised. From the relationship we can see the calcination depth at a given time. This is indicated by the density level 624.1 kgm^{-3}, i.e. the plasterboard density minus the 21% of hydration water.

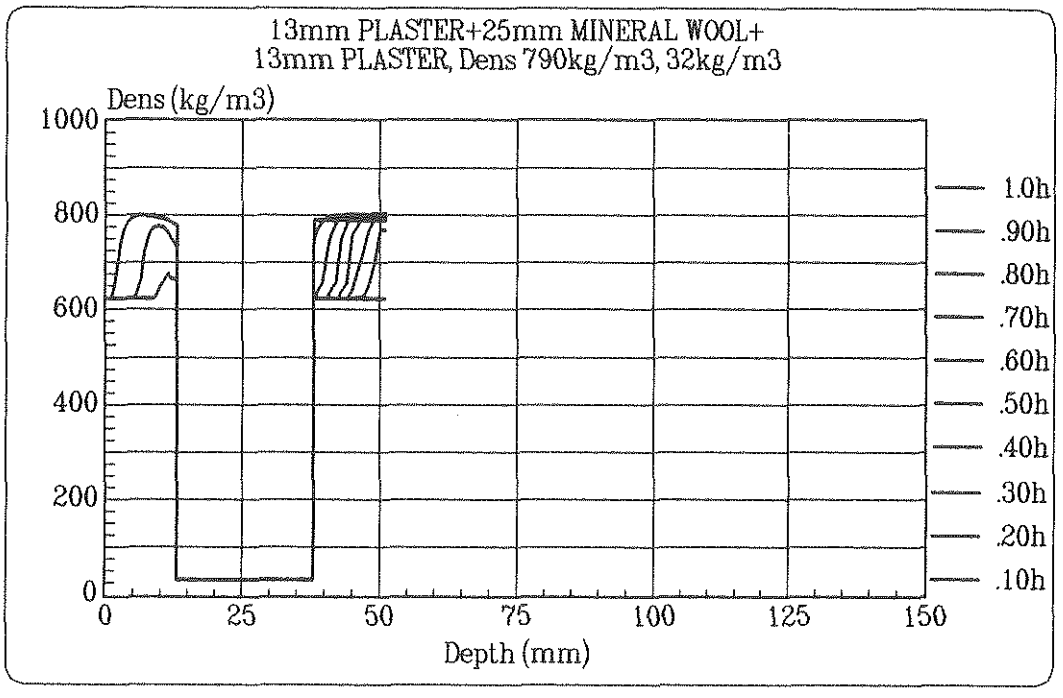

Figure 4.6b Calculation case number 22. Density distribution in a wall construction with 13 mm plasterboard + 25 mm mineral wool + 13 mm plasterboard at different times. The original density of the plasterboard is 790 kgm^{-3} including 21% hydration water and the density of the mineral wool is 32 kgm^{-3}: Fire exposure according to ISO834.

Figures on pages 85 to 93 in the Appendix set out the complete set of calculation cases 15 to 23 on wall constructions. The results from these calculations are summarised in Table 4.7.

Table 4.7 Calculated fire resistances of wall constructions

Calculation case	Material	Thickness mm	Density kgm^{-3}	Moisture content %	Fire resistance min:sec
15	Fibre board	9	800	8.0	9:07
	Glass wool	95	23	0.0	23:19
	Asphalt board	13	350	8.0	33:52
16	Chipboard	10	700	8.0	9:18
	Glass wool	70	17	0.0	24:50
	Chipboard	10	700	8.0	36:44
17	Chipboard	10	700	8.0	9:22
	Mineral wool	70	32	0.0	29:47
	Chipboard	10	700	8.0	50:45
18	Chipboard	12	700	8.0	11:24
	Mineral wool	100	32	0.0	39:00
	Chip board	12	700	8.0	71:43
19	Chipboard	19	700	8.0	21:05
	Mineral wool	25	32	0.0	35:25
	Chipboard	19	700	8.0	70:41
20	Chipboard	19	700	8.0	25:41
	Chipboard	19	700	8.0	53:02
	Mineral wool	25	32	0.0	68:08
	Chipboard	19	700	8.0	100:19
21	Chipboard	19	700	8.0	20:36
	Mineral wool	100	32	0.0	50:11
	Chipboard	19	700	8.0	105:45
22	Plasterboard	13	790	21.0	18:20
	Mineral wool	25	32	0.0	24:57
	Plasterboard	13	790	21.0	55:55
23	Plasterboard	13	790	21.0 *	18:20
	Mineral wool	45	32	0.0	31:48
	Plasterboard	13	790	21.0 *	74:40

* Hydration water included in the density of the plasterboard

From Table 4.7 we can see that the fire resistance for a material layer is influenced by the material layer behind it. As an example, compare the fire resistance of the 19 mm chipboard in case number 19 with the fire resistance of the first chipboard in case number 20. The fire resistance in case number 20 is increased by 4 min and 36 sec due to the change in material from mineral wool to chipboard. The temperature rise behind the chipboard in case number 19 is faster due to the material properties of the insulation. This implies that the total fire resistance of a wall construction cannot be determined by adding the individual fire resistance of a material layer determined from separate tests. The complete construction must be tested. An alternative method is described in the calculations.

4.6 Discussion of numerical results

The charring depth at a given time is determined from the Figures showing the density distributions. As seen from these relationships, the charring takes place as a gradual decrease of density from the original material to the final density of the charcoal. The determination of the charring rate demands a definition of a density level for the charring front.

In the calculations the final charcoal density of the building panels, with original density more than 500 kgm^{-3}, is put to 200 kgm^{-3} and for wood materials with original density less than 500 kgm^{-3} to 150 kgm^{-3}. When a visible charring starts, the density level is above the final charcoal density and below the original density.

In the calculations the beginning of the charring zone is defined as the point where the density is decreased by 20% of the original dry wood material. The data for the different materials are as follows

chipboard	($\rho_0 = 700$ kgm^{-3})	$\rho_{0.8} = 560$ kgm^{-3}
fibre board	($\rho_0 = 800$ kgm^{-3})	$\rho_{0.8} = 640$ kgm^{-3}
wood board	($\rho_0 = 500$ kgm^{-3})	$\rho_{0.8} = 400$ kgm^{-3}

These density levels are used in the calculation of the mean charring rate at 12 minutes fire exposure according to ISO834. The analysis is limited to the moisture ratio 8%. The influence of the insulation in the wall construction is not taken into consideration. In the case with wood panels, the calculations include only the moisture ratios 4 and 12%. The charring rate of a wood panel with 8% moisture ratio is approximated as the mean value of these two calculation cases.

Figure 4.7 sets out the determined charring rate of the three materials as a function of the original dry density.

The relationship in Figure 4.7 is somewhat improper because we have compared materials with the same moisture ratio 8%. But the different dry densities of the materials give different moisture content at the same moisture ratio. If the values of the wood panel with 12% moisture ratio is used instead, the comparison between the three materials is more accurate. The charring rate is then decreased from 0.63 to 0.56 mm per minute. The relationship in Figure 4.7 is then approximately linear.

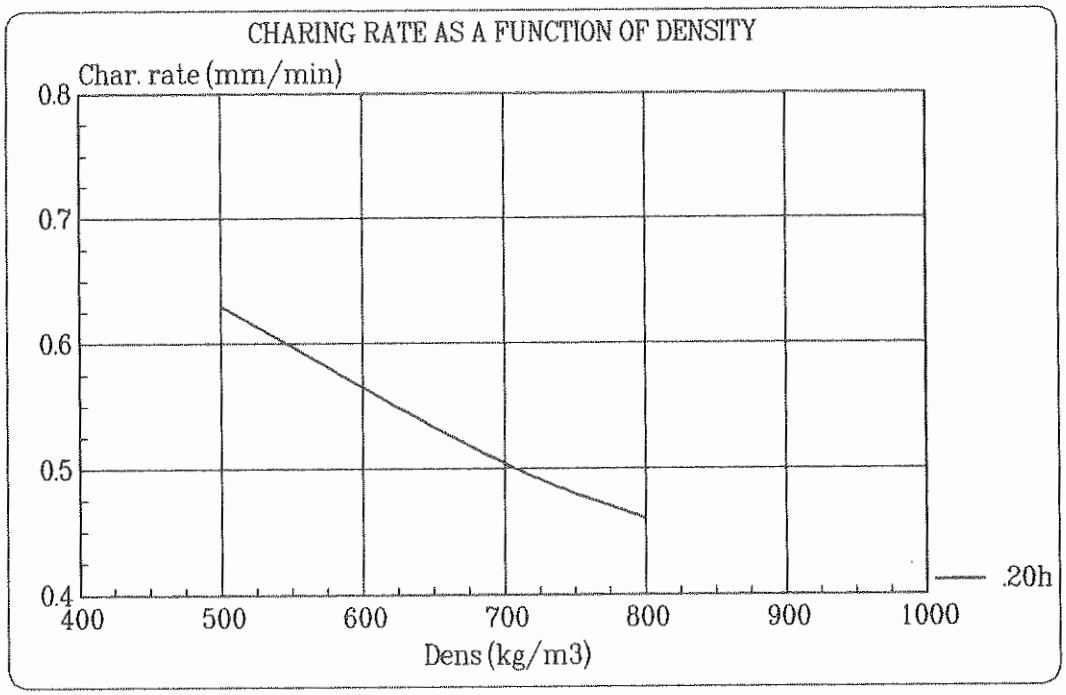

Figure 4.7 Charring rate as a function of original dry density

The influence of moisture ratio on the charring rate can be studied for the fibre board and chipboard in Figures 4.8 and 4.9 respectively.

As is clearly seen, the moisture ratio has a decisive influence on the charring rate. An insulation of the rear face influences the charring rate as well. The charring rate of the fibre board at 8% moisture ratio is increased from 0.46 mm min^{-1} to 0.58 mm min^{-1} when the rear face has an insulation.

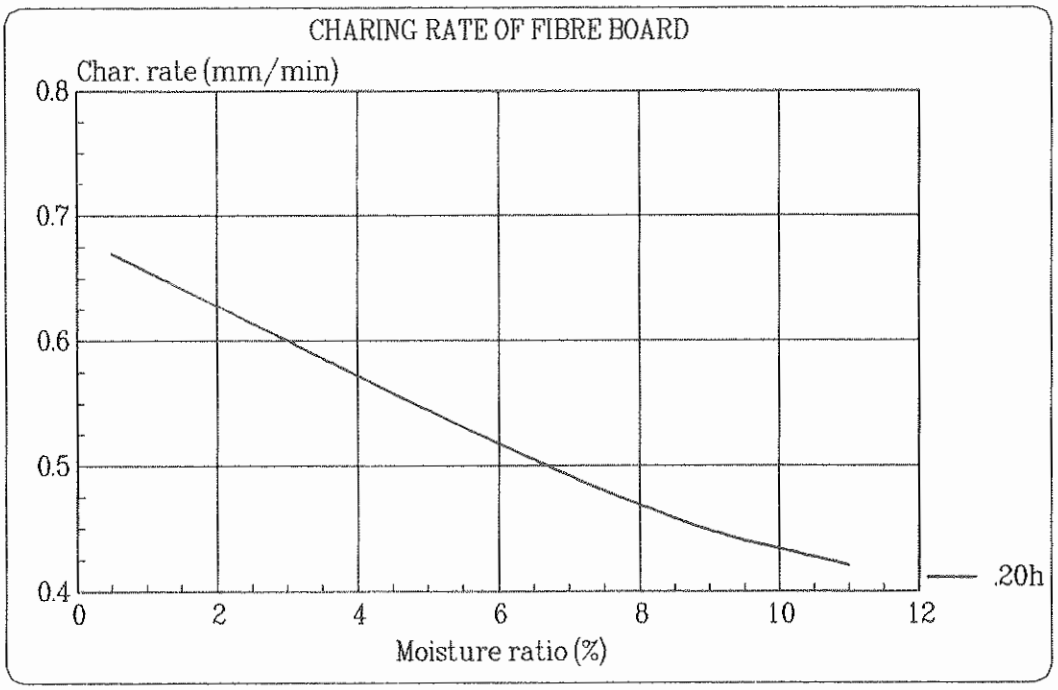

Figure 4.8 Charring rate of fibre board as a function of moisture ratio

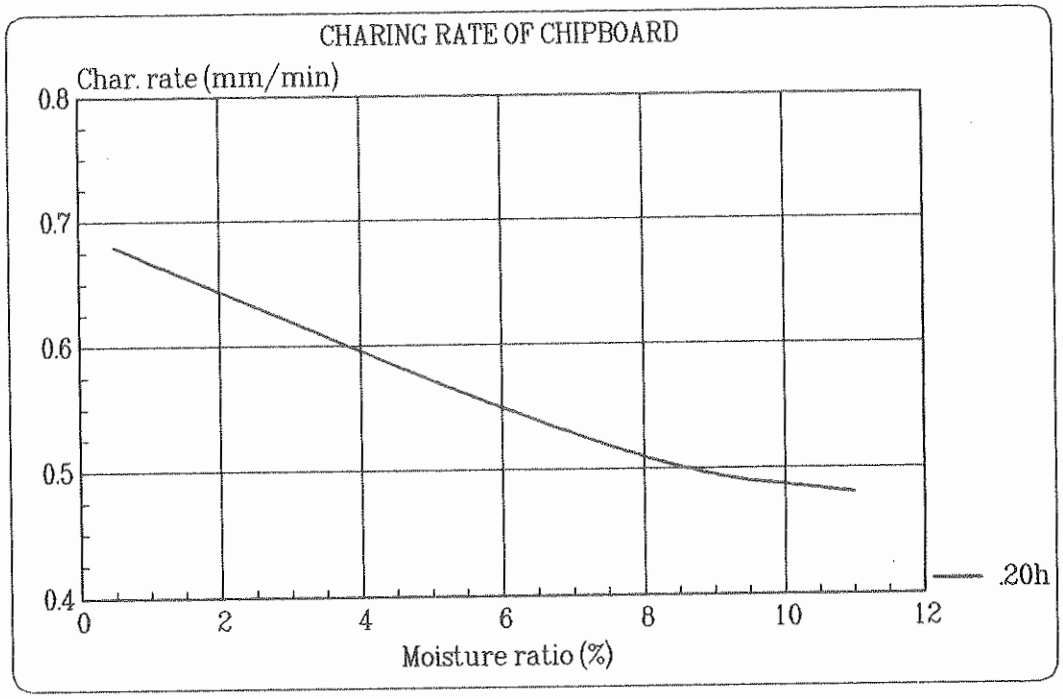

Figure 4.9 Charring rate of chipboard as a function of moisture ratio

5 COMPARISON OF CALCULATED AND MEASURED FIRE RESISTANCE

The comparison of calculated and measured fire resistance is based on an evaluation of the calculations described in Chapter 4, and experiments according to [2], [3], [12], [13] and [14]. The comparison is based on the performance requirement as set out in the internationally accepted test method ISO 834. This implies that the fire resistance is taken to be the time when the insulation requirement is no longer complied with, i.e. when the rise in temperature on the unexposed face exceeds 140 °C.

5.1 Measured fire resistance

The tests on the wood based boards have been carried out at the fire laboratory of the Swedish Institute for Wood Technology Research, Stockholm [2] and [3]. The results of tests on wall constructions are collected from several testing institutes and are summarised in [12], [13] and [14]. The test results refer to both small size and full size furnaces.

The tests on the boards [2] and [3] are performed in a small size furnace with the external size 620x525x600 mm.

The furnace consists of a steel box with the interior covered with insulating brick, type Porosil-G. The density of the brick is 850 kgm^{-3} and the thickness 70 mm. The internal surface of the furnace is covered with 3 mm thick fire resistant cement plaster. The furnace is heated with Calor gas and the regulation of oxygen and gas is operated manually in such a way that a thermal exposure according to ISO 834 is obtained.

The temperatures in the furnace and the test object are measured with thermocouples of type Cromel-Alumel.

The results from the small size furnace have been compared with test results from the full size furnace at the Fire Laboratory of National Swedish Testing Institute, Borås. The agreement between tests in small size and full size furnaces is shown to be good.

In Table 5.1 some of the results from tests in the small size furnace are summarised. The summary is based on tests reported in [2] and [3].

Table 5.1 sets out only the test result for the time when the insulation requirement T_{back}= 140 °C, is no longer complied with.

Table 5.1 Experimentally determined fire resistance of wood based boards. The fire resistance is taken to be the time when the insulation requirement T_{back}= 140 °C, is no longer complied with.

Material	Thickness mm	Density kgm^{-3}	Moisture ratio %	Fire resistance min:sec	Ref
Chipboard	12	725	8.1	16:02	[2]
Chipboard	12	720	8.1	14:45	[2]
Chipboard	19	705	8.3	24:57	[2]
Chipboard	19	705	8.3	26:30	[2]
Fibre board	9	780	0.4	8:18	[2]
Fibre board	9	780	0.4	8:51	[2]
Fibre board	9	810	8.4	11:51	[2]
Fibre board	9	810	8.4	11:21	[2]
Fibre board	9	790	10.7	12:39	[2]
Fibre board	9	800	10.7	13:01	[2]
Fibre board + insul	9	785	8.4	11:19	[2]
Fibre board + insul	9	785	8.4	10.43	[2]
Wood boarding	12.5	505	12.7	14:58	[3]
Wood boarding	12.5	560	13.2	13:57	[3]
Wood boarding	12.9	550	4.0	12:46	[3]
Wood boarding	12.9	505	3.8	12:01	[3]
Plasterboard	13	700	-	17:26	[2]
Plasterboard	13	700	-	18:27	[2]
Plasterboard	13	800		20:00	[14]

The tests on wall constructions are reported from both small size and full size furnaces. The results from tests are summarised in Table 5.2 and the size of the furnace used is indicated in the table. In cases where the temperature is measured between material layers, the fire resistance for each layer is given.

Table 5.2 Experimentally determined fire resistance of wall constructions. The fire resistance is taken to be the time when the insulation requirement T_{back}=140 °C is no longer complied with.

Material	Thick-ness mm	Density kgm^{-3}	Moisture ratio %	Furnace size	Fire resistance minutes	Ref
Fibre board	9	800	8.0			
Glass wool	95	22.5	0.0			
Asphalt board	13	350	8.0	F	35	[12]
Chipboard	10	700	8.0			
Glass wool	70	17	0.0			
Chipboard	10	700	8.0	F	37/20/31/24	[12]
Chipboard	10	700	8.0			
Mineral wool	70	32	0.0			
Chipboard	10	700	8.0	F	61/59/57/51	[12]
Chipboard	12	680	8.0			
Mineral wool	100	32	0.0			
Chip board	12	680	8.0	F	125	[13]
Chipboard	19	700	8.0	S	22	
Mineral wool	25	32	0.0	S	28	
Chipboard	19	700	8.0	S	66	[14]
Chipboard	19	700	8.0	S	26	
Chipboard	19	700	8.0	S	49	
Mineral wool	25	32	0.0	S	55	
Chipboard	19	700	8.0	S	92	[14]
Chipboard	19	700	8.0	S	21	
Mineral wool	100	32	0.0	S	40	
Chipboard	19	700	8.0	S	110	[14]
Chipboard	19	700	8.0	F	20	
Mineral wool	100	32	0.0	F	40	
Chipboard	19	700	8.0	F	100	[14]
Plasterboard	13	800	-	S	18	
Mineral wool	25	32	0.0	S	26	
Plasterboard	13	800	-	S	53	[14]
Plasterboard	13	800	-	S	19	
Mineral wool	45	32	0.0	S	27	
Plasterboard	13	800	-	S	59	[14]
Plasterboard	13	800	-	F	16	
Mineral wool	45	32	0.0	F	24	
Plasterboard	13	800	-	F	58	[14]

Notes to Table 5.2:

1 The density is in several cases very approximate
2 The moisture ratio is not explicitly given in the test reports but the 8% moisture ratio is normally a reasonable value indoors.
3 Furnace size: S = small size F = full size
4 Fire resistance: In two cases there are several tests on the same wall type. The test results are separated by slashes in the column.

As seen in Table 5.2 there is a considerable scatter in the test results of walls numbers two and three. The maximum difference for wall number two is 17 minutes and for wall number three 10 minutes. The scatter is not an exception in fire tests. In these cases the different fire resistances may be explained by the loss of the chipboard and some of the insulation in the wall.

5.2 Calculated and measured fire resistance

The calculated fire resistance is given in Tables 4.3 to 4.7 in Chapter 4. The calculated and measured fire resistance of wood based boards is summarised in Table 5.3 and Figure 5.1, and the fire resistance of wall constructions is given in Table 5.4 and Figure 5.2.

A comparison of the calculated fire resistance of boards and those measured in the tests shows very good agreement. The maximum difference between the tests and the calculations is only about 1 minute.

Table 5.3 Calculated and measured fire resistance of wood based boards

Calculation case No	Material	Thickness mm	Density kgm^{-3}	Moisture ratio %	Fire resistance calculated min:sec	measured min:sec
1	Chipboard	12	700	0.5	10:21	-
2	Chipboard	12	700	8.0	14:18	14:45/16:02
3	Chipboard	12	700	11.0	15:55	-
4	Chipboard*	12	700	8.0	11:24	-
5	Chipboard**	12	700	8.0	9:00	-
6	Chipboard	19	700	8.0	26:06	24:57/26:30
7	Fibre board	9	800	0.5	8:12	8:18/8:51
8	Fibre board	9	800	8.0	11:12	11:21/11:51
9	Fibre board	9	800	11.0	12:16	12:39/13:01
10	Fibre board***	9	800	8.0	9:48	11:19/10:43
11	Wood boarding	13	500	4.0	11:02	12:01/12:46
12	Wood boarding	13	500	13.0	14:18	13:57/14:58
13	Plasterboard	12	790	-	18:59	-
14	Plasterboard	13	790	-	19:32	17:26/18:27/20:00

* Fire compartment type A, opening factor 0.04 m$^{1/2}$, fire load 200 MJm^{-2}

** Fire compartment type A, opening factor 0.08 m$^{1/2}$, fire load 200 MJm^{-2}

*** With 100 mm mineral wool behind the fibre board, ρ=150 kgm^{-3}

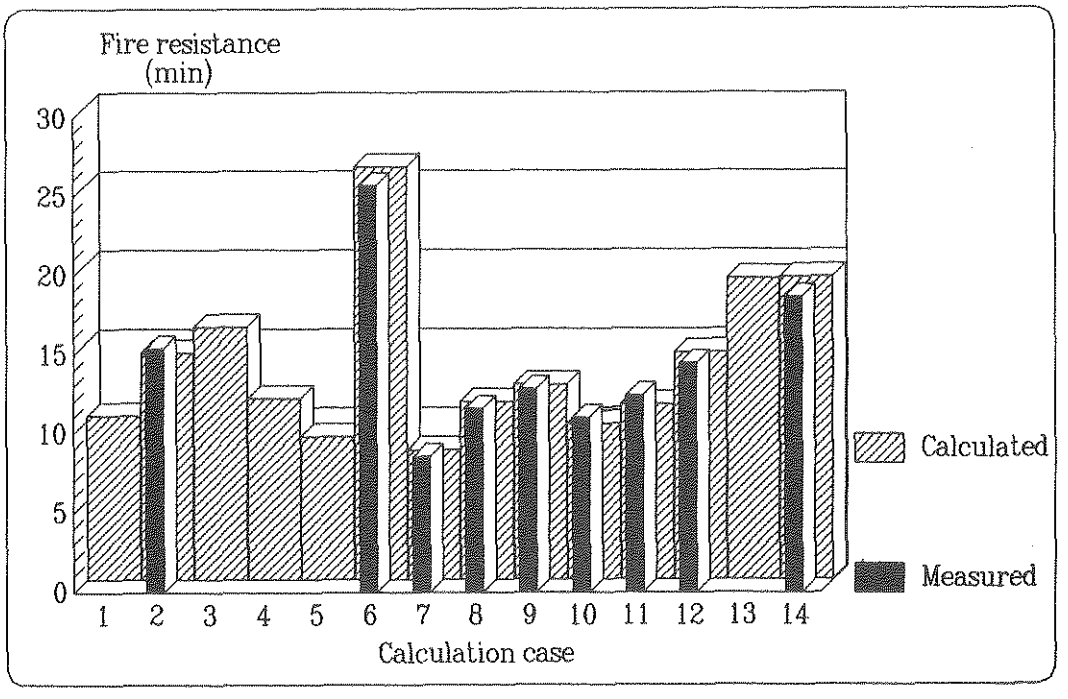

Figure 5.1 Comparison of calculated and measured fire resistance of wood based boards. In the figure the scatter from the tests is indicated. The calculation cases are numbered according to Table 5.3.

The differences between calculated and measured fire resistance are considerably larger than those for the boards. This is due to the greater difficulty in approximating the behaviour of a wall construction. We have phenomena such as the loss of the board and insulation as well as the influence of differences attributed to the manufacture of the wall. This is also reflected in the greater scatter in test results. A further complication is to measure accurately the surface temperatures of the different materials inside the wall construction.

However, the calculated fire resistances of the wall constructions in most cases give an acceptable agreement with experimentally determined fire resistances.

Table 5.4 Calculated and measured fire resistances of wall constructions

Calculation case No	Material	Thickness mm	Density kgm^{-3}	Moisture ratio %	Fire resistance calculated min	measured min
15	Fibre board	9	800	8.0	9	
	Glass wool	95	23	0.0	23	
	Asphalt board	13	350	8.0	34	35
16	Chipboard	10	700	8.0	9	
	Glass wool	70	17	0.0	25	
	Chipboard	10	700	8.0	37	37/20/31/24
17	Chipboard	10	700	8.0	9	
	Mineral wool	70	32	0.0	30	
	Chipboard	10	700	8.0	51	61/59/57/51
18	Chipboard	12	700	8.0	11	
	Mineral wool	100	32	0.0	39	
	Chipboard	12	700	8.0	72	125
19	Chipboard	19	700	8.0	21	22
	Mineral wool	25	32	0.0	35	28
	Chipboard	19	700	8.0	71	66
20	Chipboard	19	700	8.0	26	26
	Chipboard	19	700	8.0	53	49
	Mineral wool	25	32	0.0	68	55
	Chipboard	19	700	8.0	100	92
21	Chipboard	19	700	8.0	21	20/21
	Mineral wool	100	32	0.0	50	40/40
	Chipboard	19	700	8.0	106	100/110
22	Plasterboard	13	790	-	18	18
	Mineral wool	25	32	0.0	25	26
	Plasterboard	13	790	-	56	53
23	Plasterboard	13	790	-	18	16/19
	Mineral wool	45	32	0.0	32	24/27
	Plasterboard	13	790	-	75	58/59

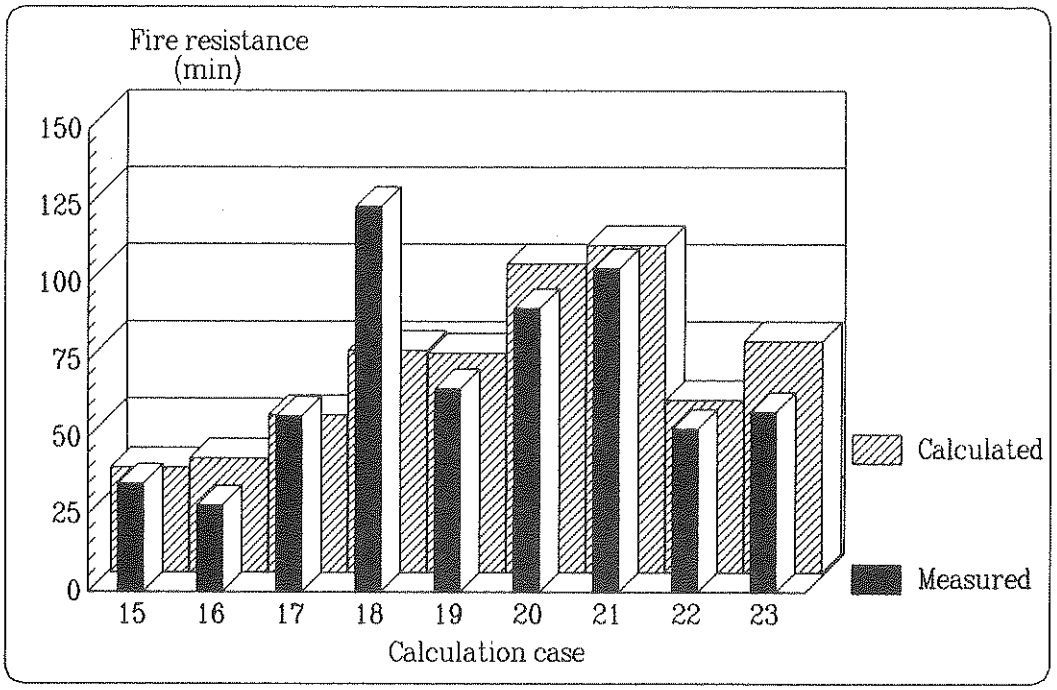

Figure 5.2 Comparison of calculated and measured fire resistances of wall constructions. The calculation cases are numbered according to Table 5.4.

The measured fire resistance of the wall corresponding to calculation case number 18 is extremely high, 125 minutes. This seems to be some misjudgement from the tests, especially as the test on wall number 21 with 19 mm chipboard only gives the fire resistance 100-110 minutes.

The calculations illustrate that the computer programme WOOD is well suited for generelisation of the test results.

6 SUMMARY

In an increasing number of countries, fire classification of elements of construction which is based on analytical treatment instead of the results of furnace tests in accordance with ISO 834 is beginning to be permitted. In Sweden, analytical fire engineering design of loadbearing and separating constructions as an alternative to design on the basis of standardised thermal action in accordance with ISO834 has been approved for a long time.

One fundamental prerequisite for analytical treatment of the design process is the development of an analytical model for the essential physical process in heated wood material. The model must be capable of treating transient temperature and moisture states in both uncharred and charred portions of the cross section, as well as the growth of the charred layer in combination with its oxidation at the surface due to variable thermal action. Material data for such a model must also be produced.

The calculations in this work are based on the model developed by the author and presented in [1]. Simulations have been made with the unidimensional computer program WOOD1. All the material data for description of the wood material have also been taken from [1].

Since the model demands a large quantity of material data which vary both with temperature and the density and moisture content of the material, it is obviously possible to modify the properties so that a satisfactory description of the physical processes is obtained. This is however a reprehensible procedure. All that this approach provides is a measure of how well the input data have been chosen. The following method for the choice of input data has therefore been decided on.

In the calculations which have been carried out, all material data have been taken from [1]. The input data which have been varied are the thickness, density, moisture content and thermal exposure of the material. These few and simple input data are of a type that are known in conjunction with a fire engineering design.

The results of all calculations are presented in diagrams in which the three different calculated quantites have been set out as a function of the distance from the surface exposed to fire at different times. The presentation comprises temperature profile, density distribution and moisture profile.

Assessment of the fire resistance of the board material is based on the same performance requirements as those set out in the internationally accepted test method, ISO 834, or its Swedish counterpart SIS 02 48 20. This implies for the calculations that the fire resistance is taken to be the time when the insulation requirement is no longer complied with, i.e. when the rise in temperature on the unexposed face exceeds 140 °C.

A comparison of the calculated fire resistances and those measured in the tests shows very good agreement. The maximum difference between the tests and the calculations is only about 1 minute for wood based boardes. For the wall constructions the maximum difference is larger but normally not more than 10 minutes.

7 REFERENCES

[1] FREDLUND, B., A model for heat and mass transfer in timber structures during fire. A theoretical, numerical and experimental study. Report LUTVDG/(TVBB-1003). Department of Fire Safety Engineering,Lund Institute of Science and Technology. Lund 1988.

[2] NORÉN, J., ÖSTMAN, B., Contribution to Fire Resistance from Building Panels. (in Swedish). Wood Technology. Report No.79. Swedish Institute for Wood Technology Research. Stockholm, March 1985.

[3] NORÉN, J., ÖSTMAN, B., Contribution to Fire Resistance from Wood Boarding. (in Swedish). Report I 8609054. Swedish Institute for Wood Technology Research. Stockholm, October 1986.

[4] CLAESSON, J., GAFFNER, D., Moisture in porous building materials. (in Swedish). Department of Mathematical Physics and Department of Building Science, Lund Institute of Science and Technology. Report BKL 1977:1. Lund, April 1977.

[5] CLAESSON, J., Fundamentals of moisture and energy flow in capillary-porous building materials. Department of Mathematical Physics, Lund Institute of Science and Technology, Sweden. Conference at the Dubrovnic's Institute for Heat and Mass Transfer 1977.

[6] MacLEAN, J.D., Thermal conductivity of wood. Transaction American Society of Heating and Ventilation 47, pp 323-354, 1941.

[7] MUNSON, T.R.and SPINDLER, R.J., Transient thermal behaviour of decomposing materials. Part I. General Theory and Application to Convective Heating, presented at the 30th Institute of Aerospace Science Annual Meeting, New York, June 1962.

[8] CHAN, W-C.,R., Analysis of chemical and physical processes during the pyrolysis of large biomass pellets. University of Washington, 1983.

[9] ANDERSSON, L. and JANSSON, B., Investigation of thermal properties of plasterboard - Theory and experiments. (in Swedish).Report LUTVDG/ (TVBB-5001). Department of Fire Safety Engineering,Lund Institute of Science and Technology. Lund 1986.

[10] LANGES HANDBOOK OF CHEMISTRY, Twelfth Edition. McGraw-Hill Book Company, New York, 1979.

[11] KRONVALL, J., Air flows in building components. Report TVBH-1002. Division of Building Technology, Lund Institute of Science and Technology. Lund 1980.

[12] NORÉN, J., Fire resistance of wood constructions. - A summary of test results. (in Swedish). Report P8611070. Swedish Institute for Wood Technology Research. Stockholm 1986.

[13] Calculation method for the fire resistance of non-loadbearing stud walls with boards. TR-Project 133/612-79.195 and TR-Project 133/361-79.210, UDK 69.022.5:614.84. Dansk Brandværns-Komité. Dantest, Dansk Institut for Prøvning og justering. Instituttet for Husbygning, DTH. Rockwool. Denmark, 1984.

[14] Calculation method for the fire resistance of non-loadbearing stud walls with boards. Part 3. UDK 69.022.5:614.84. Dansk Brandværns-Komité. Dantest, Dansk Institut for Prøvning og justering. Instituttet for Husbygning DTH. Nordisk Gipspladeforening, Rockwool, Træbranchens Oplysningsråd. Denmark, 1984.

APPENDIX

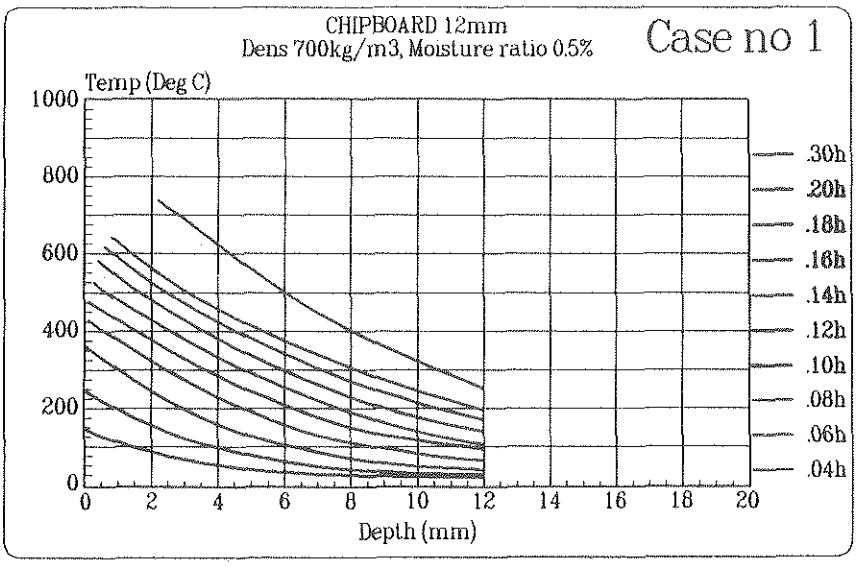
CHIPBOARD 12mm
Dens 700kg/m3, Moisture ratio 0.5%
Case no 1
Temp (Deg C)
1000
800
600
400
200
0
0 2 4 6 8 10 12 14 16 18 20
Depth (mm)
.30h
.20h
.18h
.16h
.14h
.12h
.10h
.08h
.06h
.04h

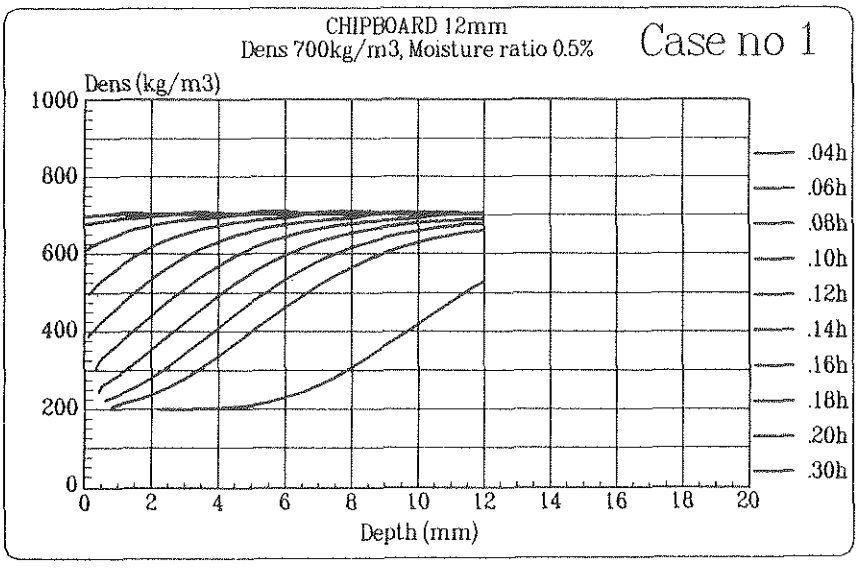
CHIPBOARD 12mm
Dens 700kg/m3, Moisture ratio 0.5%
Case no 1
Dens (kg/m3)
1000
800
600
400
200
0
0 2 4 6 8 10 12 14 16 18 20
Depth (mm)
.04h
.06h
.08h
.10h
.12h
.14h
.16h
.18h
.20h
.30h

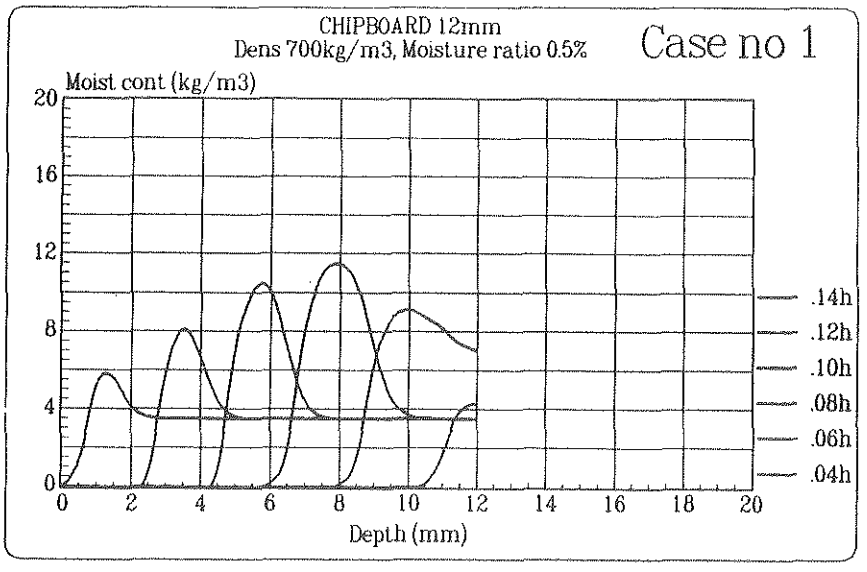
CHIPBOARD 12mm
Dens 700kg/m3, Moisture ratio 0.5%
Case no 1
Moist cont (kg/m3)
20
16
12
8
4
0
0 2 4 6 8 10 12 14 16 18 20
Depth (mm)
.14h
.12h
.10h
.08h
.06h
.04h

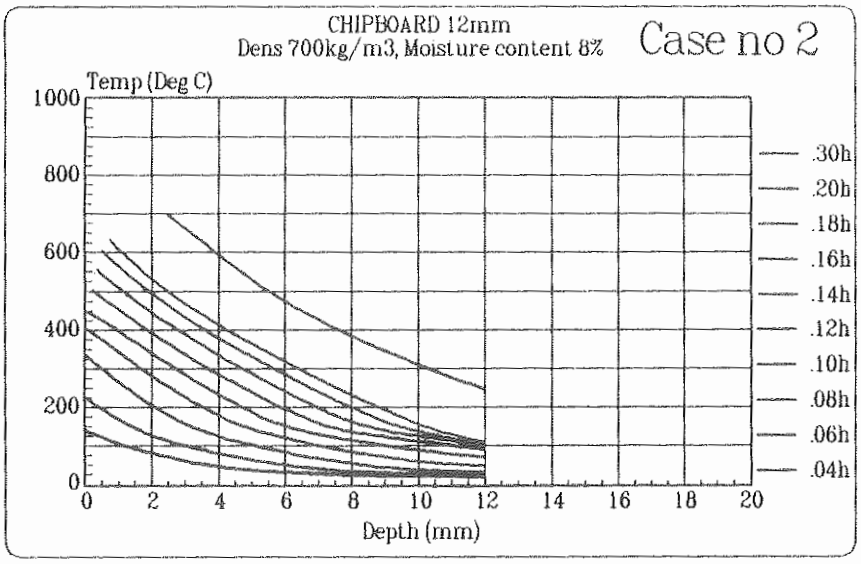
CHIPBOARD 12mm
Dens 700kg/m3, Moisture content 8%
Case no 2
Temp (Deg C)
1000
800
600
400
200
0
0 2 4 6 8 10 12 14 16 18 20
Depth (mm)
.30h
.20h
.18h
.16h
.14h
.12h
.10h
.08h
.06h
.04h

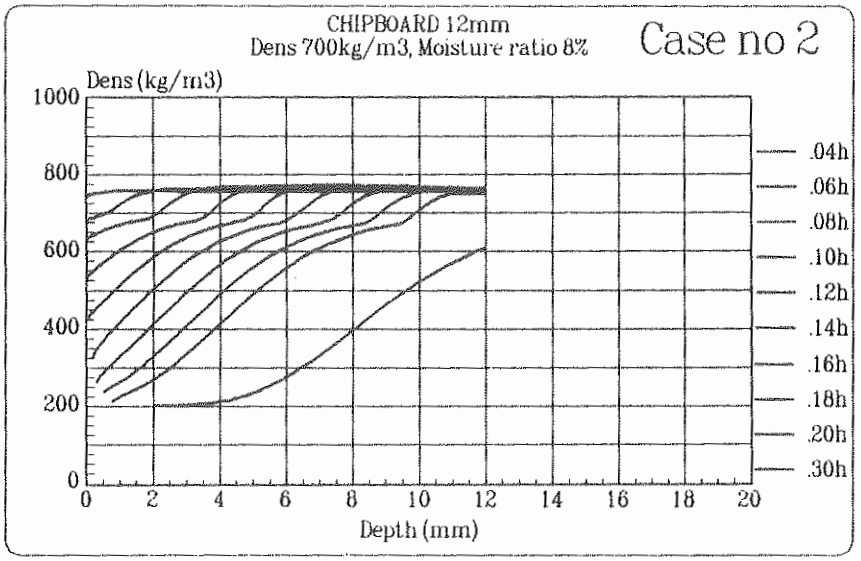
CHIPBOARD 12mm
Dens 700kg/m3, Moisture ratio 8%
Case no 2
Dens (kg/m3)
1000
800
600
400
200
0
0 2 4 6 8 10 12 14 16 18 20
Depth (mm)
.04h
.06h
.08h
.10h
.12h
.14h
.16h
.18h
.20h
.30h

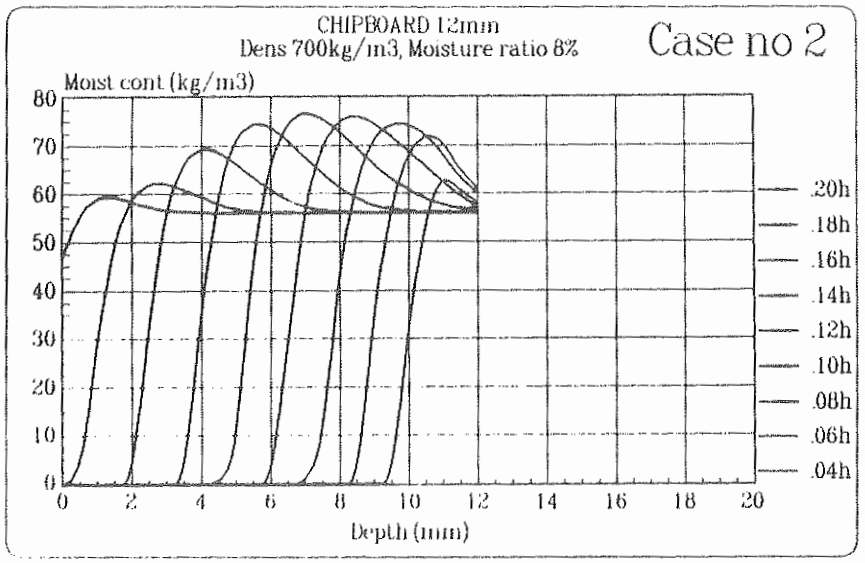
CHIPBOARD 12mm
Dens 700kg/m3, Moisture ratio 8%
Case no 2
Moist cont (kg/m3)
80
70
60
50
40
30
20
10
0
0 2 4 6 8 10 12 14 16 18 20
Depth (mm)
.20h
.18h
.16h
.14h
.12h
.10h
.08h
.06h
.04h

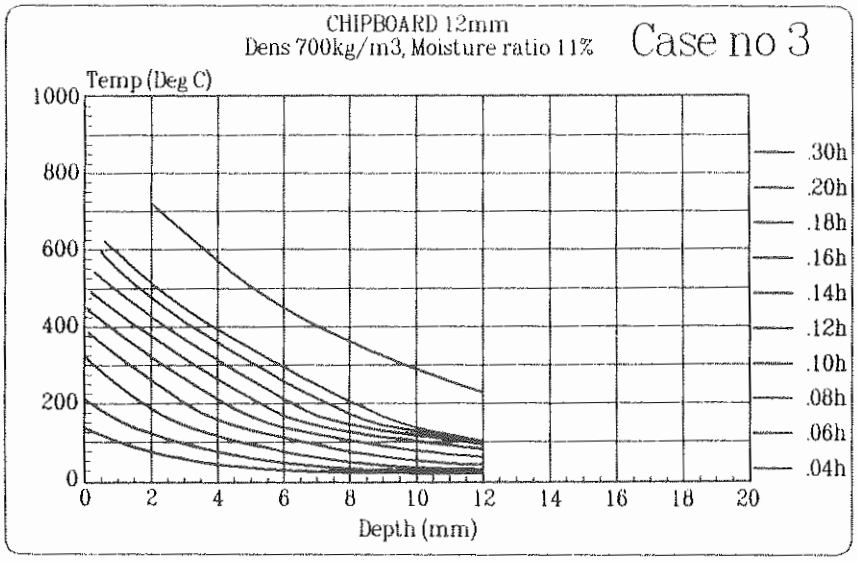
CHIPBOARD 12mm
Dens 700kg/m3, Moisture ratio 11%
Case no 3
Temp (Deg C)
1000
800
600
400
200
0
0 2 4 6 8 10 12 14 16 18 20
Depth (mm)
.30h
.20h
.18h
.16h
.14h
.12h
.10h
.08h
.06h
.04h

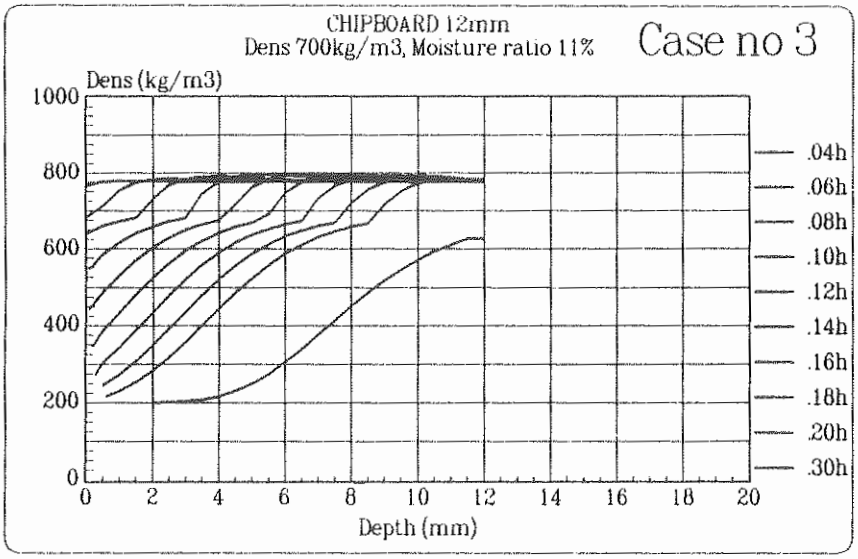
CHIPBOARD 12mm
Dens 700kg/m3, Moisture ratio 11%
Case no 3
Dens (kg/m3)
1000
800
600
400
200
0
0 2 4 6 8 10 12 14 16 18 20
Depth (mm)
.04h
.06h
.08h
.10h
.12h
.14h
.16h
.18h
.20h
.30h

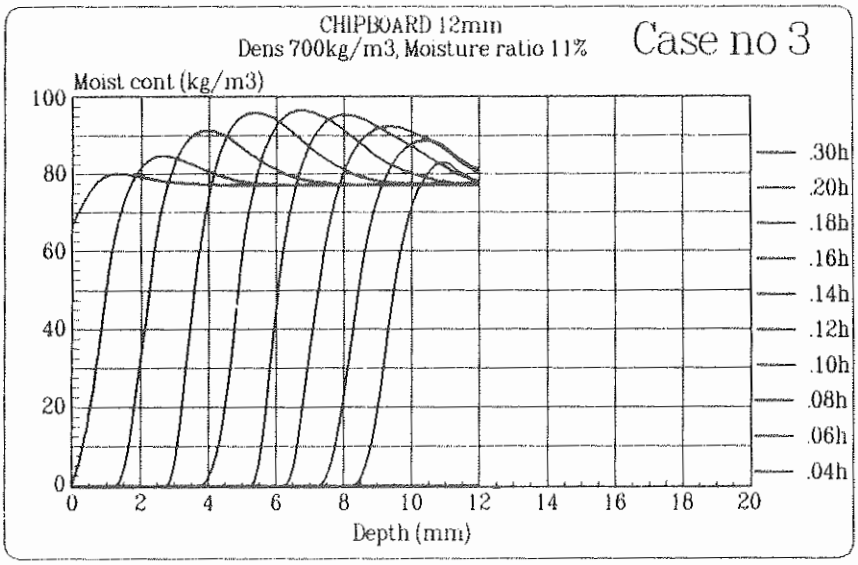
CHIPBOARD 12mm
Dens 700kg/m3, Moisture ratio 11%
Case no 3
Moist cont (kg/m3)
100
80
60
40
20
0
0 2 4 6 8 10 12 14 16 18 20
Depth (mm)
.30h
.20h
.18h
.16h
.14h
.12h
.10h
.08h
.06h
.04h

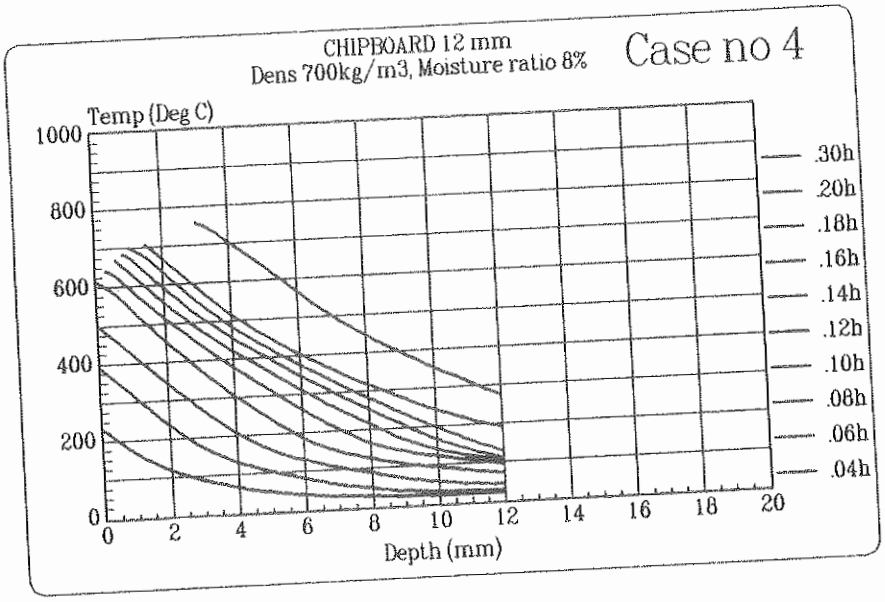
CHIPBOARD 12 mm
Dens 700kg/m3, Moisture ratio 8%
Case no 4
Temp (Deg C)
1000
800
600
400
200
0
0 2 4 6 8 10 12 14 16 18 20
Depth (mm)
.30h
.20h
.18h
.16h
.14h
.12h
.10h
.08h
.06h
.04h

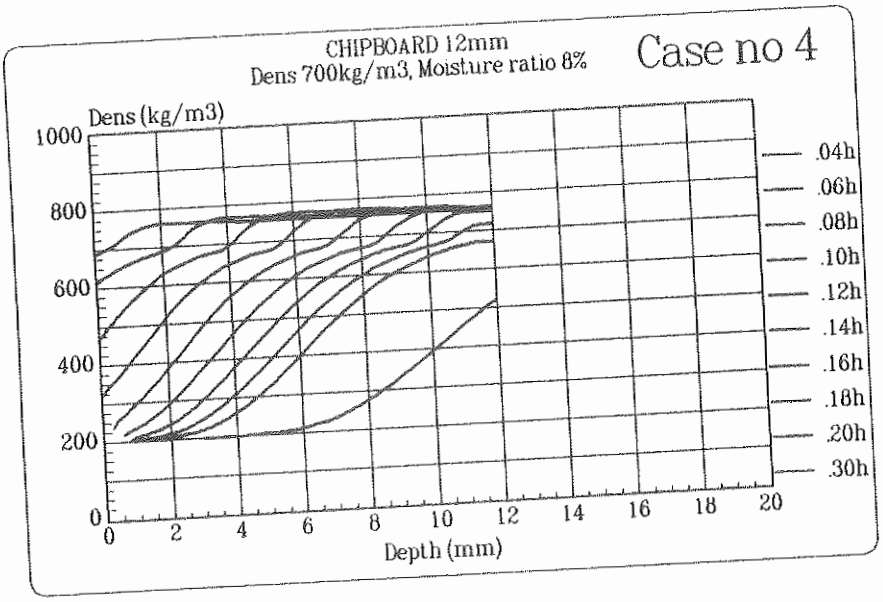
CHIPBOARD 12mm
Dens 700kg/m3, Moisture ratio 8%
Case no 4
Dens (kg/m3)
1000
800
600
400
200
0
0 2 4 6 8 10 12 14 16 18 20
Depth (mm)
.04h
.06h
.08h
.10h
.12h
.14h
.16h
.18h
.20h
.30h

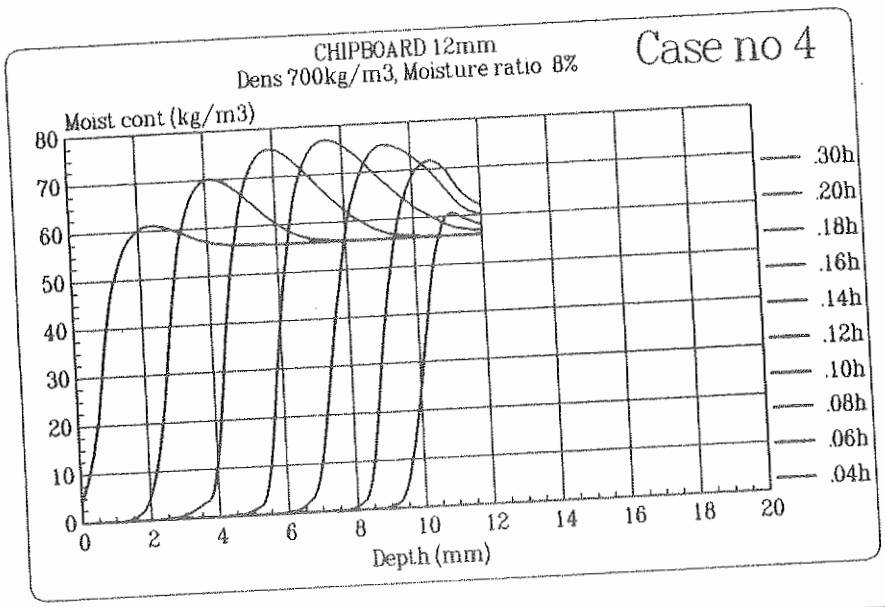
CHIPBOARD 12mm
Dens 700kg/m3, Moisture ratio 8%
Case no 4
Moist cont (kg/m3)
80
70
60
50
40
30
20
10
0
0 2 4 6 8 10 12 14 16 18 20
Depth (mm)
.30h
.20h
.18h
.16h
.14h
.12h
.10h
.08h
.06h
.04h

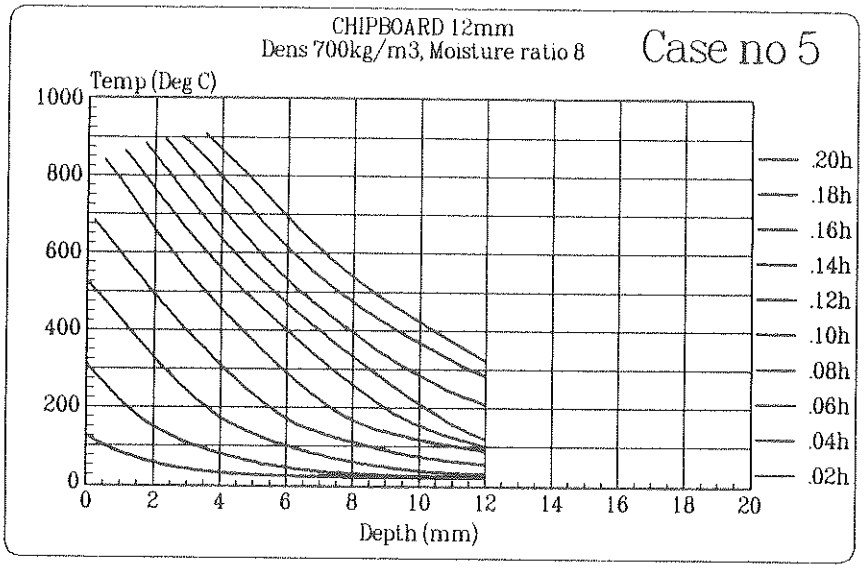
CHIPBOARD 12mm
Dens 700kg/m3, Moisture ratio 8
Case no 5
Temp (Deg C)
1000
800
600
400
200
0
0 2 4 6 8 10 12 14 16 18 20
Depth (mm)
.20h
.18h
.16h
.14h
.12h
.10h
.08h
.06h
.04h
.02h

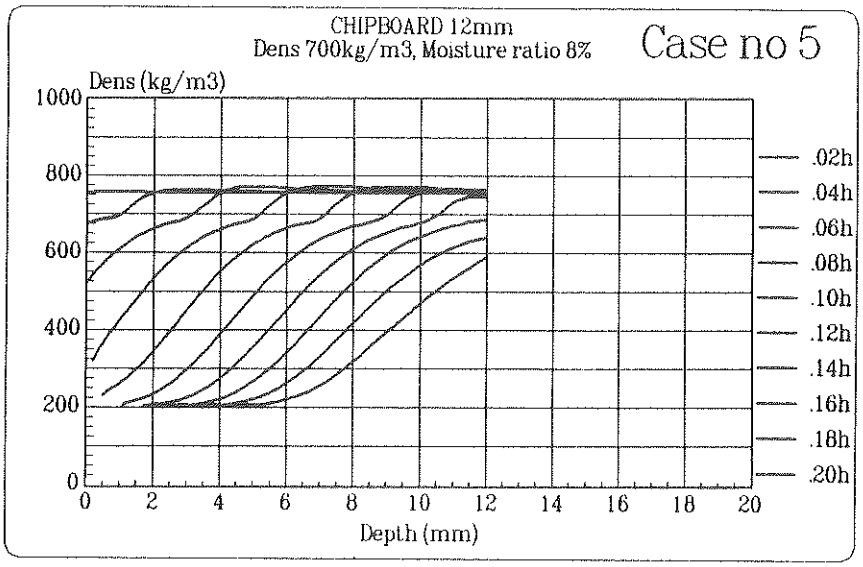
CHIPBOARD 12mm
Dens 700kg/m3, Moisture ratio 8%
Case no 5
Dens (kg/m3)
1000
800
600
400
200
0
0 2 4 6 8 10 12 14 16 18 20
Depth (mm)
.02h
.04h
.06h
.08h
.10h
.12h
.14h
.16h
.18h
.20h

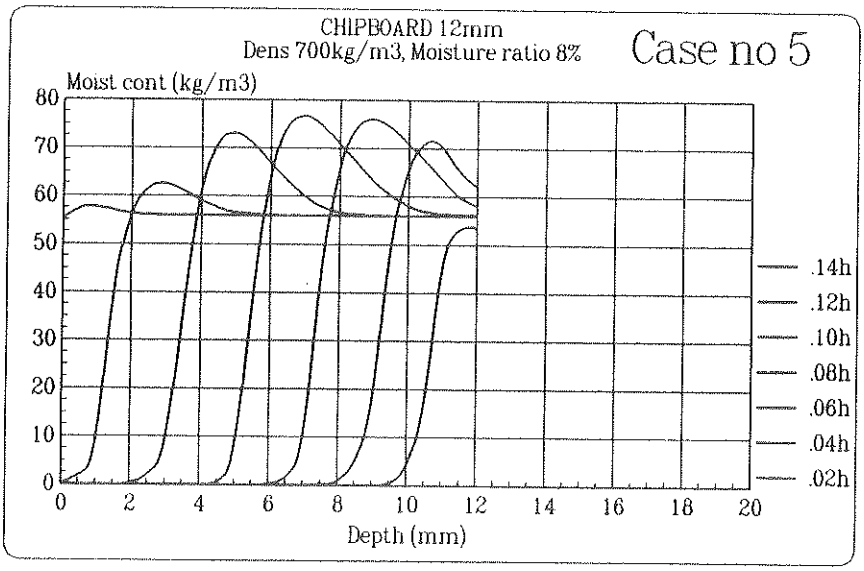
CHIPBOARD 12mm
Dens 700kg/m3, Moisture ratio 8%
Case no 5
Moist cont (kg/m3)
80
70
60
50
40
30
20
10
0
0 2 4 6 8 10 12 14 16 18 20
Depth (mm)
.14h
.12h
.10h
.08h
.06h
.04h
.02h

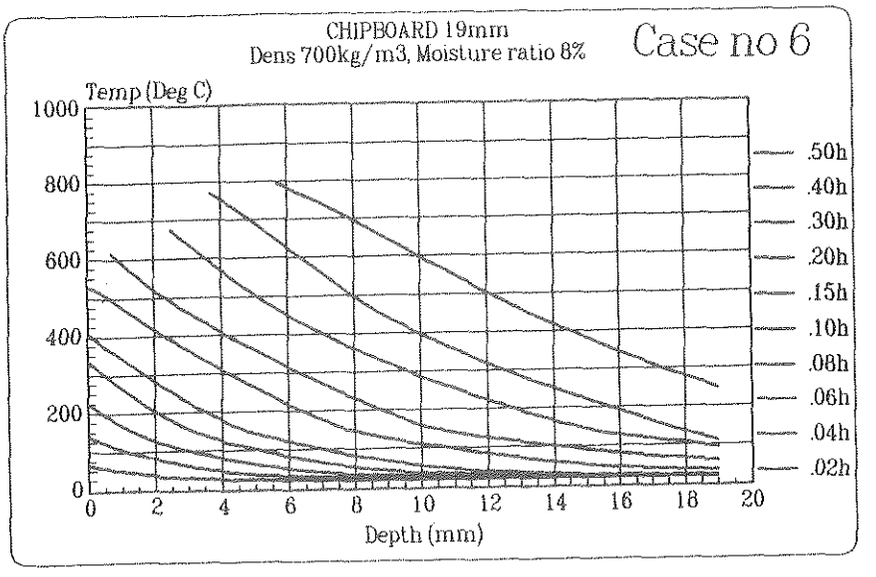
CHIPBOARD 19mm
Dens 700kg/m3, Moisture ratio 8%
Case no 6
Temp (Deg C)
1000
800
600
400
200
0
0 2 4 6 8 10 12 14 16 18 20
Depth (mm)
.50h
.40h
.30h
.20h
.15h
.10h
.08h
.06h
.04h
.02h

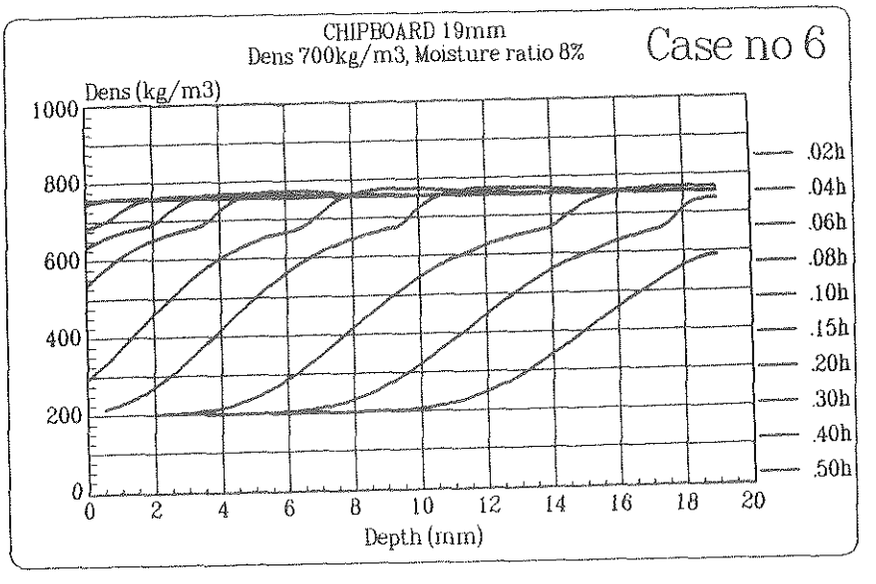
CHIPBOARD 19mm
Dens 700kg/m3, Moisture ratio 8%
Case no 6
Dens (kg/m3)
1000
800
600
400
200
0
0 2 4 6 8 10 12 14 16 18 20
Depth (mm)
.02h
.04h
.06h
.08h
.10h
.15h
.20h
.30h
.40h
.50h

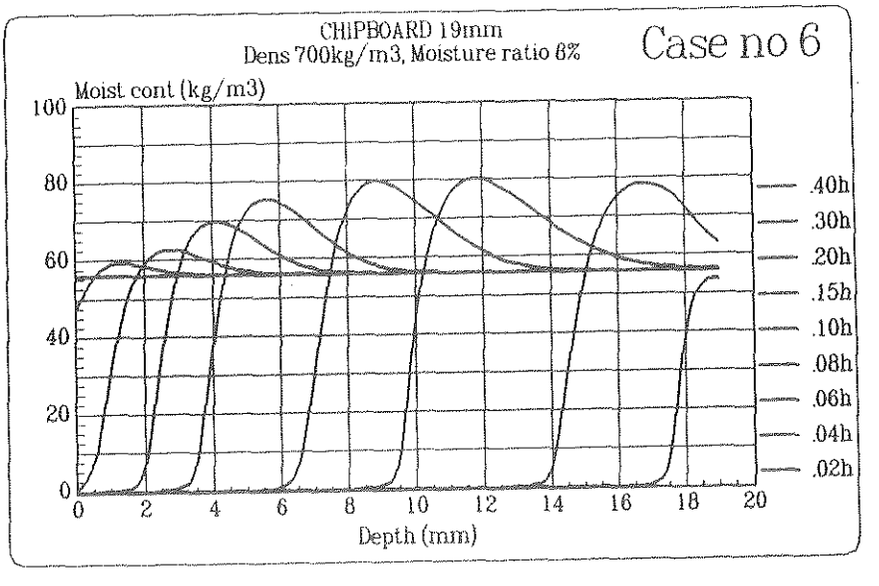
CHIPBOARD 19mm
Dens 700kg/m3, Moisture ratio 8%
Case no 6
Moist cont (kg/m3)
100
80
60
40
20
0
0 2 4 6 8 10 12 14 16 18 20
Depth (mm)
.40h
.30h
.20h
.15h
.10h
.08h
.06h
.04h
.02h

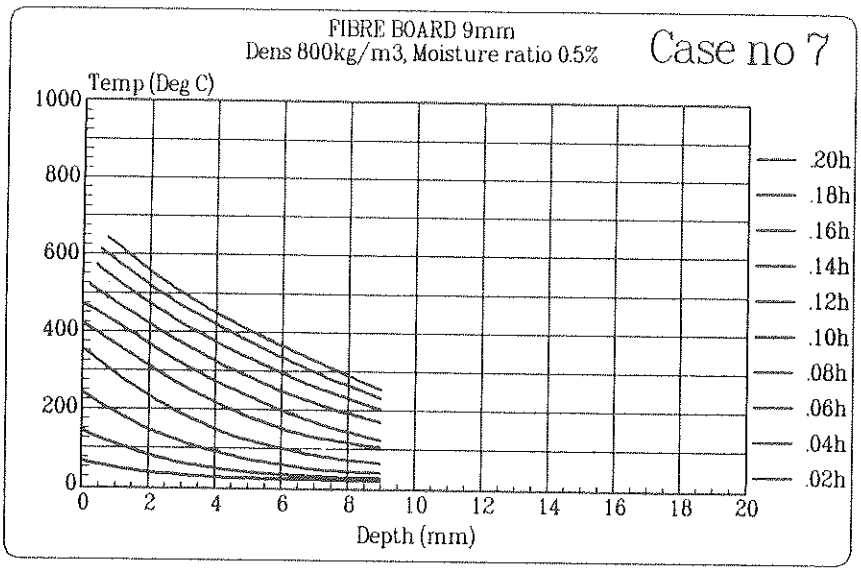
FIBRE BOARD 9mm
Dens 800kg/m3, Moisture ratio 0.5%
Case no 7
Temp (Deg C)
1000
800
600
400
200
0
0 2 4 6 8 10 12 14 16 18 20
Depth (mm)
.20h
.18h
.16h
.14h
.12h
.10h
.08h
.06h
.04h
.02h

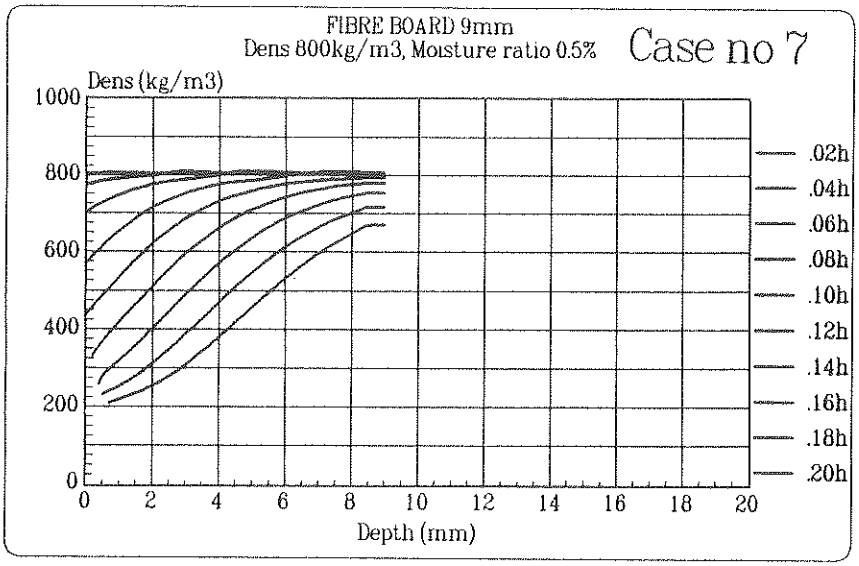
FIBRE BOARD 9mm
Dens 800kg/m3, Moisture ratio 0.5%
Case no 7
Dens (kg/m3)
1000
800
600
400
200
0
0 2 4 6 8 10 12 14 16 18 20
Depth (mm)
.02h
.04h
.06h
.08h
.10h
.12h
.14h
.16h
.18h
.20h

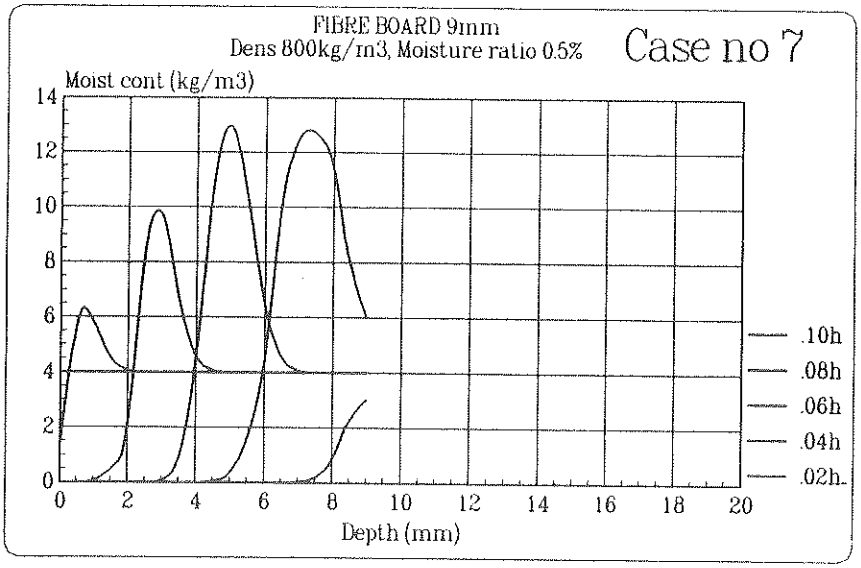
FIBRE BOARD 9mm
Dens 800kg/m3, Moisture ratio 0.5%
Case no 7
Moist cont (kg/m3)
14
12
10
8
6
4
2
0
0 2 4 6 8 10 12 14 16 18 20
Depth (mm)
.10h
.08h
.06h
.04h
.02h

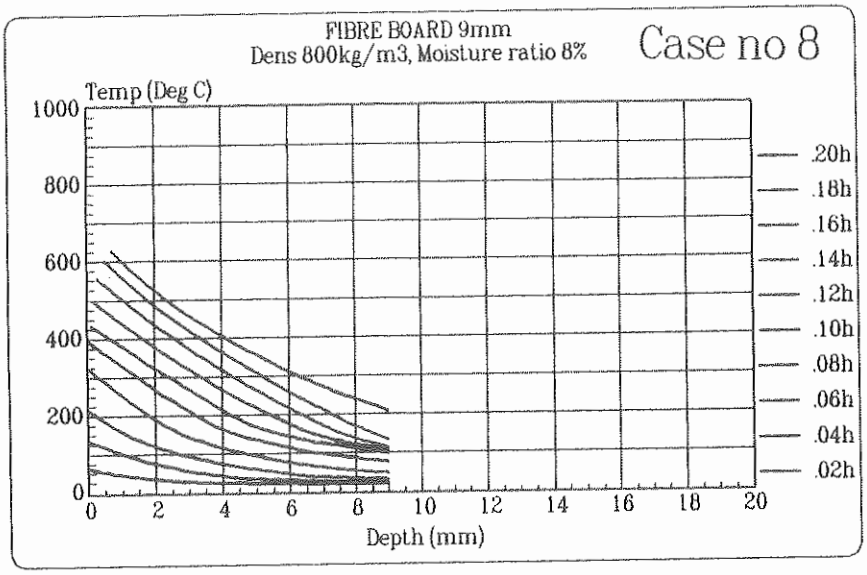
FIBRE BOARD 9mm
Dens 800kg/m3, Moisture ratio 8%
Case no 8
Temp (Deg C)
1000
800
600
400
200
0
0 2 4 6 8 10 12 14 16 18 20
Depth (mm)
.20h
.18h
.16h
.14h
.12h
.10h
.08h
.06h
.04h
.02h

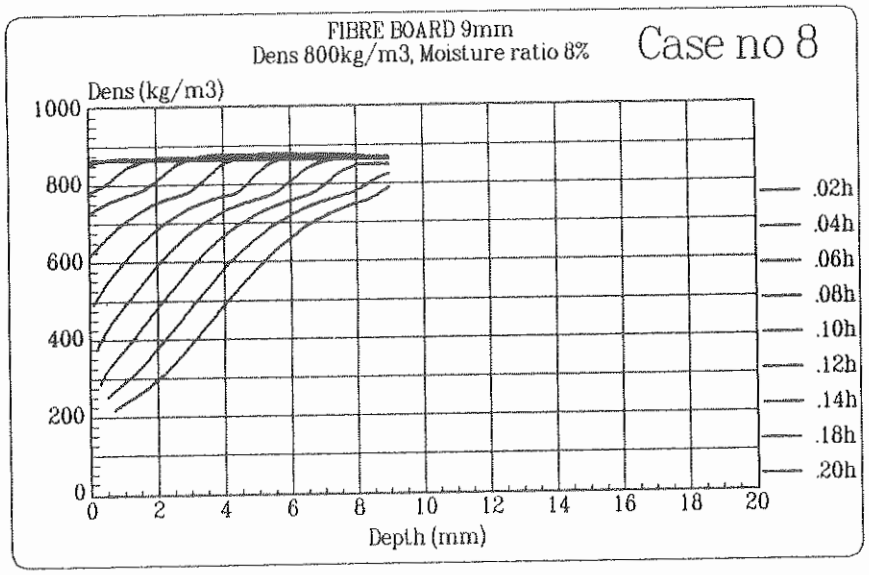
FIBRE BOARD 9mm
Dens 800kg/m3, Moisture ratio 8%
Case no 8
Dens (kg/m3)
1000
800
600
400
200
0
0 2 4 6 8 10 12 14 16 18 20
Depth (mm)
.02h
.04h
.06h
.08h
.10h
.12h
.14h
.18h
.20h

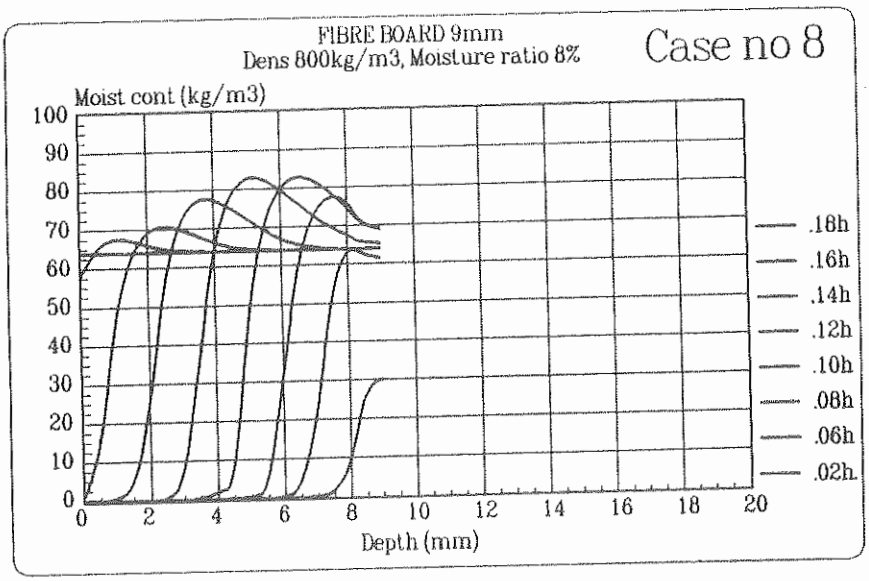
FIBRE BOARD 9mm
Dens 800kg/m3, Moisture ratio 8%
Case no 8
Moist cont (kg/m3)
100
90
80
70
60
50
40
30
20
10
0
0 2 4 6 8 10 12 14 16 18 20
Depth (mm)
.18h
.16h
.14h
.12h
.10h
.08h
.06h
.02h

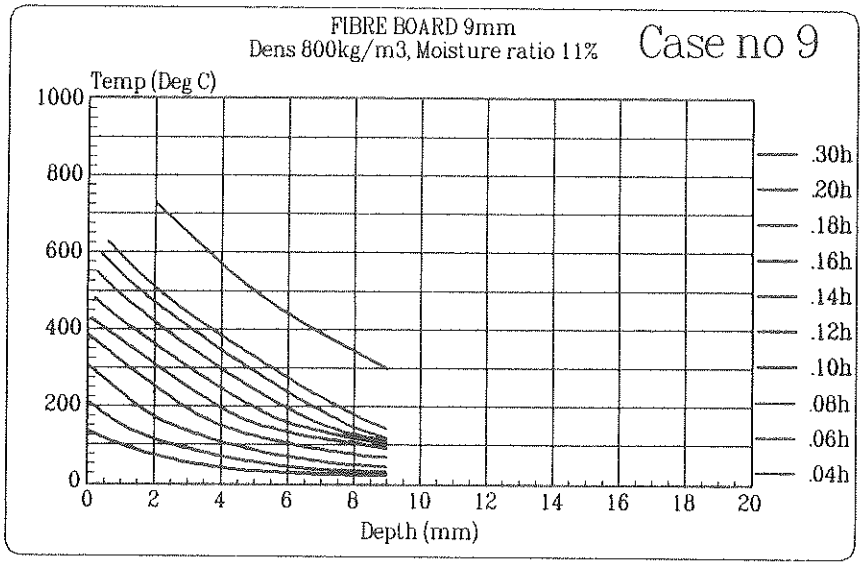
FIBRE BOARD 9mm
Dens 800kg/m3, Moisture ratio 11%
Case no 9
Temp (Deg C)
1000
800
600
400
200
0
0 2 4 6 8 10 12 14 16 18 20
Depth (mm)
.30h
.20h
.18h
.16h
.14h
.12h
.10h
.08h
.06h
.04h

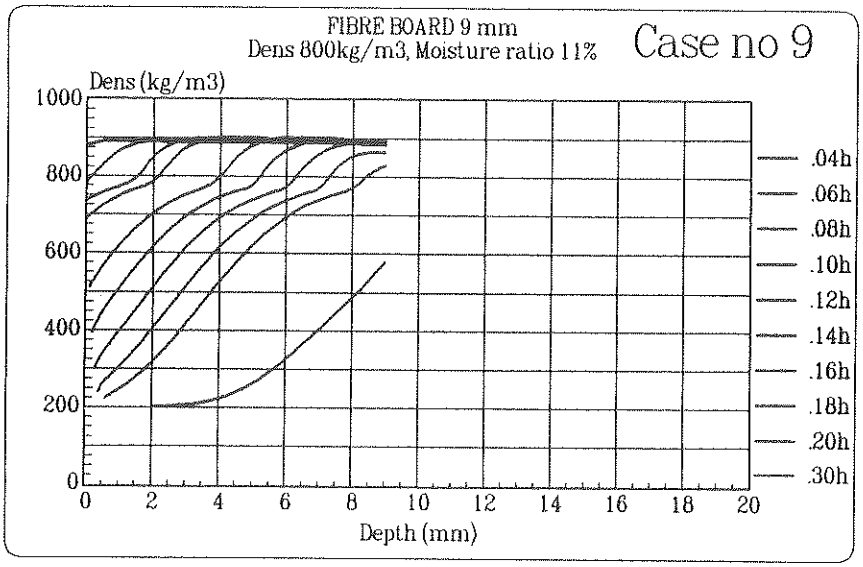
FIBRE BOARD 9 mm
Dens 800kg/m3, Moisture ratio 11%
Case no 9
Dens (kg/m3)
1000
800
600
400
200
0
0 2 4 6 8 10 12 14 16 18 20
Depth (mm)
.04h
.06h
.08h
.10h
.12h
.14h
.16h
.18h
.20h
.30h

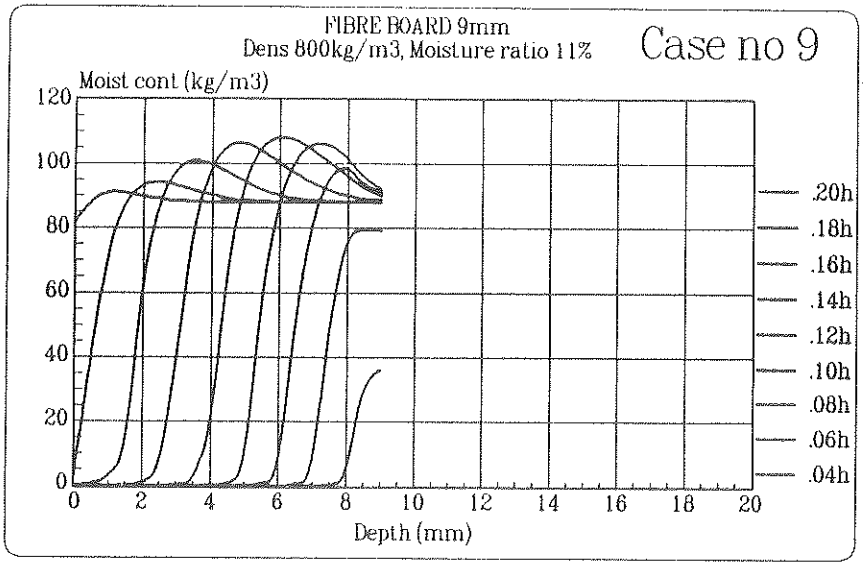
FIBRE BOARD 9mm
Dens 800kg/m3, Moisture ratio 11%
Case no 9
Moist cont (kg/m3)
120
100
80
60
40
20
0
0 2 4 6 8 10 12 14 16 18 20
Depth (mm)
.20h
.18h
.16h
.14h
.12h
.10h
.08h
.06h
.04h

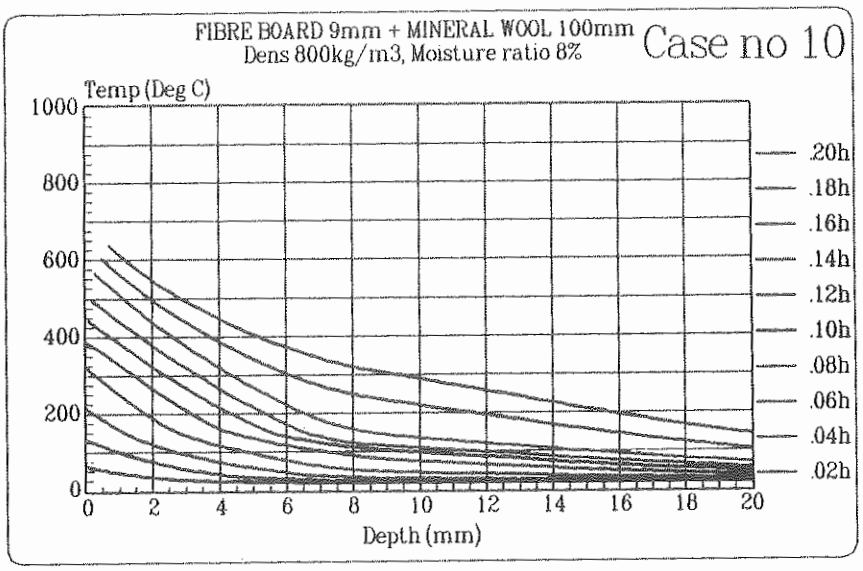
FIBRE BOARD 9mm + MINERAL WOOL 100mm
Dens 800kg/m3, Moisture ratio 8%
Case no 10
Temp (Deg C)
1000
800
600
400
200
0
0 2 4 6 8 10 12 14 16 18 20
Depth (mm)
.20h
.18h
.16h
.14h
.12h
.10h
.08h
.06h
.04h
.02h

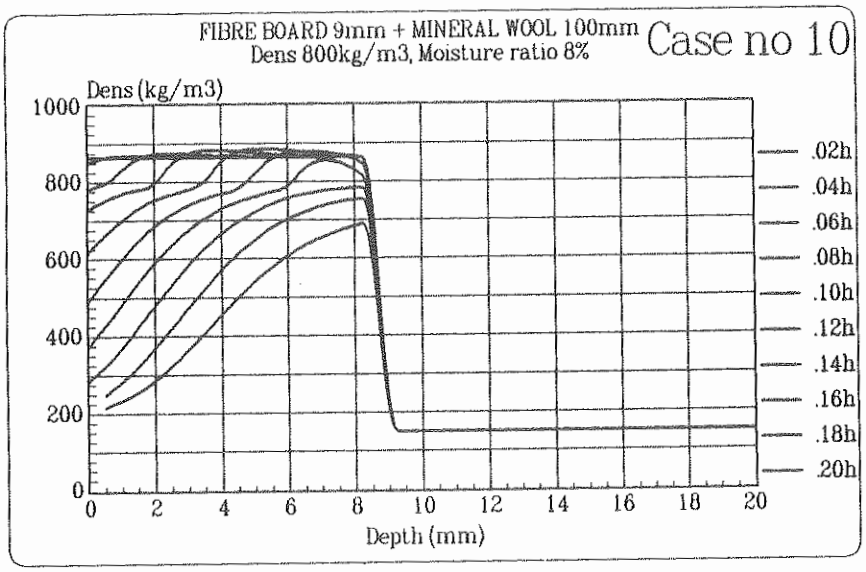
FIBRE BOARD 9mm + MINERAL WOOL 100mm
Dens 800kg/m3, Moisture ratio 8%
Case no 10
Dens (kg/m3)
1000
800
600
400
200
0
0 2 4 6 8 10 12 14 16 18 20
Depth (mm)
.02h
.04h
.06h
.08h
.10h
.12h
.14h
.16h
.18h
.20h

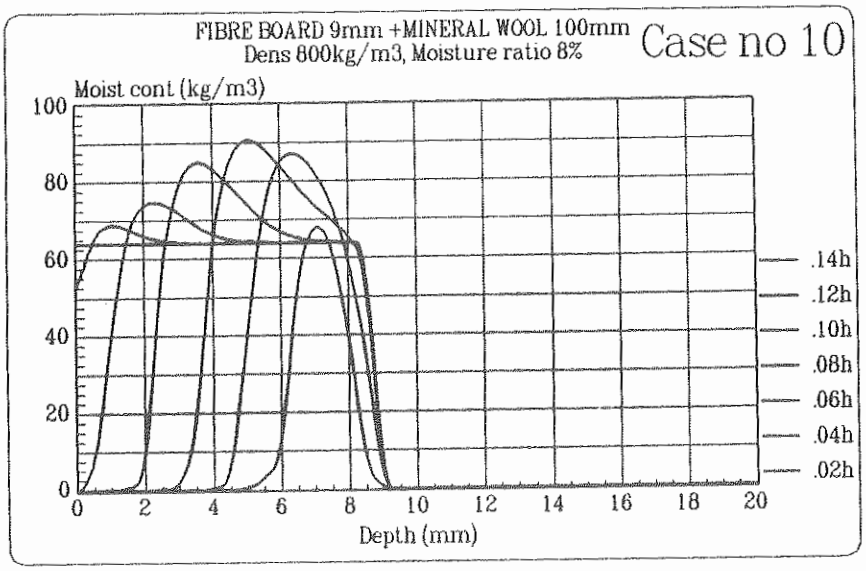
FIBRE BOARD 9mm +MINERAL WOOL 100mm
Dens 800kg/m3, Moisture ratio 8%
Case no 10
Moist cont (kg/m3)
100
80
60
40
20
0
0 2 4 6 8 10 12 14 16 18 20
Depth (mm)
.14h
.12h
.10h
.08h
.06h
.04h
.02h

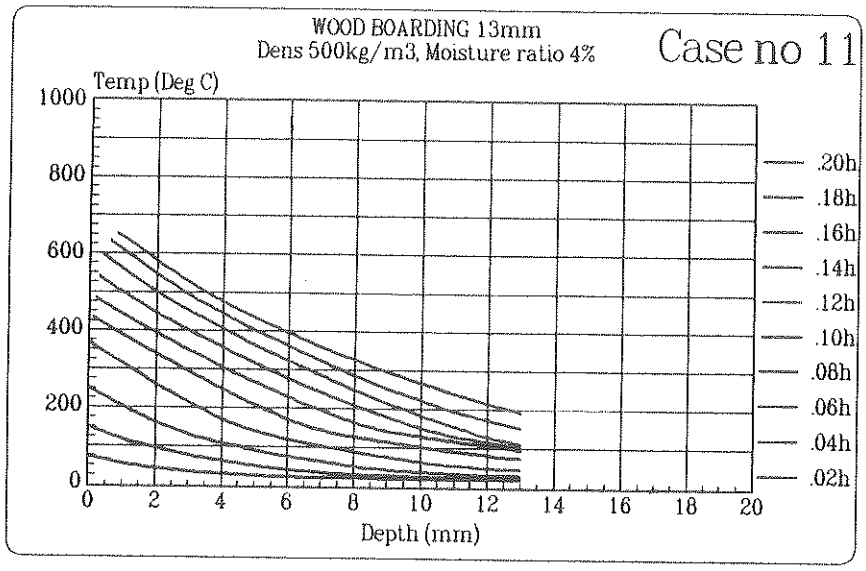
WOOD BOARDING 13mm
Dens 500kg/m3, Moisture ratio 4%
Case no 11
Temp (Deg C)
1000
800
600
400
200
0
0 2 4 6 8 10 12 14 16 18 20
Depth (mm)
.20h
.18h
.16h
.14h
.12h
.10h
.08h
.06h
.04h
.02h

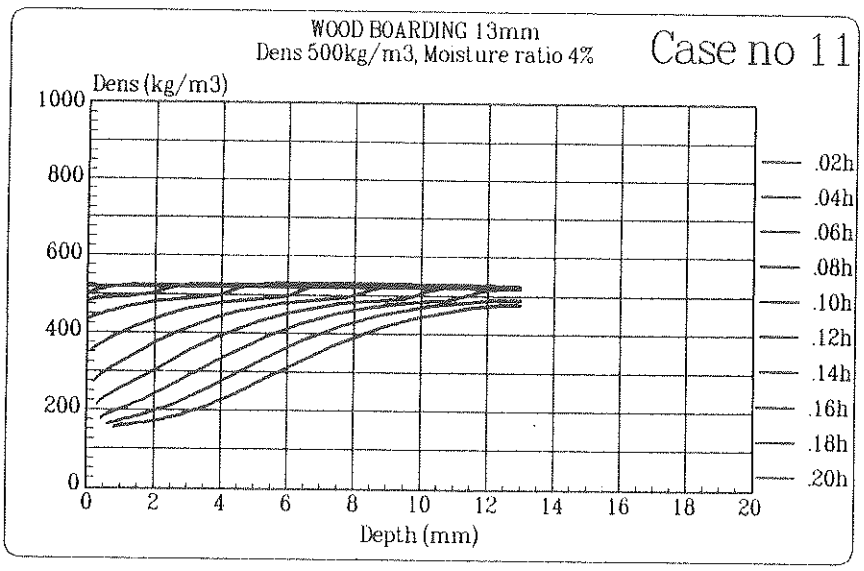
WOOD BOARDING 13mm
Dens 500kg/m3, Moisture ratio 4%
Case no 11
Dens (kg/m3)
1000
800
600
400
200
0
0 2 4 6 8 10 12 14 16 18 20
Depth (mm)
.02h
.04h
.06h
.08h
.10h
.12h
.14h
.16h
.18h
.20h

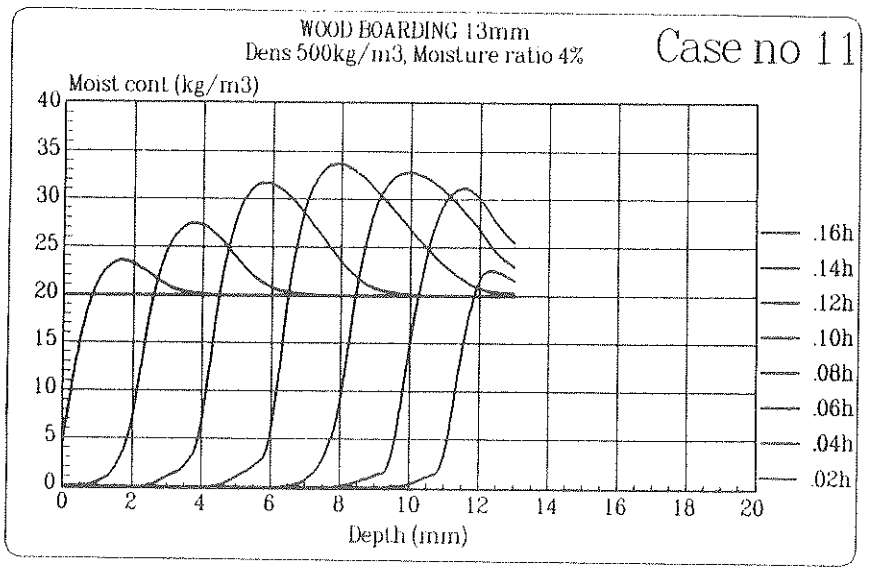
WOOD BOARDING 13mm
Dens 500kg/m3, Moisture ratio 4%
Case no 11
Moist cont (kg/m3)
40
35
30
25
20
15
10
5
0
0 2 4 6 8 10 12 14 16 18 20
Depth (mm)
.16h
.14h
.12h
.10h
.08h
.06h
.04h
.02h

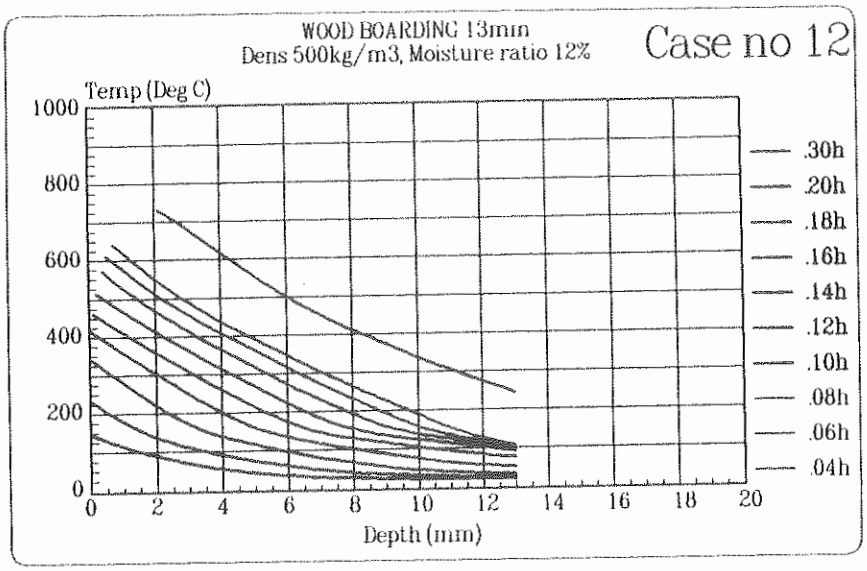
WOOD BOARDING 13mm
Dens 500kg/m3, Moisture ratio 12%
Case no 12
Temp (Deg C)
1000
800
600
400
200
0
0 2 4 6 8 10 12 14 16 18 20
Depth (mm)
.30h
.20h
.18h
.16h
.14h
.12h
.10h
.08h
.06h
.04h

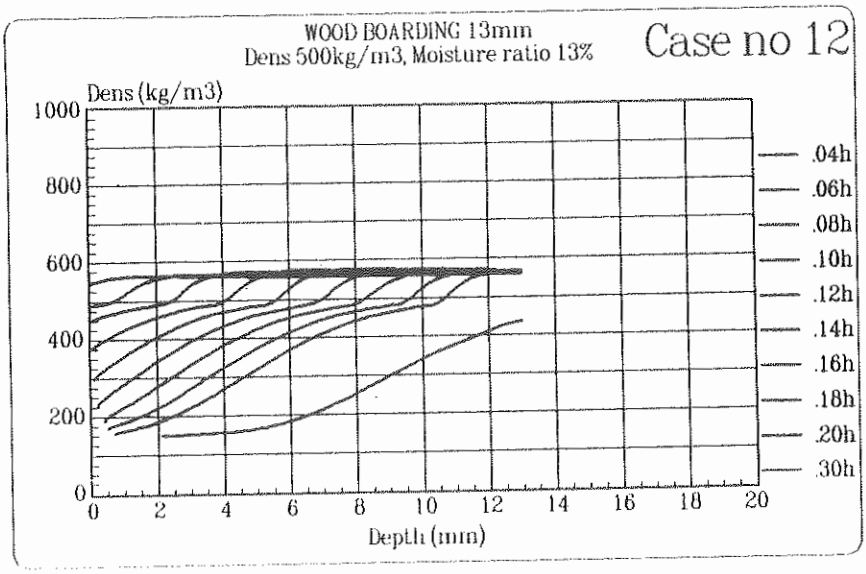
WOOD BOARDING 13mm
Dens 500kg/m3, Moisture ratio 13%
Case no 12
Dens (kg/m3)
1000
800
600
400
200
0
0 2 4 6 8 10 12 14 16 18 20
Depth (mm)
.04h
.06h
.08h
.10h
.12h
.14h
.16h
.18h
.20h
.30h

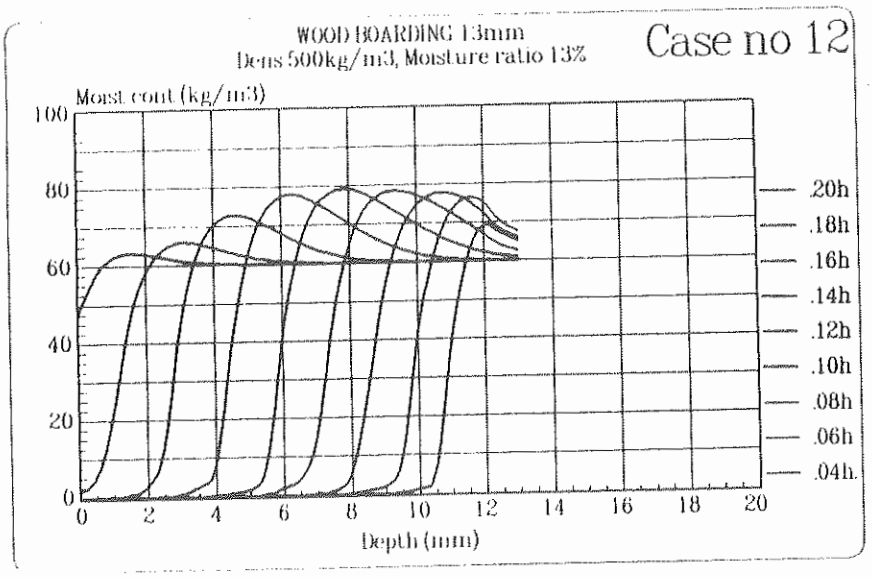
WOOD BOARDING 13mm
Dens 500kg/m3, Moisture ratio 13%
Case no 12
Moist cont (kg/m3)
100
80
60
40
20
0
0 2 4 6 8 10 12 14 16 18 20
Depth (mm)
.20h
.18h
.16h
.14h
.12h
.10h
.08h
.06h
.04h

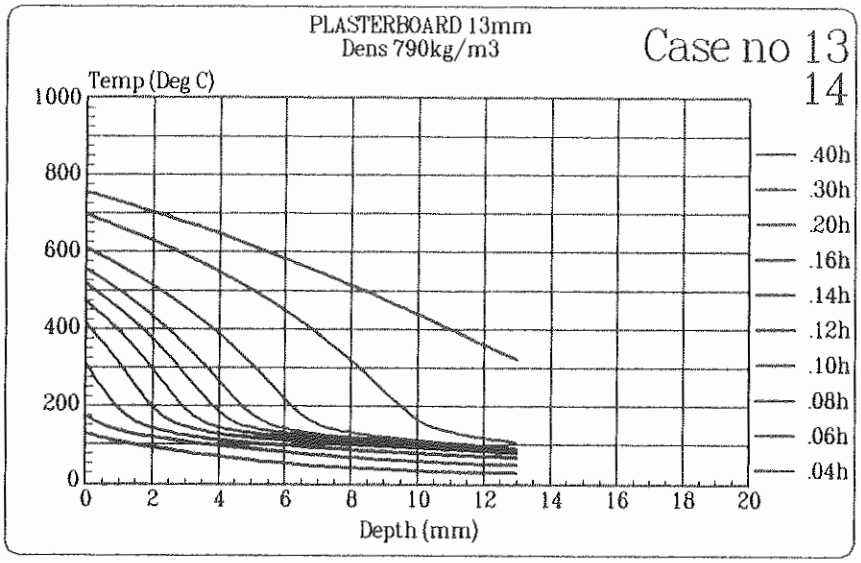
PLASTERBOARD 13mm
Dens 790kg/m3
Case no 13
14
Temp (Deg C)
1000
800
600
400
200
0
0 2 4 6 8 10 12 14 16 18 20
Depth (mm)
.40h
.30h
.20h
.16h
.14h
.12h
.10h
.08h
.06h
.04h

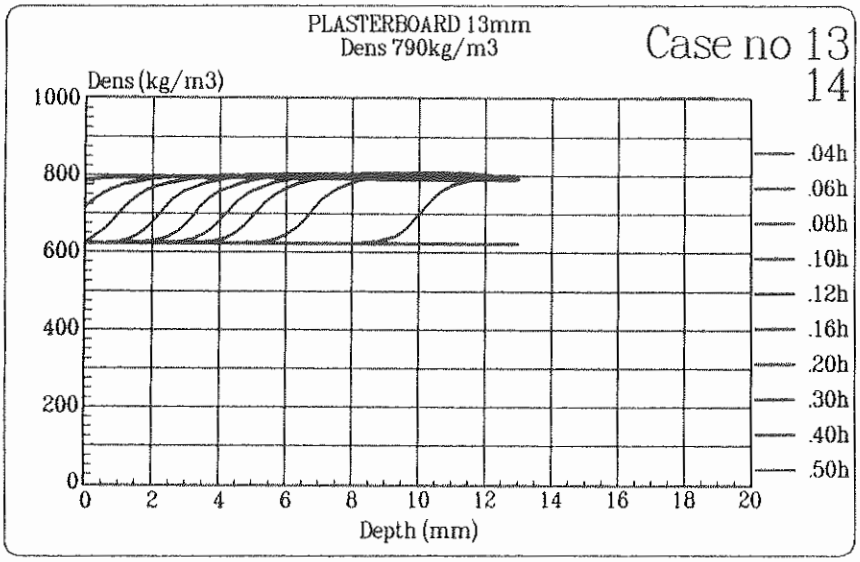
PLASTERBOARD 13mm
Dens 790kg/m3
Case no 13
14
Dens (kg/m3)
1000
800
600
400
200
0
0 2 4 6 8 10 12 14 16 18 20
Depth (mm)
.04h
.06h
.08h
.10h
.12h
.16h
.20h
.30h
.40h
.50h

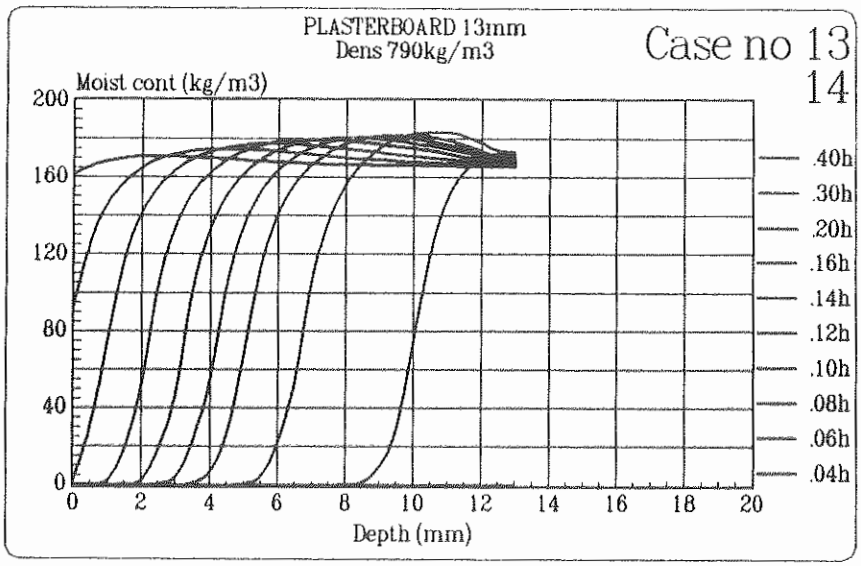
PLASTERBOARD 13mm
Dens 790kg/m3
Case no 13
14
Moist cont (kg/m3)
200
160
120
80
40
0
0 2 4 6 8 10 12 14 16 18 20
Depth (mm)
.40h
.30h
.20h
.16h
.14h
.12h
.10h
.08h
.06h
.04h

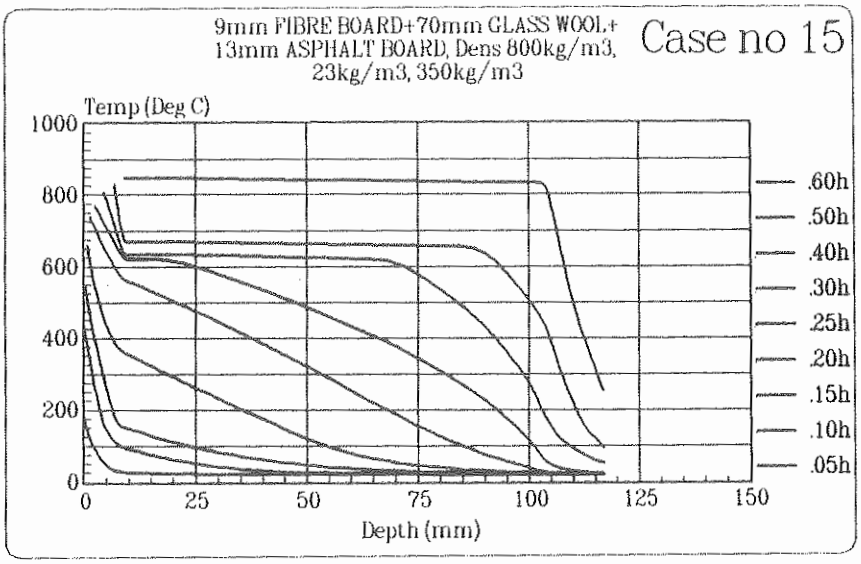
9mm FIBRE BOARD+70mm GLASS WOOL+
13mm ASPHALT BOARD, Dens 800kg/m3,
23kg/m3, 350kg/m3
Case no 15
Temp (Deg C)
1000
800
600
400
200
0
0
25
50
75
100
125
150
Depth (mm)
.60h
.50h
.40h
.30h
.25h
.20h
.15h
.10h
.05h

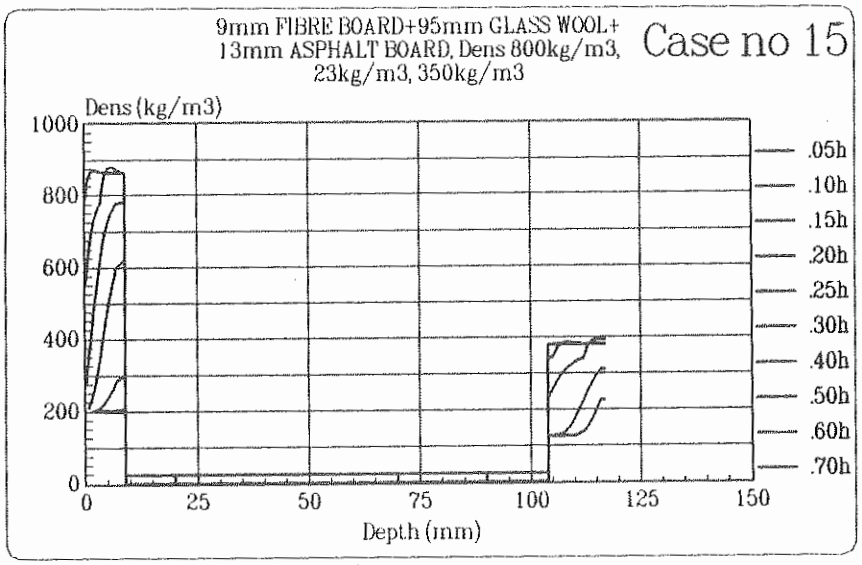
9mm FIBRE BOARD+95mm GLASS WOOL+
13mm ASPHALT BOARD, Dens 800kg/m3,
23kg/m3, 350kg/m3
Case no 15
Dens (kg/m3)
1000
800
600
400
200
0
0
25
50
75
100
125
150
Depth (mm)
.05h
.10h
.15h
.20h
.25h
.30h
.40h
.50h
.60h
.70h

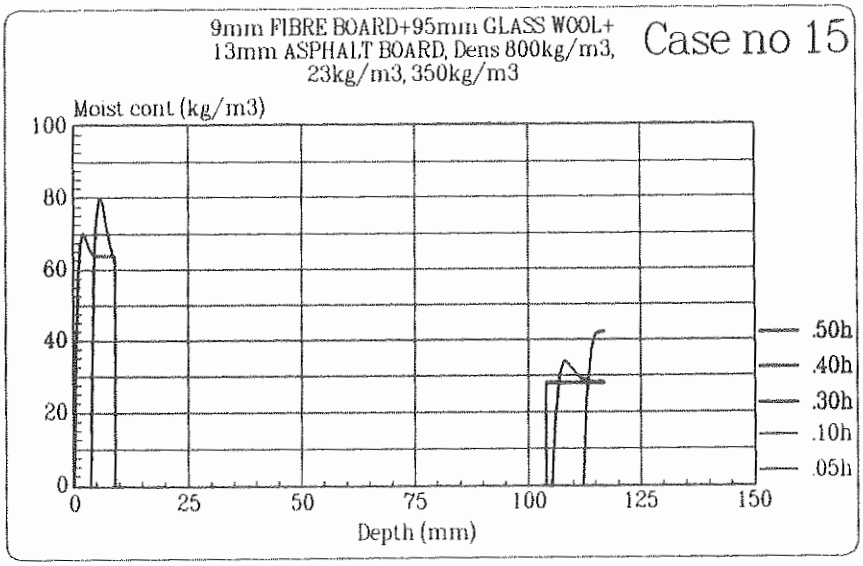
9mm FIBRE BOARD+95mm GLASS WOOL+
13mm ASPHALT BOARD, Dens 800kg/m3,
23kg/m3, 350kg/m3
Case no 15
Moist cont (kg/m3)
100
80
60
40
20
0
0
25
50
75
100
125
150
Depth (mm)
.50h
.40h
.30h
.10h
.05h

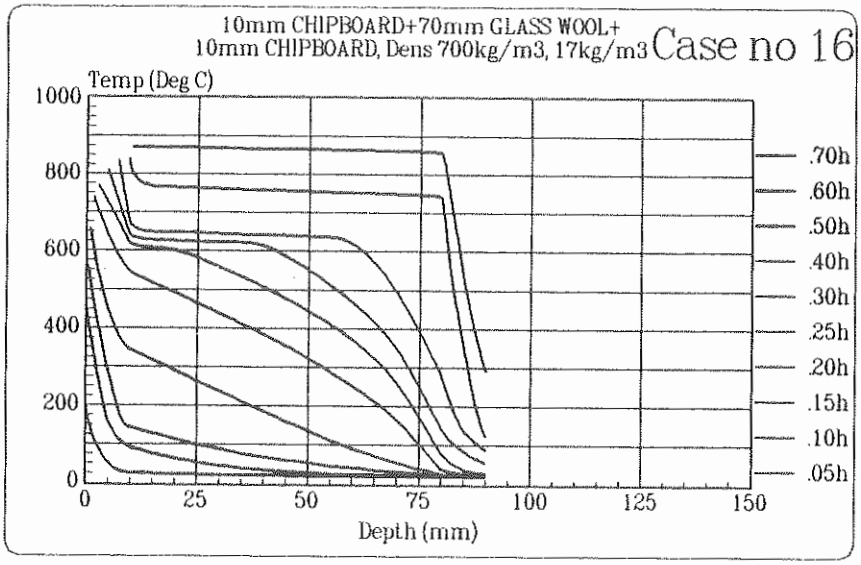
10mm CHIPBOARD+70mm GLASS WOOL+
10mm CHIPBOARD, Dens 700kg/m3, 17kg/m3
Case no 16
Temp (Deg C)
1000
800
600
400
200
0
0
25
50
75
100
125
150
Depth (mm)
.70h
.60h
.50h
.40h
.30h
.25h
.20h
.15h
.10h
.05h

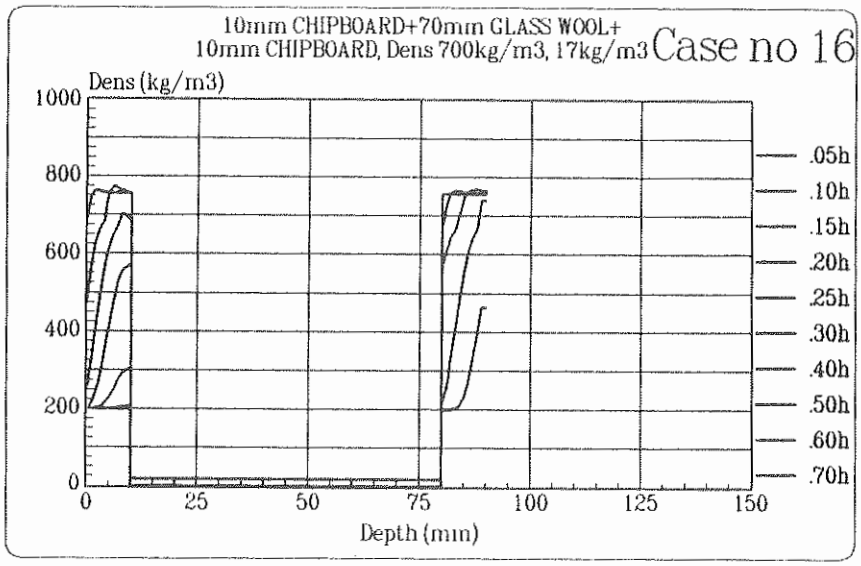
10mm CHIPBOARD+70mm GLASS WOOL+
10mm CHIPBOARD, Dens 700kg/m3, 17kg/m3
Case no 16
Dens (kg/m3)
1000
800
600
400
200
0
0
25
50
75
100
125
150
Depth (mm)
.05h
.10h
.15h
.20h
.25h
.30h
.40h
.50h
.60h
.70h

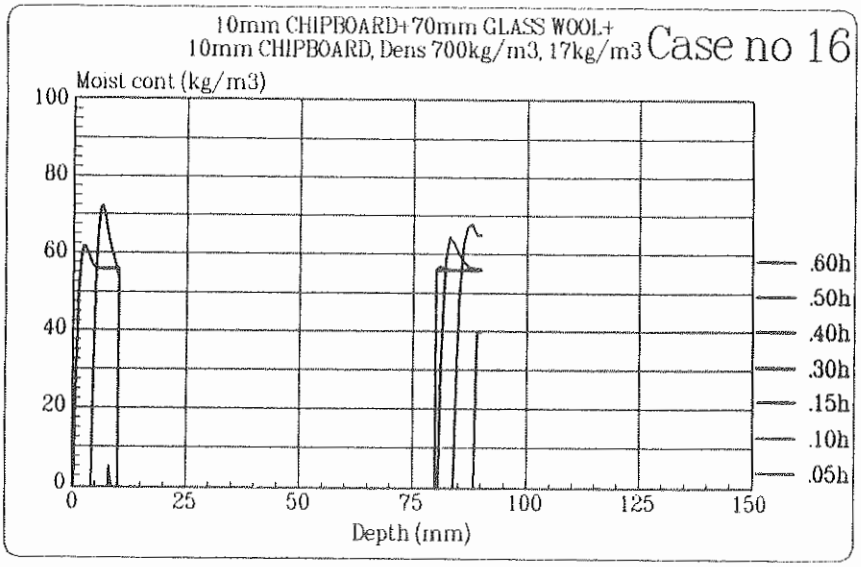
10mm CHIPBOARD+70mm GLASS WOOL+
10mm CHIPBOARD, Dens 700kg/m3, 17kg/m3
Case no 16
Moist cont (kg/m3)
100
80
60
40
20
0
0
25
50
75
100
125
150
Depth (mm)
.60h
.50h
.40h
.30h
.15h
.10h
.05h

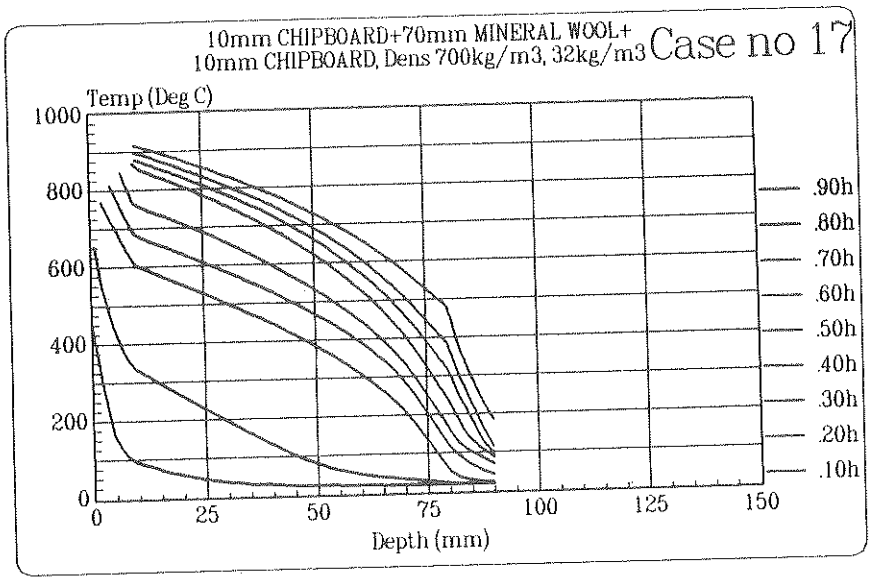
10mm CHIPBOARD+70mm MINERAL WOOL+
10mm CHIPBOARD, Dens 700kg/m3, 32kg/m3 Case no 17
Temp (Deg C)
1000
800
600
400
200
0
0
25
50
75
100
125
150
Depth (mm)
.90h
.80h
.70h
.60h
.50h
.40h
.30h
.20h
.10h

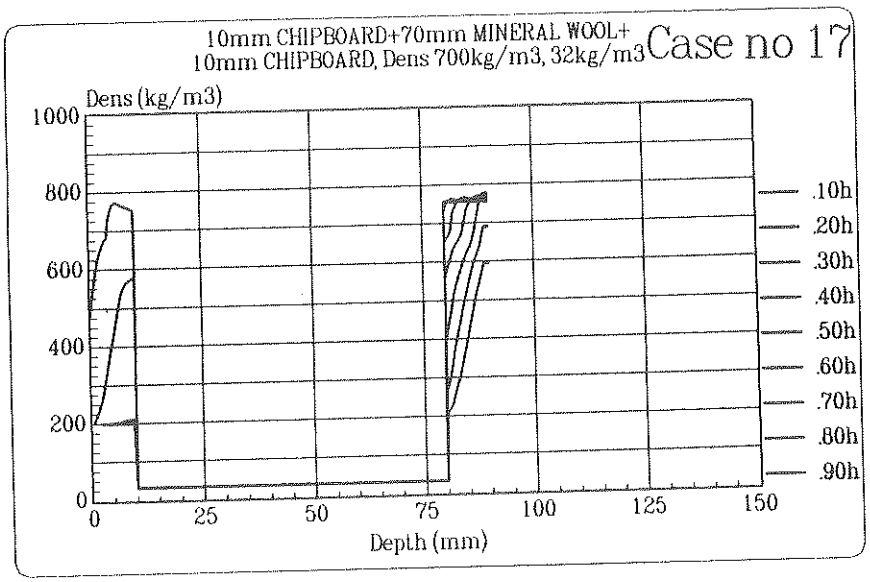
10mm CHIPBOARD+70mm MINERAL WOOL+
10mm CHIPBOARD, Dens 700kg/m3, 32kg/m3 Case no 17
Dens (kg/m3)
1000
800
600
400
200
0
0
25
50
75
100
125
150
Depth (mm)
.10h
.20h
.30h
.40h
.50h
.60h
.70h
.80h
.90h

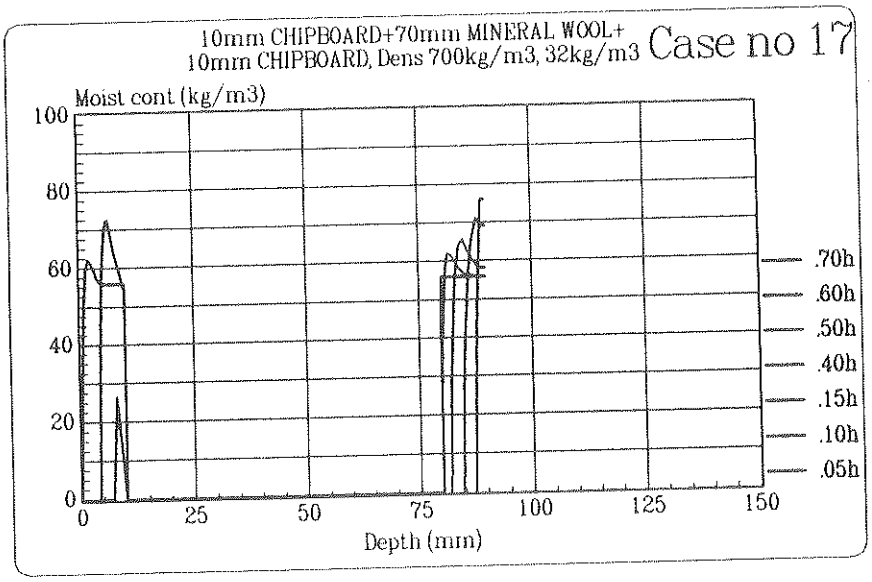
10mm CHIPBOARD+70mm MINERAL WOOL+
10mm CHIPBOARD, Dens 700kg/m3, 32kg/m3 Case no 17
Moist cont (kg/m3)
100
80
60
40
20
0
0
25
50
75
100
125
150
Depth (mm)
.70h
.60h
.50h
.40h
.15h
.10h
.05h

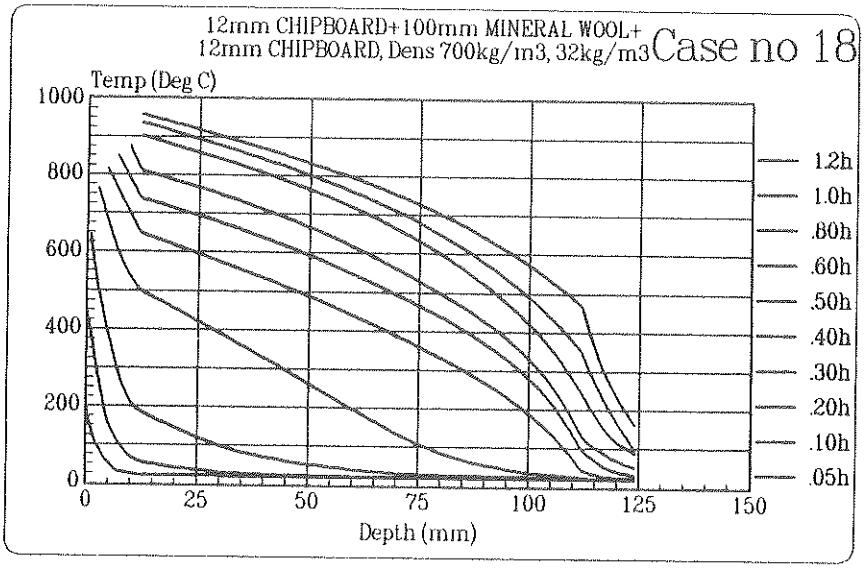
12mm CHIPBOARD+100mm MINERAL WOOL+
12mm CHIPBOARD, Dens 700kg/m3, 32kg/m3
Case no 18
Temp (Deg C)
1000
800
600
400
200
0
0
25
50
75
100
125
150
Depth (mm)
1.2h
1.0h
.80h
.60h
.50h
.40h
.30h
.20h
.10h
.05h

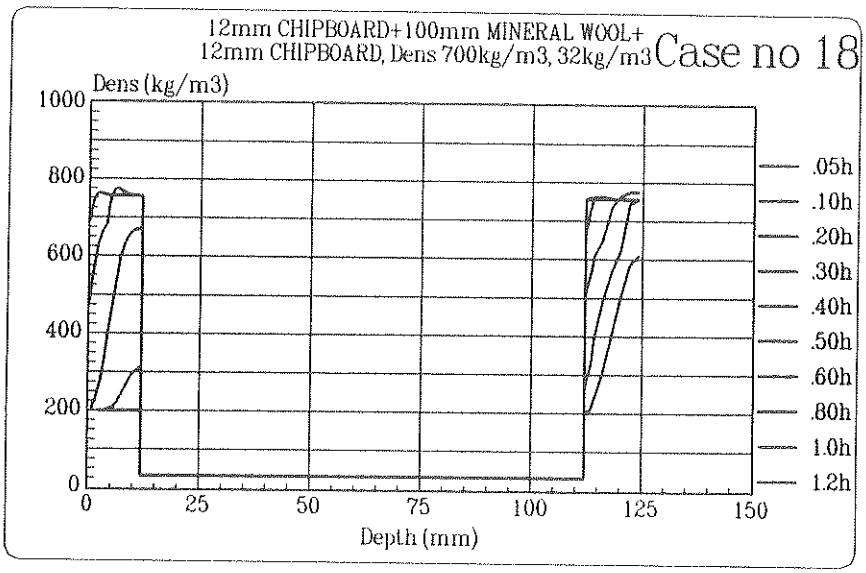
12mm CHIPBOARD+100mm MINERAL WOOL+
12mm CHIPBOARD, Dens 700kg/m3, 32kg/m3
Case no 18
Dens (kg/m3)
1000
800
600
400
200
0
0
25
50
75
100
125
150
Depth (mm)
.05h
.10h
.20h
.30h
.40h
.50h
.60h
.80h
1.0h
1.2h

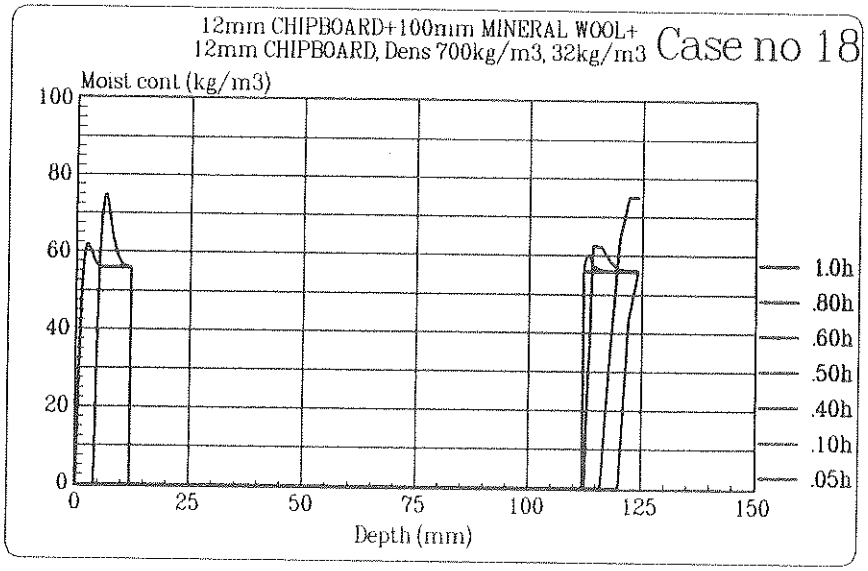
12mm CHIPBOARD+100mm MINERAL WOOL+
12mm CHIPBOARD, Dens 700kg/m3, 32kg/m3
Case no 18
Moist cont (kg/m3)
100
80
60
40
20
0
0
25
50
75
100
125
150
Depth (mm)
1.0h
.80h
.60h
.50h
.40h
.10h
.05h

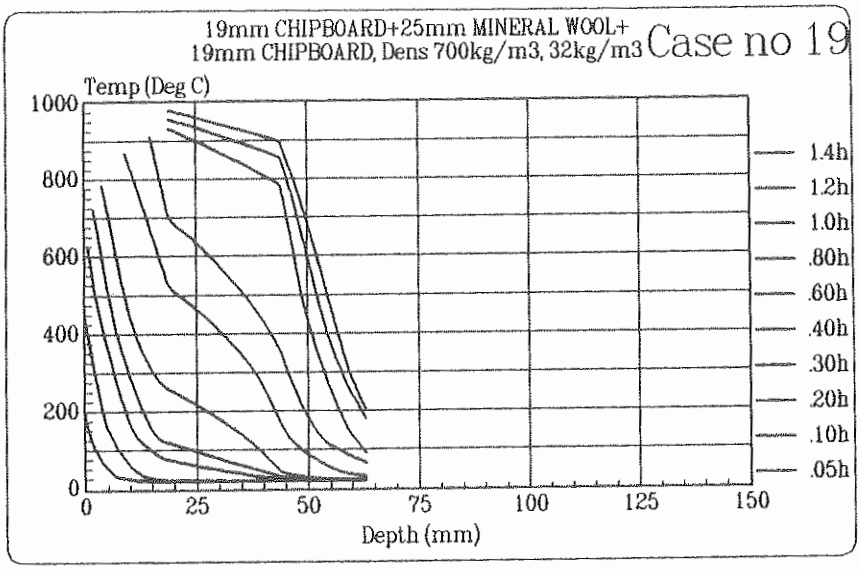
19mm CHIPBOARD+25mm MINERAL WOOL+
19mm CHIPBOARD, Dens 700kg/m3, 32kg/m3
Case no 19
Temp (Deg C)
1000
800
600
400
200
0
0
25
50
75
100
125
150
Depth (mm)
1.4h
1.2h
1.0h
.80h
.60h
.40h
.30h
.20h
.10h
.05h

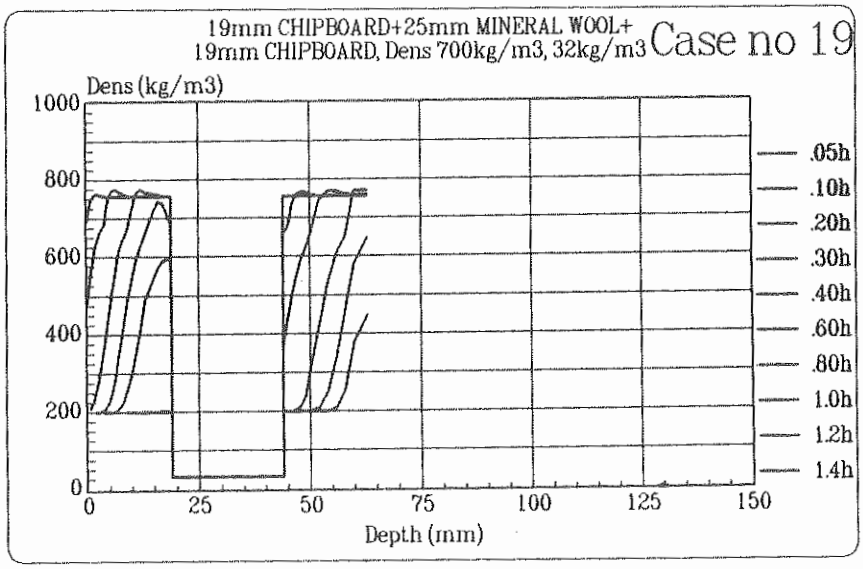
19mm CHIPBOARD+25mm MINERAL WOOL+
19mm CHIPBOARD, Dens 700kg/m3, 32kg/m3
Case no 19
Dens (kg/m3)
1000
800
600
400
200
0
0
25
50
75
100
125
150
Depth (mm)
.05h
.10h
.20h
.30h
.40h
.60h
.80h
1.0h
1.2h
1.4h

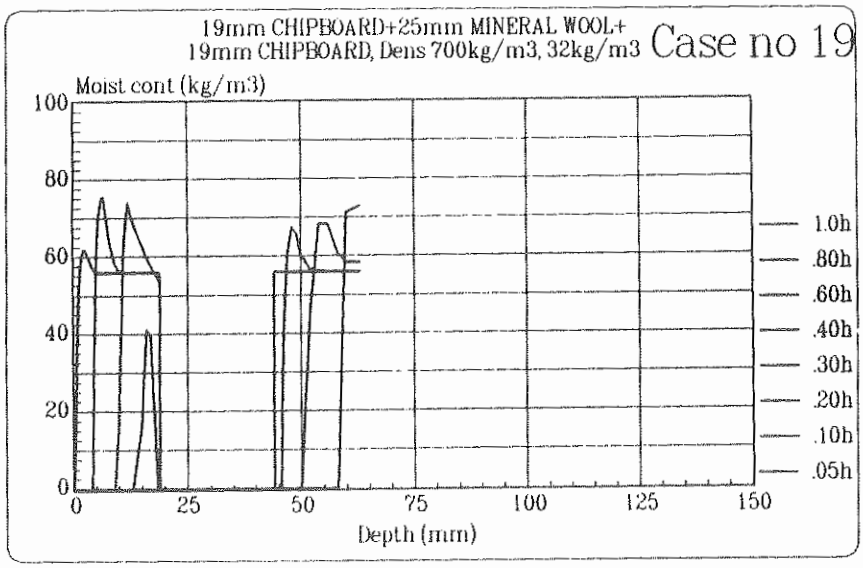
19mm CHIPBOARD+25mm MINERAL WOOL+
19mm CHIPBOARD, Dens 700kg/m3, 32kg/m3
Case no 19
Moist cont (kg/m3)
100
80
60
40
20
0
0
25
50
75
100
125
150
Depth (mm)
1.0h
.80h
.60h
.40h
.30h
.20h
.10h
.05h

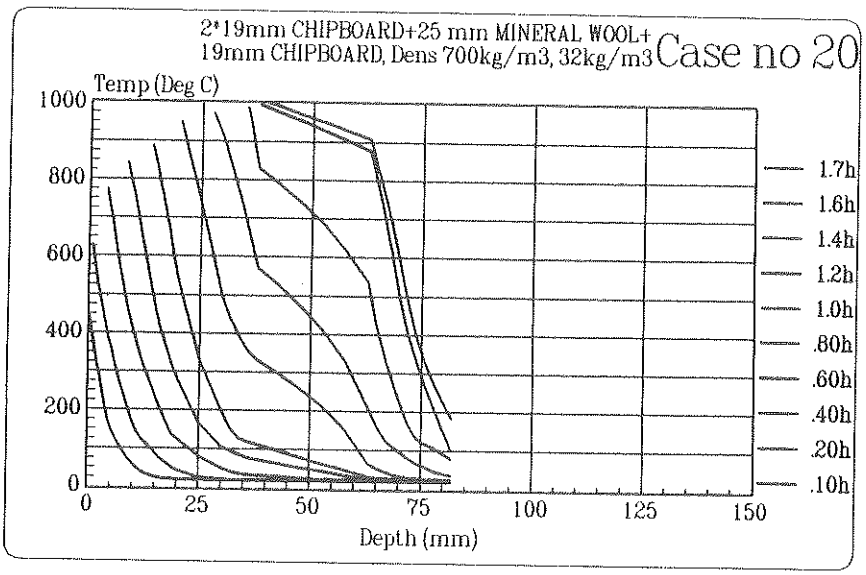
2*19mm CHIPBOARD+25 mm MINERAL WOOL+
19mm CHIPBOARD, Dens 700kg/m3, 32kg/m3
Case no 20
Temp (Deg C)
1000
800
600
400
200
0
0
25
50
75
100
125
150
Depth (mm)
1.7h
1.6h
1.4h
1.2h
1.0h
.80h
.60h
.40h
.20h
.10h

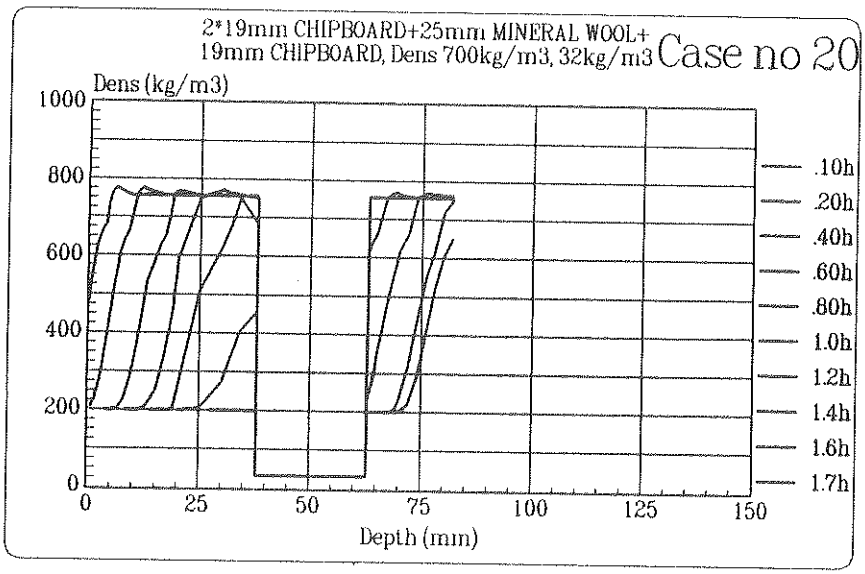
2*19mm CHIPBOARD+25mm MINERAL WOOL+
19mm CHIPBOARD, Dens 700kg/m3, 32kg/m3
Case no 20
Dens (kg/m3)
1000
800
600
400
200
0
0
25
50
75
100
125
150
Depth (mm)
.10h
.20h
.40h
.60h
.80h
1.0h
1.2h
1.4h
1.6h
1.7h

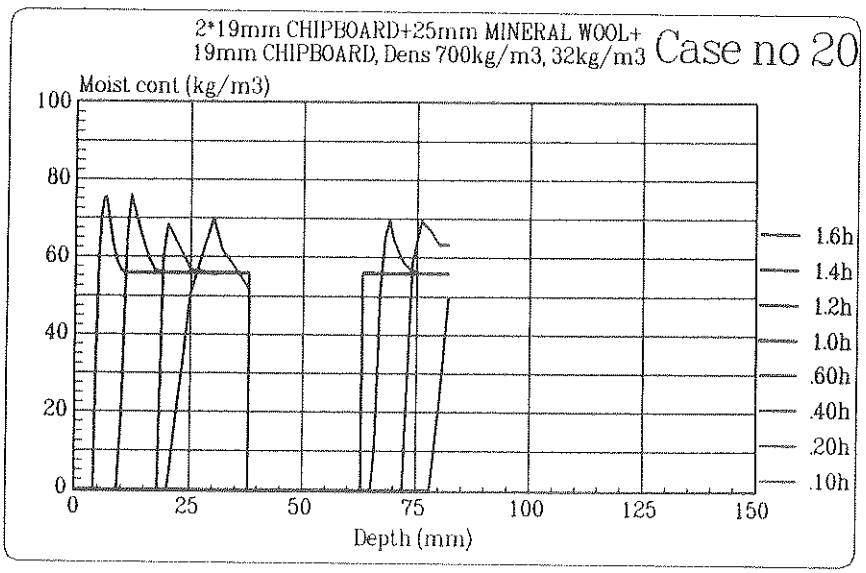
2*19mm CHIPBOARD+25mm MINERAL WOOL+
19mm CHIPBOARD, Dens 700kg/m3, 32kg/m3
Case no 20
Moist cont (kg/m3)
100
80
60
40
20
0
0
25
50
75
100
125
150
Depth (mm)
1.6h
1.4h
1.2h
1.0h
.60h
.40h
.20h
.10h

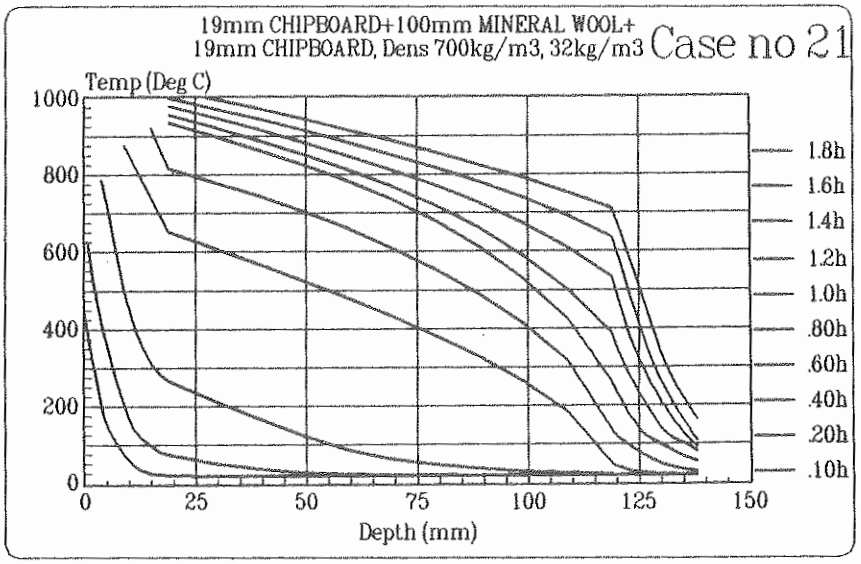
19mm CHIPBOARD+100mm MINERAL WOOL+
19mm CHIPBOARD, Dens 700kg/m3, 32kg/m3
Case no 21
Temp (Deg C)
1000
800
600
400
200
0
0
25
50
75
100
125
150
Depth (mm)
1.8h
1.6h
1.4h
1.2h
1.0h
.80h
.60h
.40h
.20h
.10h

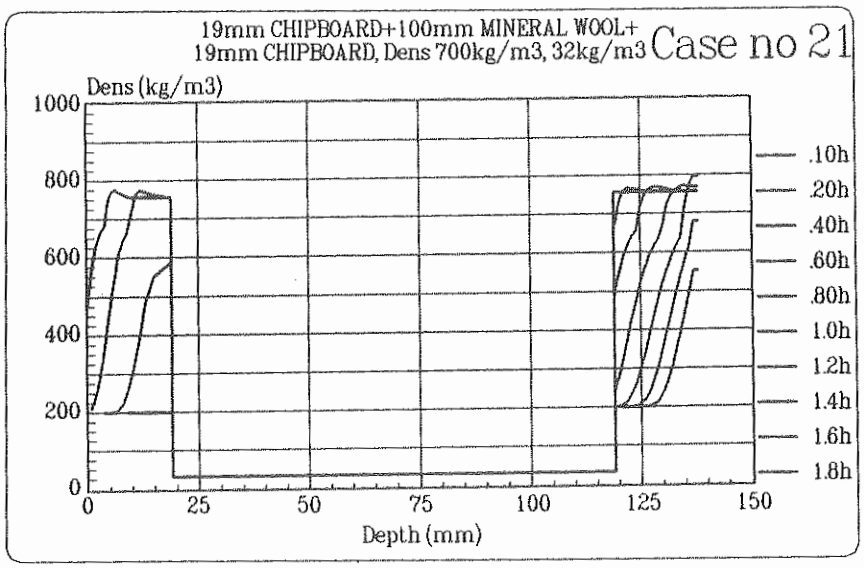
19mm CHIPBOARD+100mm MINERAL WOOL+
19mm CHIPBOARD, Dens 700kg/m3, 32kg/m3
Case no 21
Dens (kg/m3)
1000
800
600
400
200
0
0
25
50
75
100
125
150
Depth (mm)
.10h
.20h
.40h
.60h
.80h
1.0h
1.2h
1.4h
1.6h
1.8h

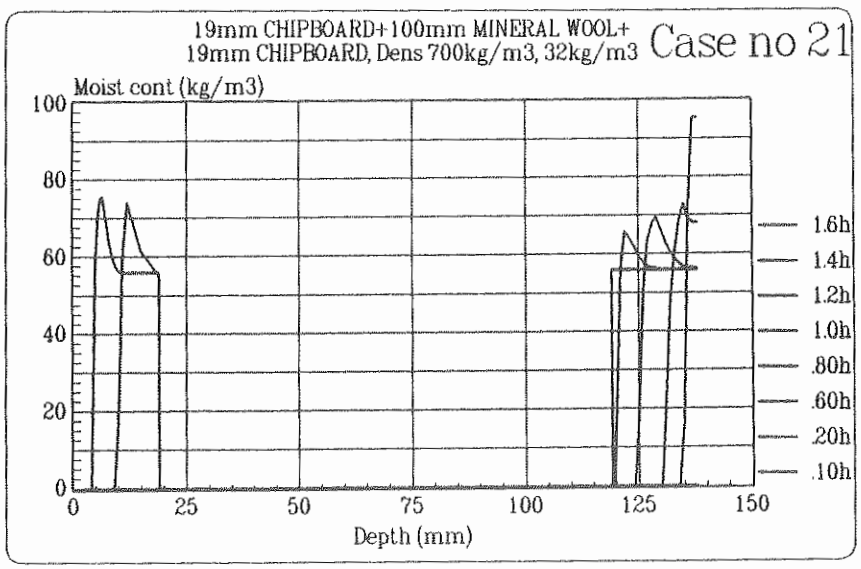
19mm CHIPBOARD+100mm MINERAL WOOL+
19mm CHIPBOARD, Dens 700kg/m3, 32kg/m3
Case no 21
Moist cont (kg/m3)
100
80
60
40
20
0
0
25
50
75
100
125
150
Depth (mm)
1.6h
1.4h
1.2h
1.0h
.80h
.60h
.20h
.10h

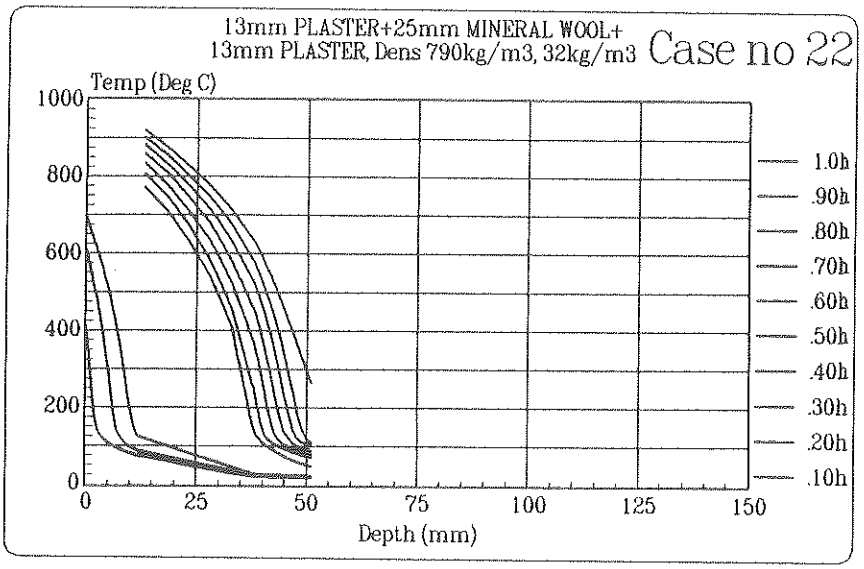
13mm PLASTER+25mm MINERAL WOOL+
13mm PLASTER, Dens 790kg/m3, 32kg/m3
Case no 22
Temp (Deg C)
1000
800
600
400
200
0
0
25
50
75
100
125
150
Depth (mm)
1.0h
.90h
.80h
.70h
.60h
.50h
.40h
.30h
.20h
.10h

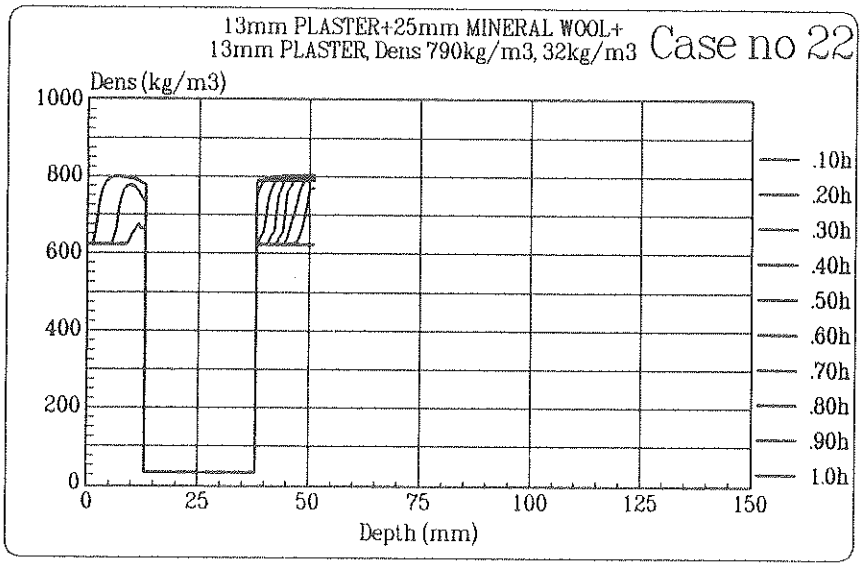
13mm PLASTER+25mm MINERAL WOOL+
13mm PLASTER, Dens 790kg/m3, 32kg/m3
Case no 22
Dens (kg/m3)
1000
800
600
400
200
0
0
25
50
75
100
125
150
Depth (mm)
.10h
.20h
.30h
.40h
.50h
.60h
.70h
.80h
.90h
1.0h

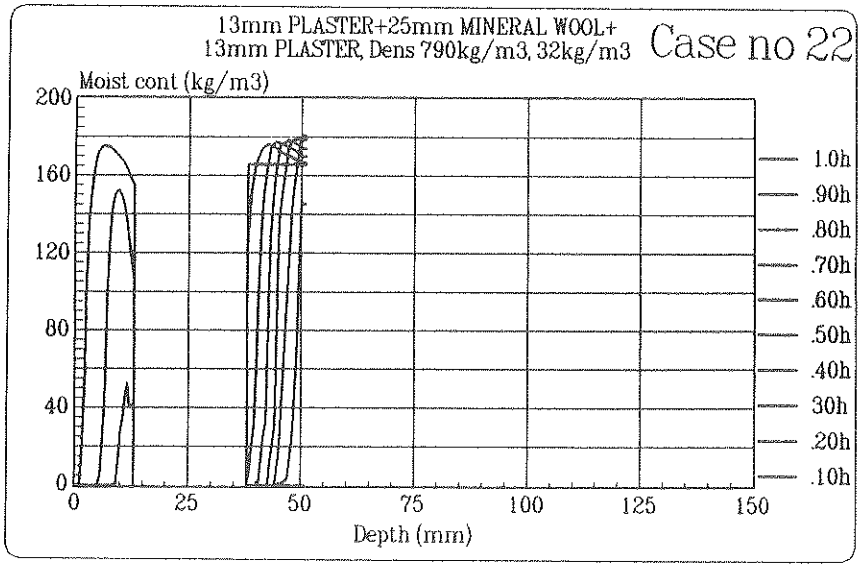
13mm PLASTER+25mm MINERAL WOOL+
13mm PLASTER, Dens 790kg/m3, 32kg/m3
Case no 22
Moist cont (kg/m3)
200
160
120
80
40
0
0
25
50
75
100
125
150
Depth (mm)
1.0h
.90h
.80h
.70h
.60h
.50h
.40h
30h
.20h
.10h

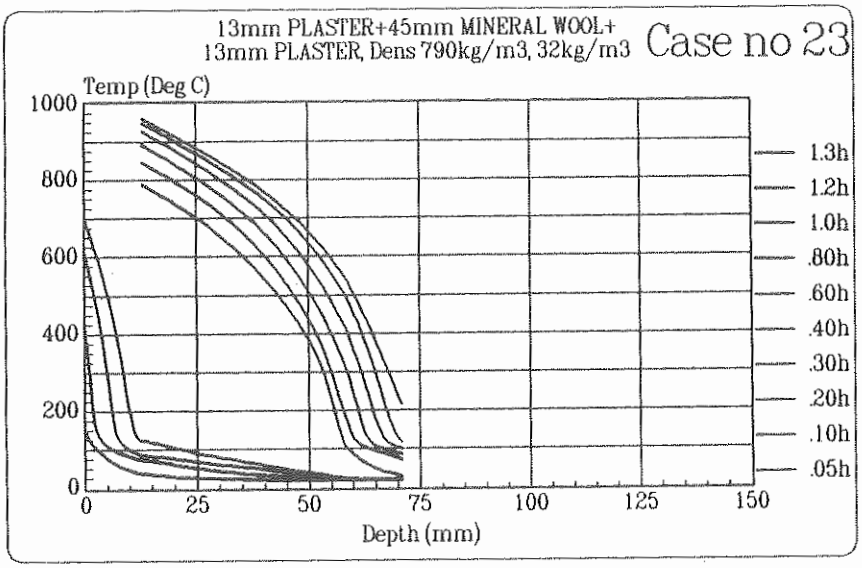
13mm PLASTER+45mm MINERAL WOOL+
13mm PLASTER, Dens 790kg/m3, 32kg/m3
Case no 23
Temp (Deg C)
1000
800
600
400
200
0
0
25
50
75
100
125
150
Depth (mm)
1.3h
1.2h
1.0h
.80h
.60h
.40h
.30h
.20h
.10h
.05h

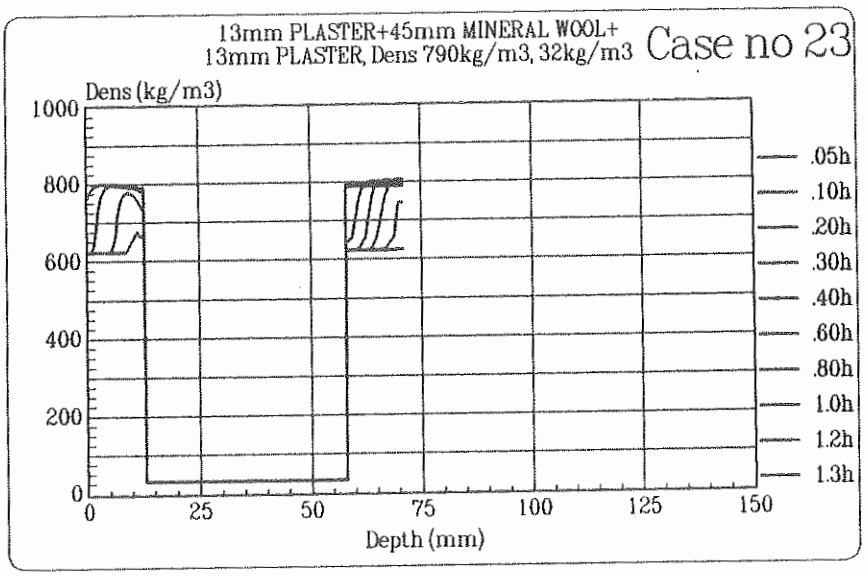
13mm PLASTER+45mm MINERAL WOOL+
13mm PLASTER, Dens 790kg/m3, 32kg/m3
Case no 23
Dens (kg/m3)
1000
800
600
400
200
0
0
25
50
75
100
125
150
Depth (mm)
.05h
.10h
.20h
.30h
.40h
.60h
.80h
1.0h
1.2h
1.3h

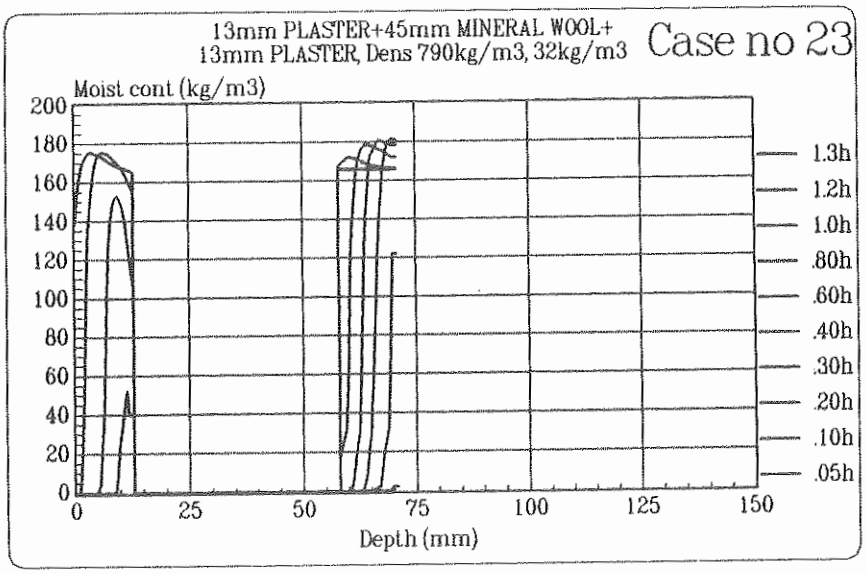
13mm PLASTER+45mm MINERAL WOOL+
13mm PLASTER, Dens 790kg/m3, 32kg/m3
Case no 23
Moist cont (kg/m3)
200
180
160
140
120
100
80
60
40
20
0
0
25
50
75
100
125
150
Depth (mm)
1.3h
1.2h
1.0h
.80h
.60h
.40h
.30h
.20h
.10h
.05h